SYNTHESES OF AMORPHOUS POLYMERS
WITH RIGID MAIN-CHAIN OR PENDANT STRUCTURES
BY CATIONIC POLYMERIZATION

TOSHIHIRO SAGANE

1992

CONTENTS

INTRODUCTION

Unlike small organic compounds, most of synthetic polymers are inherently heterogeneous in the molecular level: heterogeneous in molecular weight [i.e., involving a molecular weight distribution (MWD)] and heterogeneous in structure in solid state, where crystalline and amorphous domains coexist in varying properties. Depending on which of the two domains predominates, therefore, polymers are designated as either "crystalline" or "amorphous".

Among the various properties of polymer materials, thermal properties are the most important and often critical in both processing stages and end uses.[1] Polymers undergo various phase transitions, such as melting and glassy-rubbery transitions. Importantly, the phase-transition phenomena and their onset temperatures critically depend not only on primary chemical structures but on the molecular weights and MWDs of respective polymers. This dependence, in turn, implies that one can control the thermal properties of polymers by designing and regulating these chemical/structural factors. Therefore, it is one of the strategies in developing high-performance polymeric materials to create "polymers with characteristic thermal properties" (e.g., controlled solid-liquid transition).

In general, the thermal properties of amorphous polymers are primarily determined by the primary chemical structure, molecular weight and MWD, whereas those of crystalline polymers depend not only on these factors but also on such factors as stereostructures, annealing and rate of crystallization.[2] Therefore, in investigations of the relationships between polymer structure and thermal properties, amorphous polymers are more suited than crystalline counterparts. Depending on temperature and structure, amorphous polymers exhibit widely

different physical and mechanical behaviors. At low temperatures, for example, amorphous polymers are glassy, hard and brittle; as temperature is raised, they undergo the glass-rubber transition. The glass-transition temperature (Tg) is defined as the temperature at which a polymer softens or begins long-range coordinated molecular (segmental) motions. The glass-rubber transition is known to be controlled mainly by the molecular structures of polymers. In general, factors that increase the energy required for the onset of molecular motion and thereby raise Tg include (i) intermolecular forces, (ii) high cohesive energy density and (iii) bulky and rigid structures.[3]

As expected from these factors, polymers of excellent thermal performance often contain rigid cyclic structures (such as phenyl rings), complex aromatic heterocycles and alicyclic structures primarily in the main chains.[4] Another interesting aspect of the rigid cyclic-type polymers is the possible development of liquid crystallinity, as evidenced by the recent extensive studies.[5] These polymers, on the other hand, often consist of rigid cyclic structures with flexible chain sequences either in the main chains or in the pendant groups, and the rigid cyclic units serve as mesogenic cores. Therefore well-designed rigid cyclic structures are important in controlling the thermal properties and liquid crystallinity of polymers.

Polymers with rigid cyclic structures have been synthesized mostly by condensation polymerization. Recently, however, it has been found that cationic polymerization can be controlled to provide interesting polymers.[6] Examples include cationic polymerizations with controlled chain transfer (selective oligomerization)[7] and with controlled propagation (living polymerization)[7, 8]. In cationic polymerization,

however, there have been few investigations directed towards controlling the thermal properties of polymers by regulating their molecular structures. This is rather surprising in view of a very large number and variety of cationically polymerizable monomers (as many as 500) and the low cost and high efficiency of initiators.[9]

Therefore, as shown in Figure 1, the author decided to employ cationic polymerization for the synthesis of amorphous polymers with rigid cyclic aliphatic structures in the main chain [Figure 1(a)] and with rigid-rod aromatic structures in the pendant groups [Figure 1(b)]. Relative to these synthetic efforts, this doctoral study is specifically focused on the effects of the molecular structures, molecular weight and MWD on the thermal properties of the polymers thus prepared.

The present thesis consists of two parts. Figure 1 serves to visualize the framework and basic concepts of this study. Part I [Figure 1(a)] concerns the synthesis of amorphous polymers with rigid alicyclic (norbornyl) structures in the main chain and the control of their thermal properties (glass-rubber transition).

Chapter 1 describes the synthesis of soluble norbornyl unit-containing polymers with a moderately high Tg (100-200 ℃) (Eq. 1). The polymers were prepared by cationic copolymerization of norbornadiene (NBD) with styrene (St) with the ethylaluminum dichloride/$\underline{t}$-butyl chloride (AlEtCl$_2$/$\underline{t}$-BuCl) catalyst system at -50 ℃ in CH$_2$Cl$_2$, and the effects of NBD/St molar ratio in feed on the polymer solubility, molecular weight, and Tg were investigated. A totally soluble random-copolymer was prepared with 40 mole% or more St fed, in contrast to the corresponding NBD homopolymer that contained an insoluble fraction (ca. 30 wt%). The Tg of the amorphous copolymer was controlled by the NBD/St composition in the range

(a) : Part I (Control of Glass Transition)

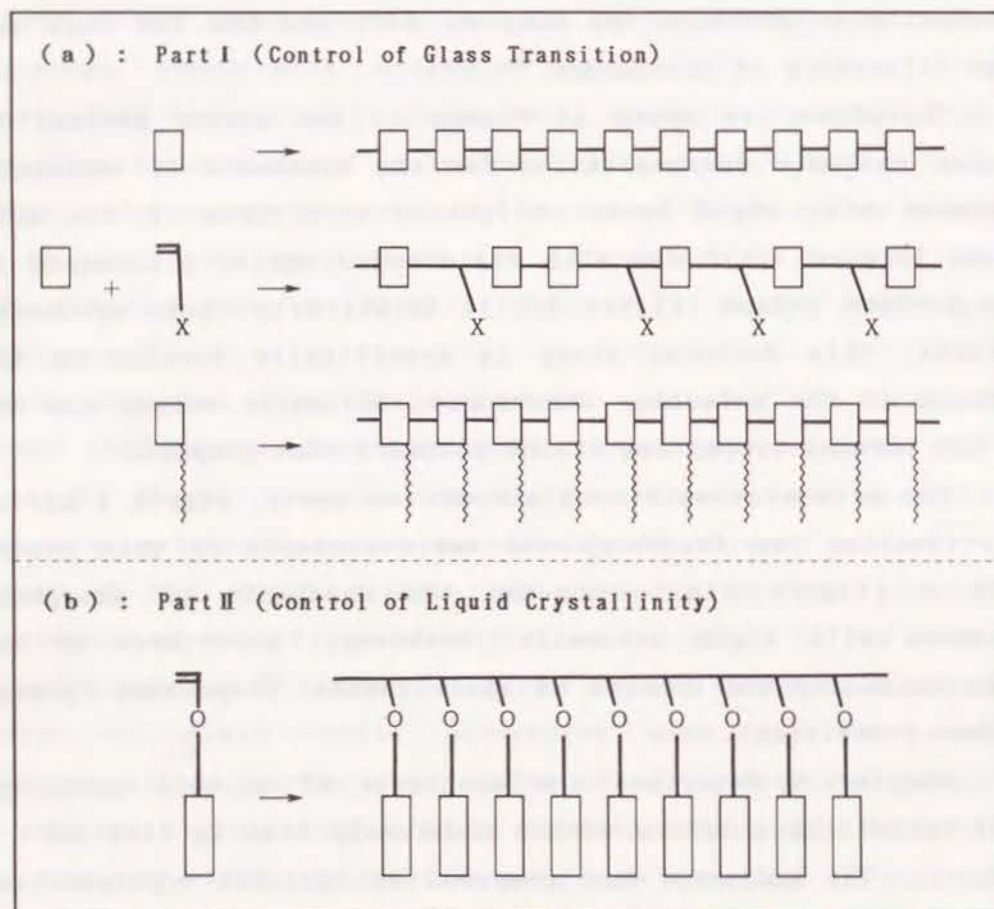(b) : Part II (Control of Liquid Crystallinity)

Figure 1. Framework and basic concepts of this thesis: Introduction of rigid-cyclic structures into either (a) polymer main chains (aliphatic) or (b) side chains (aromatic).

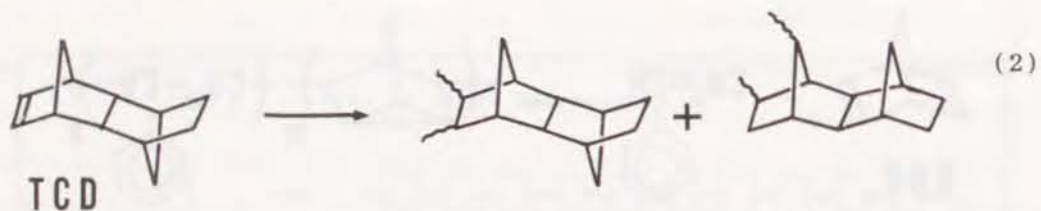▭ or □ : rigid cyclic structure

〰〰 : flexible alkyl chain

from 100 ℃ to 290 ℃, and the soluble copolymer with the highest Tg (ca. 170 ℃) could be prepared at the NBD/St (6/4 mole/mole) feed.
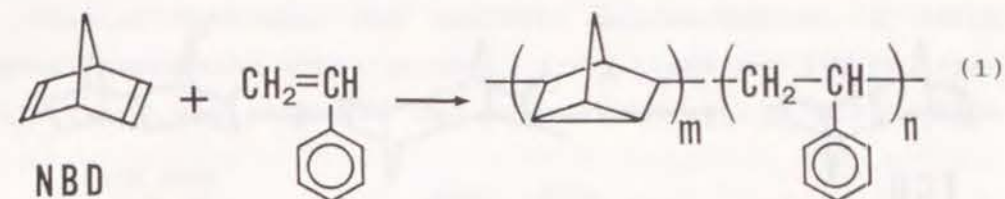

Chapter 2 discusses the effects of reaction conditions on intermolecular reactions which occur in the above mentioned NBD/St copolymerization; that is, a "crosslinking" reaction to form an insoluble polymer, and a "polymer linking" reaction to form a soluble polymer where the intermolecular reaction via two NBD repeat units is not very extensive. On the basis of the effect of the NBD/St molar ratio in the polymerization on polymer solubility, two mechanisms of the crosslinking processes were proposed. The "polymer linking" reaction was, on the other hand, concluded to begin only after the complete consumption of the monomers, where a longer polymerization time, a lower temperature, the initial monomer concentrations $[M]_0$ around 1.0-1.5 M, the $[AlEtCl_2]_0/[\underline{t}\text{-BuCl}]_0$ ratio around 0.75-1.0, and a higher $[AlEtCl_2]_0$ were the factors that facilitate the "polymer linking" to form soluble polymers with high molecular weights.

Chapter 3 deals with the cationic homo- and co-polymerizations of tetracyclo$[4.4.0.1^{2,5}.1^{7,10}]$dodecene-3 (TCD), a tetracyclic monomer bulkier than NBD, where a bicyclic norbornene ring is fused to a norbornane structure (Eq. 2). With the AlEtCl$_2$/t-BuCl catalyst system, soluble oligomers with a molecular weight of 1,000 were obtained in the homopolymerization at +10 ℃ or in the copolymerization with St (higher than 4 mole% in the feed) at -50 ℃. TCD/St copolymers with

controlled Tg (100-260 ℃) could also be prepared by selecting the TCD/St composition, in the same manner as with the NBD/St copolymer (Chapter 1).

$$\text{(2)}$$

TCD

Chapter 4 delineates another method for controlling the thermal properties of alicyclic structure-containing polymers, which is based on the design of norbornenes (R-NB) with flexible alkyl pendant groups (R), rather than the incorporation of a second monomer component (copolymerization) discussed in Chapters 1-3. For a series of R-NB (R = H, CH₃, C₂H₅, C₆H₁₁, C₇H₁₅, C₁₀H₂₁), the alkyl pendant groups R at the 5-position were found to reduce the Tg of polymers by acting as internal diluents. The alkyl substituents also invariably reduced the monomer reactivity and the polymer molecular weight, although their length did not affect them. In contrast, the Tg of the polymers were indeed controlled by the length of alkyl chain; this effect was discussed on the basis of the mobility of the carbons in the substituents.

R-NB
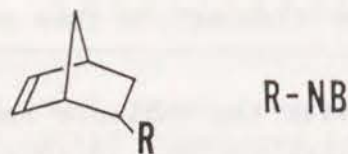
Part II of this thesis [see Figure 1(b)] is devoted to the (living) cationic polymerizations of seven vinyl ethers that contain rigid aromatic pendant groups, such as biphenyl and naphthyl. This part specifically discusses the relationship between the structure of the rigid aromatic groups and the liquid crystallinity, of the resulting poly(vinyl ether)s. One of the features of this part is the synthesis of new side-chain liquid crystalline polymers with controlled molecular weights and MWDs by living cationic polymerization.

Chapter 5 treats the cationic polymerization of three biphenyl-containing vinyl ethers (1 - 3) and the liquid crystallinity of the polymers. The polymers of 1 - 3 with narrow

1

2

3
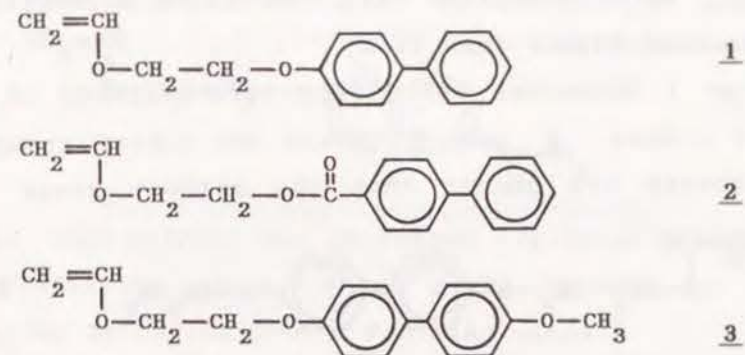
MWDs were prepared by the living polymerization with the hydrogen iodide/iodine (HI/I₂) initiating system,[8] whereas those with broader MWDs by the non-living process with boron trifluoride etherate (BF₃OEt₂). Poly 1 and poly 2 with narrow MWDs formed only isotropic melts, but poly 3 with a narrow MWD showed enantiotropic, liquid-crystalline behavior, and formed both smectic and nematic phases after one heating and cooling cycle. Based on the narrow MWDs of these polymers, this chapter also discusses the effects of polymer molecular weight on liquid crystallinity, free from undue influence of low and high MW components, perhaps for the first time in this field.[10]

Chapter 6 concerns a poly(vinyl ether) with a biphenyl mesogen having an electron-withdrawing cyano group, which was obtained by the living cationic polymerization of vinyl ether 4 with the HI/I₂ or HI/ZnI₂ initiating system. Poly 4 with $\overline{M}n$

4
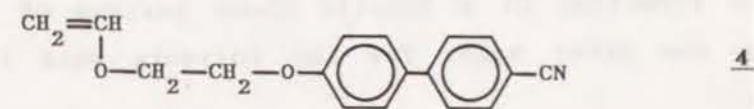
below 2,600 and a narrow MWD ($\overline{M}w/\overline{M}n$=1.02-1.1) showed an enantiotropic liquid-crystalline behavior (a smectic phase after one heating cycle), whereas samples with $\overline{M}n$ above 2,600 and a similar MWD ($\overline{M}w/\overline{M}n$= 1.2-1.3) formed isotropic melts only. These phenomena were interpreted in terms of the difference between Tg and Ti-s (the transition temperature from isotropic to smectic), which decreases with increasing molecular weights until Tg becomes higher than Ti-s.

Chapter 7 discusses the liquid crystallinity of polymers from vinyl ethers, **5** and **6**, where the alkoxy groups in the biphenyl moiety are longer than the methoxy group in their

5

6
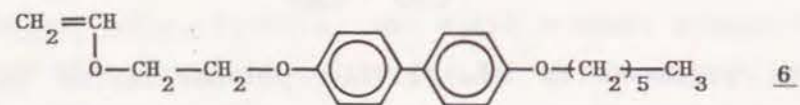
analog **3** discussed in Chapter 5. The HI/I₂ or HI/ZnI₂ system yielded polymers with narrow MWDs from both monomers. Although these polymers were invariably liquid crystalline independent of their molecular weights, the phase patterns depended on the polymer structures and molecular weights: with poly **5**, smectic and nematic after one heating cycle for $\overline{M}w$ < 8,000 and nematic alone for $\overline{M}w$ > 8,000; with poly **6**, nematic alone for $\overline{M}w$=2,600-7,300.

To summarize Chapters 5-7, this chapter also discusses the effect of the substituent in the biphenyl group on the basis of its possible steric and polarity effects. Namely, the cyano substituent in **4** (Chapter 6) is not only small but also highly polar, and the enhanced interaction between mesogens may facilitate formation of a smectic phase instead of a nematic phase. On the other hand, for the polymers with less polar

alkoxy terminal groups (**3** in Chapter 5; **5** and **6** in Chapter 7), there may be an optimum size of the alkoxy group to form a smectic phase.
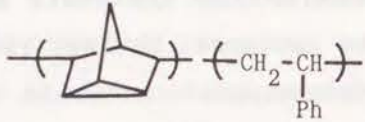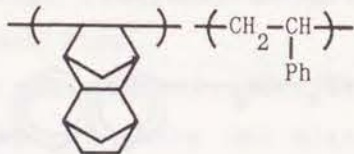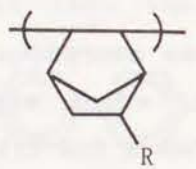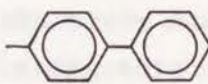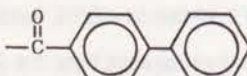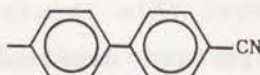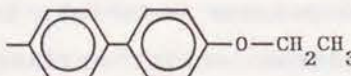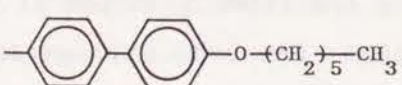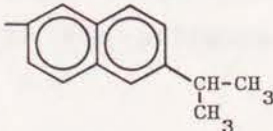
Chapter 8 concerns the synthesis and thermal properties of a novel comb-like polymer having isopropylnaphthoxy pendant groups by the conventional cationic polymerization of vinyl ether **7** with AlEtCl₂ catalyst. In contrast to the polymers

7
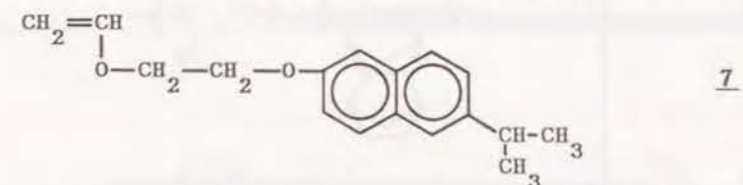
of **3** ~ **6**, this polymer was amorphous (Tg=22-45 ℃) without any liquid crystalline phase, which might be due to the bulky pendant group deviating from a rod-like shape.

In conclusion, the relation of the structure and thermal properties (glass-transition behavior and liquid crystallinity) of the polymers described in this thesis is illustrated in Table 1 (pages 10-11). This study has shown it possible to synthesize polymers with rigid cyclic structures, either in the main chain or in the side chain, by cationic polymerization. Furthermore, this research has provided strategies for controlling thermal properties (glass-transition behavior and liquid crystallinity) of these polymers, as shown in the wide range of Tg and other phase transition temperatures in Table 1. The author wishes that this thesis would contribute not only to the molecular design and development of high-performance and functionalized polymer materials in cationic polymerization but also to the macromolecular engineering in other polymerization reactions.

Table 1. Thermal properties of cationically obtained polymers described in this thesis.

Chapter	Polymer Structure		TEMPERATURE (°C)

Part I : alicyclic structure in the main chain

Chapter	Polymer Structure	No.	Thermal behavior
1 and 2	alicyclic polymer with norbornane and $-(CH_2-CH(Ph))-$ units		Tg (ca. 100–280 °C)
3	alicyclic polymer and $-(CH_2-CH(Ph))-$ units		Tg (ca. 90–280 °C)
4	alicyclic polymer, R = H		Tg (ca. 75–230 °C)
	R = CH₃		Tg (ca. 50–175 °C)
	R = C₂H₅		Tg (ca. 30–130 °C)
	R = C₅H₁₁ – C₁₀H₂₁		Tg (ca. –50 °C)

Part II : aromatic structure in the side chain

$-(CH_2-CH(O-CH_2-CH_2-O-R))-$

Chapter	R =	No.	Thermal behavior
5	biphenyl	1	Tg (ca. 65 °C)
5	$-OC-$ phenyl–phenyl (benzoate biphenyl)	2	Tg (ca. 90 °C)
5	biphenyl $-O-CH_3$	3	Tg (ca. 130 °C)
			Ts-n / Tn-i
6	biphenyl $-CN$	4	Tg (ca. 115 °C), Ts-i
7	biphenyl $-O-CH_2CH_3$	5	Tg (ca. 150–200 °C)
			Ts-n / Tn-i
7	biphenyl $-O-(CH_2)_5-CH_3$	6	Tg (ca. 110 °C), Tn-i
8	naphthyl $-CH-CH_3$ with CH_3	7	Tg (ca. 55 °C)

Tg   : Glass-Transition Temp.
Ts-n : Smectic to Nematic Transition Temp.
Ts-i : Smectic to Isotropic Transition Temp.
Tn-i : Nematic to Isotropic Transition Temp.

REFERENCES AND NOTES

1) E.V. Thompson, "Encyclopedia of Polymer Science and Engineering", H.F. Mark, N.M. Bikals, C.G. Overberger, G. Menges, and J.I. Kroschwitz, Eds., 2nd Edn., Vol.16, John Wiley & Sons, New York, 1989, p. 711.

2) J.W.S. Hearle, "Polymers and Their Properties", Vol. 1, "Fundamentals of Structures and Mechanics", Halsted Press, New York, 1982, Chap. 7.

3) L.H. Sperling, "Introduction to Physical Polymer Science", Wiley-Interscience, New York, 1985, Chap. 6.

4) For a review, H.-G. Elias and F. Vohwinkel, "New Commercial Polymers 2", Gordon and Breach Science, New York, 1986.

5) For reviews, (a) A. Ciferri W.R. Krigbaum, and R.B. Meyer, Eds., "Polymer Liquid Crystals", Academic Press, New York, 1982. (b) A.C. Griffin and J.F. Johnson, Eds., "Liquid Crystals and Ordered Fluid", Vol. 4, Plenum, New York, 1984. (c) L.L. Chapoy, Ed., "Recent Advances in Liquid Crystalline Polymers", Elsevier, New York, 1985.

6) For reviews, (a) J.P. Kennedy, "Cationic Polymerization of Olefins: A Critical Inventory", John Wiley & Sons, New York, 1975. (b) P.H. Plesch, Ed., "The Chemistry of Cationic Polymerization", Pergamon Press, Oxford, 1963.
(C) T. Higashimura, "Cationic Polymerization", Kagakudojin, Kyoto, 1971. (d) G.C. Eastmond, A. Ledwith, S. Russo, and P. Sigwalt, Eds., "Comprehensive Polymer Science", Vol. 3, Pergamon Press, Oxford, 1989, Chaps. 39-44.

7) For a review, T. Higashimura and M. Sawamoto, Adv. Polym. Sci., 62, 49 (1984).

8) For reviews, (a) M. Sawamoto and T. Higashimura, "Encyclopedia of Polymer Science and Engineering", 2nd Edn (Suppl.), John Wiley & Sons, New York, 1989, p.399. (b) T. Higashimura and M. Sawamoto, Koubunshi Ronbunshu (Jap. J. Polym. Sci. Technol.), 46, 189 (1986).

9) J.P. Kennedy and E. Maréchal, "Carbocationic Polymerization", John Wiley & Sons, New York, 1982.

10) One example of such control was the preparation of polymethacrylates by group-transfer polymerization [W. Kreuder and O.W. Webster, Makromol. Chem., Rapid Commun., 7, 5 (1986)], but the MWD's of these polymers were still quite broad ($\overline{M}w/\overline{M}n=1.2-1.8$).

PART I

SYNTHESIS OF AMORPHOUS POLYMERS WITH RIGID ALICYCLIC MAIN-CHAIN STRUCTURES: CONTROL OF GLASS-TRANSITION TEMPERATURE

CHAPTER 1

CATIONIC COPOLYMERIZATION OF NORBORNADIENE WITH STYRENE BY AlEtCl$_2$/tert-BUTYL CHLORIDE CATALYST SYSTEM: EFFECTS OF NORBORNADIENE/STYRENE FEED RATIO

ABSTRACT

The cationic copolymerizations of norbornadiene (NBD) and styrene (St) were carried out with the AlEtCl$_2$/tert-butyl chloride catalyst system in CH$_2$Cl$_2$ at -50 ℃, and the effect of NBD/St molar ratio in the polymerization on the solubility, the glass-transition temperature (Tg) and the molecular weight of the copolymer was investigated. A soluble copolymer was prepared with 40 mole% or more St fed, although the NBD homopolymer comprised an insoluble fraction which might have been formed by a crosslinking reaction between the double bonds in the NBD units of the polymer. The sequential distribution of the two monomer units in the copolymer was statistically random not only in a polymer chain but also over the whole molecular weight range (from 10^3 to 10^6). The Tg of the amorphous copolymer was controlled by the NBD/St composition in the range from 100 ℃ to 290 ℃. The soluble copolymer with the highest Tg (ca.170 ℃) could be prepared with the NBD/St molar ratio of 60/40 in the polymerization.
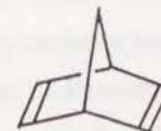
NBD

INTRODUCTION

Amorphous polymers with high-glass transition temperature (Tg) and crystalline polymers with high melting temperature (Tm) are thought to be promising candidates for heat-resistant materials of engineering plastics, and are of interest both in the theoretical field and for practical use. The Tg of the polymer from 2,5-norbornadiene (NBD, bicyclo[2.2.1]hepta-2,5-diene) synthesized cationically (320 ℃) is presumably the highest known for linear hydrocarbon polymers synthesized by addition-type polymerization.[1, 2, 3] This polymer is a typical example of a high-Tg amorphous polymer achieved by incorporating a bulky-rigid alicyclic structure into a polymer main chain.

For the cationic polymerization of NBD, Kennedy[1] proposed the following cationic reaction mechanism with a transannular rearrangement to form a nortricyclene structure, I. In their
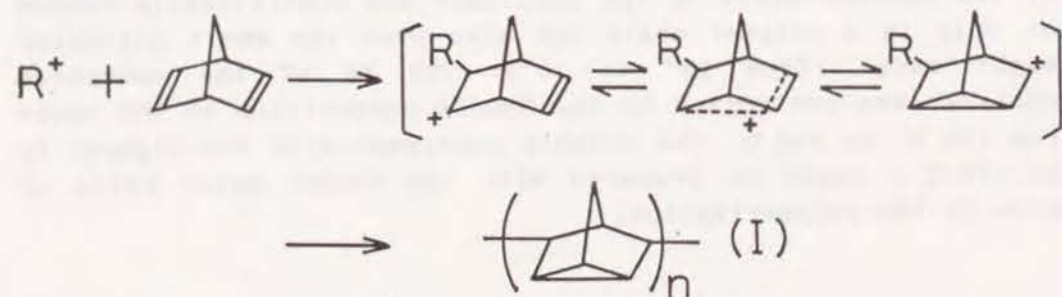
investigation, the cationic polymerization (AlCl$_3$ catalyst, in ethyl chloride and/or methylene dichloride solvent) of NBD was carried out in a temperature range from +40 to -123 ℃. They have concluded that only the polymer obtained at a very low temperature of -123 ℃ was completely soluble and mainly consisted of structure I. On the other hand, crosslinking reaction took place at higher temperatures by the consecutive "2,3-type" addition reaction to form insoluble polymers with structural units Ⅲ via polymers containing unsaturation units of structure Ⅱ.
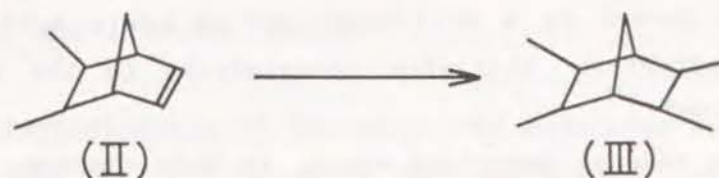
The author and coworkers have recently studied the structure of cationically obtained poly(NBD) by high-resolution ^{13}C-NMR technique and revealed that the repeating monomer units were only the structures of I-a and I-b and that the structure I-c did not exist. Furthermore, the author has proposed a stereoregular homopolymerization mechanism of NBD.[4]
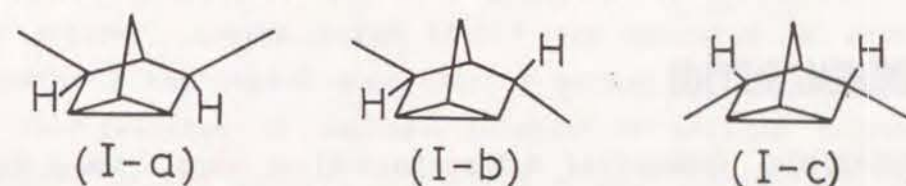
From the industrial point of view, Kennedy's process has two drawbacks, that is, (i) the polymerization temperature has to be very low (-123 ℃) in order to obtain soluble poly(NBD), (ii) the NBD homopolymer so formed is difficult to handle as a thermoplastic material, because its Tg (320 ℃) is high and very close to the polymer decomposition temperature. The aim of this chapter, therefore, was to obtain a soluble NBD copolymer with a moderately high Tg (100-200 ℃) by cationic polymerization at a relatively high polymerization temperature of -50 ℃. More specifically, styrene, which gives a typical amorphous polymer (Tg ~ 100 ℃) and is one of cheap monomers, was selected as a comonomer. In these conditions the probability of forming the insoluble structure Ⅲ via structure Ⅱ might decrease, while the Tg of polymer might be lowered to a moderate region. AlEtCl$_2$/tert-butyl chloride was selected as the catalyst/cocatalyst system, which was expected to lead to a high polymer

yield within an acceptable polymerization time of 1 h for practical use. The selection of initiator system was made also because the former is a well-known strong Lewis acid and the latter an effective initiator (cocatalyst) in the isobutene polymerization[5].

For the reasons described above, in this chapter, the cationic copolymerizations of NBD with styrene (St) were carried out by the AlEtCl$_2$/tert-butyl chloride catalyst system in CH$_2$Cl$_2$ at -50 ℃, and the effect of NBD/St molar ratio in feed on the polymer solubility, molecular weight, and Tg was investigated.

EXPERIMENTAL SECTION

Materials. Commercial 2,5-norbornadiene (NBD, Tokyo Kasei Kogyo Co.) and styrene (St, Wako Pure Chemical Ind.) were freshly distilled over calcium hydride under atmospheric or reduced pressure, respectively. AlEtCl$_2$ was commercially obtained as an n-hexane solution (Tosoh Akzo Corp.) and used without further purification. CH$_2$Cl$_2$ and tert-butyl chloride (t-BuCl, Wako Pure Chemical Ind.) were purified by the usual method and distilled over calcium hydride before use.

Polymerization Procedures. Copolymerization was carried out under a dry nitrogen atmosphere in a baked glass reactor equipped with a stirrer and a condenser. The reaction was initiated by addition of an AlEtCl$_2$ solution into a monomer solution, and terminated with ammoniacal methanol. The cocatalyst (or initiator), t-BuCl, was added to a monomer solution before the addition of AlEtCl$_2$. The quenched polymerization mixture was sequentially washed with a dilute aqueous acid and water to remove catalyst residues. The product was recovered as a white powder from the organic layer by precipitation with methanol, and dried in vacuum.

Characterization of Polymers. The molecular weight distribution (MWD) of the polymers was measured by gel-permeation chromatography (GPC) in o-dichlorobenzene solutions at 140 ℃ on a Waters liquid chromatograph (150-C ALC/GPC) equipped with a column containing polystyrene gel (TSKgel GMH-HT, 7.5mmID × 60cm) and a refractive index (RI) detector. The $\overline{M}$n and $\overline{M}$w were calculated from GPC curves on the basis of a calibration with the polystyrene standard. For the content of unsaturation in the polymer, iodine value (I.V.) was measured as previously reported (the iodine monochloride method).[6] The percentage of the fraction of polymer soluble in boiling toluene was obtained by the Soxhlet extraction method (extraction time = 5 h). ^{1}H-NMR spectra were obtained on JOEL FX-100 spectrometer operating at 99.5MHz in CDCl$_3$ at room temperature. The molecular weight dependency of the styrene-unit content of the copolymer was determined by GPC-FT-IR (GPC: Waters 150-CALC/GPC, hexachlorobutadiene solution; FT-IR: Perkin-Elmer FT-IR Spectrometer 1760X), using the absorption at 3028 cm^{-1} due to phenyl group as a key absorption for the styrene-unit content and the total absorption from 2800 to 3000 cm^{-1} for molecular weight distribution. The content of styrene unit was calculated from 3028cm^{-1}/2935cm^{-1} intensity ratio by using a calibration which was obtained beforehand with a series of NBD/St copolymers with known styrene contents. The Tg of the polymers was measured by differential scanning calorimetry (DSC) on a Seiko DSC-20 differential scanning calorimeter with polymer samples of about 10 mg under a nitrogen flow at a scanning rate of 10 ℃ per min.

RESULTS AND DISCUSSION

1. Effect of NBD/St feed ratio

Cationic copolymerizations of NBD and St with various NBD/St molar ratios were carried out using the AlEtCl$_2$/t-BuCl catalyst system. All data are listed in Table 1. Figure 1 shows the dependency of the polymer yield and the amount of polymer fraction soluble in boiling toluene on the NBD/St molar ratio. As the St content in the feed was in a range from 10 to 30 mole%, the polymer yield attained a maximum of ca. 95 wt% on
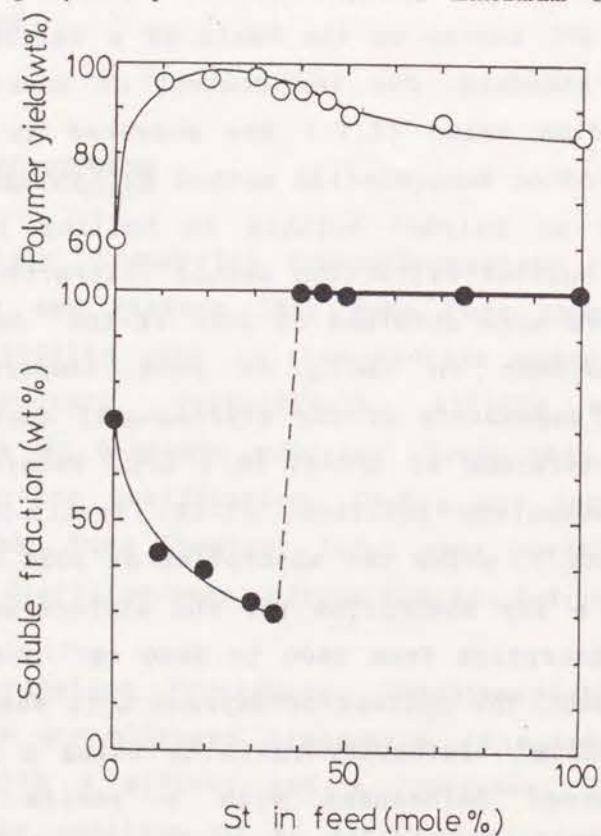
Figure 1. Dependency of polymer yield and boiling toluene-soluble fraction on the molar ratio of monomers in the copolymerization of NBD with St at -50 ℃ in CH$_2$Cl$_2$ for 1 h; [NBD]$_0$+[St]$_0$ = 1.0 M, [AlEtCl$_2$]$_0$ = 10.0 mM, [t-BuCl]$_0$ = 5.0 mM.

Table 1.
Copolymerization of NBD with St by AlEtCl$_2$/t-BuCl catalyst system.[a]

Run No.	[NBD]$_0$/[St]$_0$ (mole%)	Polymer Yeild (wt%)	Soluble Fraction (wt%)	$\overline{M}_n$ [b]	$\overline{M}_w/\overline{M}_n$ [b]	I.V. [b] (g-I$_2$/ 100g-poly.)	St-unit Content [b] (mole%)	Tg (℃) Whole Polymer	Tg (℃) Soluble Fraction
1	0/100	85.5	100	16,900	5.6	~0	100	101	98
2	25/75	88.5	100	11,400	10.0	7.7	69.5	122	123
3	50/50	89.8	99	10,200	10.6	14.8	46.3	158	151
4	55/45	92.1	100	8,900	21.1	16.8	43.1	171	166
5	60/40	93.9	100	7,100	73.0	20.0	38.7	175	171
6	65/35	94.3	29	(4,700)	(9.3)	(21.5)	(33.0)	188	178
7	70/30	97.0	32	(4,600)	(14.4)	(24.4)	(28.9)	198	188
8	80/20	96.5	36	(4,200)	(13.0)	(30.7)	(19.3)	230	220
9	90/10	96.5	43	(4,800)	(10.0)	(30.1)	(11.7)	262	252
10	100/0	60.9	72	(4,800)	(7.6)	(31.0)	(0)	274	292

a) Polymerization conditions: [NBD]$_0$ + [St]$_0$ = 1.0 M, [AlEtCl$_2$]$_0$/[t-BuCl]$_0$ = 10.0/5.0 mM, in CH$_2$Cl$_2$, at -50℃, for 60 min.

b) Numbers in parentheses are taken by the soluble fractions.

the basis of total monomers. A further increase in St content in feed led to a slight decrease in the polymer yield, and eventually a pure St feed gave a yield of ca. 85 wt%. These results show that the polymer yield (at a polymerization time of 1 h) in the copolymerization is larger than that of the homopolymerization of either NBD or St. The boiling toluene soluble fraction of the polymer decreased with increasing St content in the feed up to 35 mole%, and then, above 40 mole% St in the feed, completely soluble polymers were formed (Figure 1). This behavior will be discussed in the next chapter.[7]

The $\bar{M}n$ and $\bar{M}w$ of the soluble copolymers, obtained at the St molar ratio above 40 mole%, are shown in Table 1. The molecular weight distribution of the copolymers are also shown in Figure 2. On decreasing the St (increasing NBD) content in

NBD/St (mol%)

0 / 100

25 / 75

50 / 50

55 / 45

60 / 40

LOG(MW) (PSt)
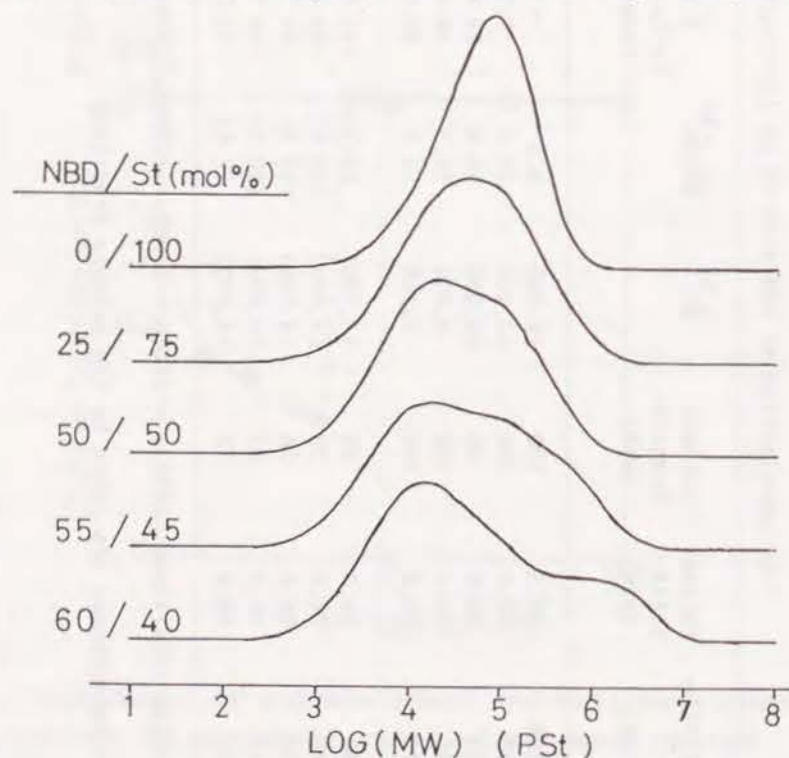
Figure 2. Effect of NBD/St feed ratio on the MWD of the polymers. For reaction conditions: see Table 1.

the feed, $\bar{M}n$ decreased, while $\bar{M}w$ increased and MWD became broader. The decrease of $\bar{M}n$ can be explained by an increase of the number of NBD cations, which tend to undergo a transfer reaction (see below). The increase of $\bar{M}w$ is interpreted by the frequent occurrence of "polymer linking" by the intermolecular reaction via two carbon-carbon double bonds in NBD repeat units (structure II). As shown by the MWD curves in Figure 2, broadening of a shoulder at high MW region, which could ascribed to species formed by the "polymer linking" reaction, is also observed with increasing NBD/St molar ratio.

In order to obtain quantitative values of the double bonds in the polymer chains, which may be the reaction sites both of the "crosslinking" reaction (defined as an interpolymer reaction to form an insoluble polymer) and the "polymer linking" reaction (defined as an interpolymer reaction to form a soluble polymer), the iodine values (I.V.) of the polymers were measured. In the case of the insoluble polymers, I.V. was determined on the boiling toluene-soluble fraction. As shown in Table 1, I.V. increased from 0 to 31 with decreasing St molar ratio (or with increasing NBD molar ratio) in the polymerization. The relationship between the content of double bond and the solubility of polymer (which may depend on the degree of crosslinking of the polymer) will be discussed in the next chapter[7].

With reference to a transfer reaction, the system behaved in the normal way of cationic copolymerization, that is, the molecular weight of the cationically formed copolymers is generally smaller than that of the homopolymer of each monomer.[8, 9] As shown in Table 1, the $\bar{M}n$ of the copolymer was smaller than that of St homopolymer. The transfer reaction shown in eq.(1), which involves an elimination of a proton from the propagating chain end ~ St-NBD$^+$, might be the reason of the

molecular weight decrease.

$$\sim C - C^+ + N\,B\,D \quad \rightarrow \quad \sim C - C$$
$$\underset{P\,h}{\mid} \qquad\qquad \underset{P\,h\ +}{\mid}$$

$$\rightarrow \quad \sim C - C \qquad\qquad + \ H^+ \quad (1)$$
$$\underset{P\,h}{\mid}$$
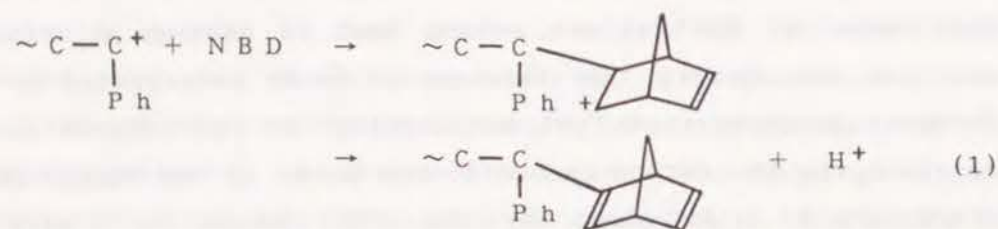
Figure 3 shows the relationship between the copolymer composition and the monomer composition in the NBD/St copolymerization. The curve shown in Figure 3 indicates that the copolymer composition is almost the same as the monomer composition. This result does not represent an azeotropic copolymerization, but is due to higher conversion of monomers than 80 wt%.
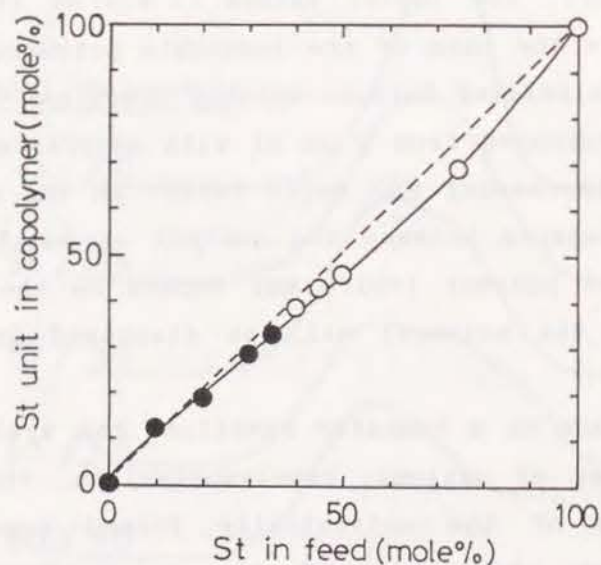
Figure 3. Copolymer composition as a function of St feed; ○ : whole polymer, ● : soluble fraction. For reaction conditions: see Table 1.

2. Proof of random-copolymer formation

In order to investigate the sequential distribution of St units and the relation of the molecular weight of copolymer with the content of St units in the NBD/St copolymers, ^{1}H-NMR analysis of the St unit (phenyl protons) and GPC-FTIR analysis of the copolymer were carried out. Figure 4 shows the aromatic proton resonance of the copolymer. The following NMR analysis is based on the fact that the aromatic proton resonance of polystyrene consists of two well-resolved peaks with an intensity ratio of 3:2 [=(meta+para):ortho], as described elsewhere.[10] As shown in Figure 4, with decreasing St content in the polymerization, the peak intensity of the ortho-protons (H^a, δ = ca. 6.5ppm) decreased, and then, at a NBD/St molar ratio of 50/50 to 90/10, this peak shifted towards and ultimately overlapped with the signal due to meta- or para-protons appearing at lower magnetic field (H^b, δ = ca.7.1 ppm). These data indicate that the homosequences of more than two continuing St units are rare throughout the chain of copolymers obtained in the copolymerization containing more than 50 mole% of NBD. The results of GPC-FTIR analysis are showing in Figure 5, indicating almost the same content of St units (or NBD units) over a wide range of molecular weight (from 10^3 to 10^6).

As shown in Figure 6, Tg's of the copolymers are in the range from ca. 100 to 290 °C and exhibit a strong dependency on the ratio of rigid NBD units to comparatively flexible St units. This result demonstrates the additivity of the copolymer composition on Tg. In other words, it suggests a random distribution of the two types of monomeric units in the polymer chain. Considering also the data in Figure 1, a soluble NBD/St copolymer with the highest Tg (Tg=170 °C) can be prepared at a NBD/St molar ratio of 60/40 mole%.
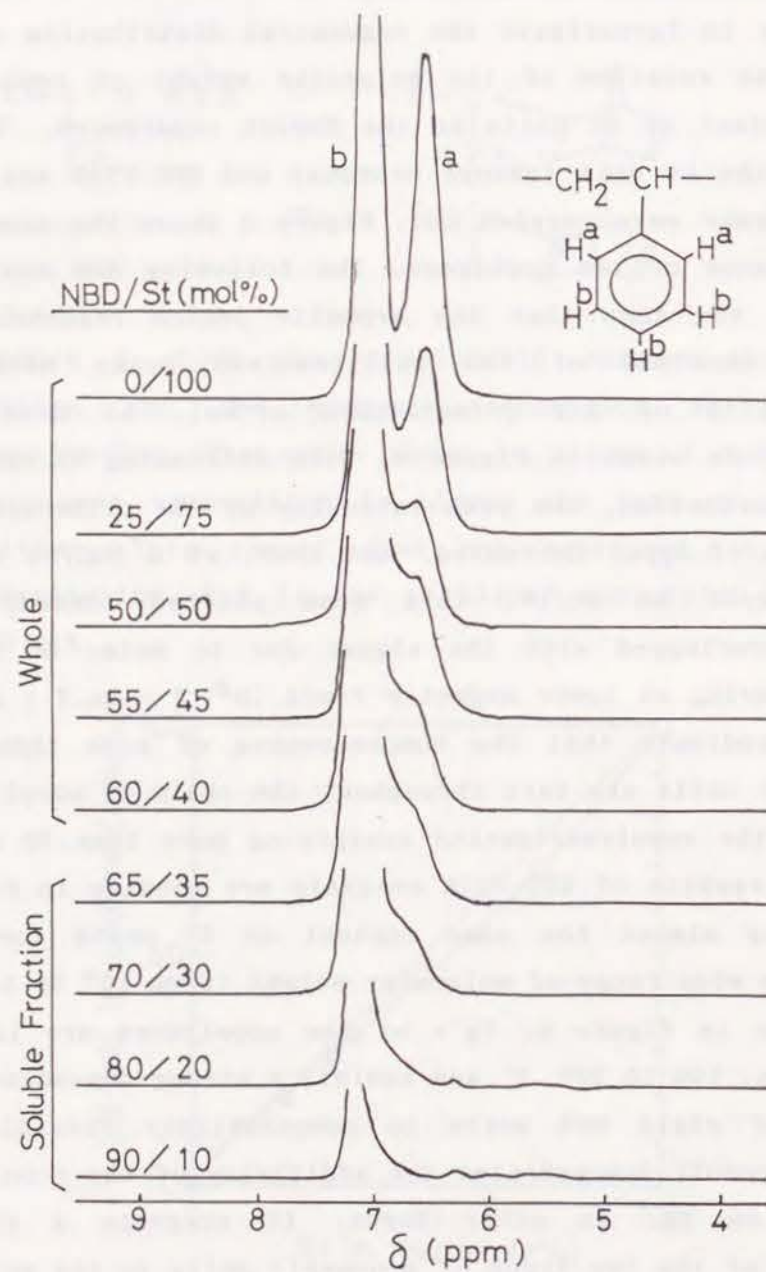
Figure 4. Aromatic protons region in ¹H-NMR spectra of NBD/St copolymers. For reaction conditions: see Table 1.
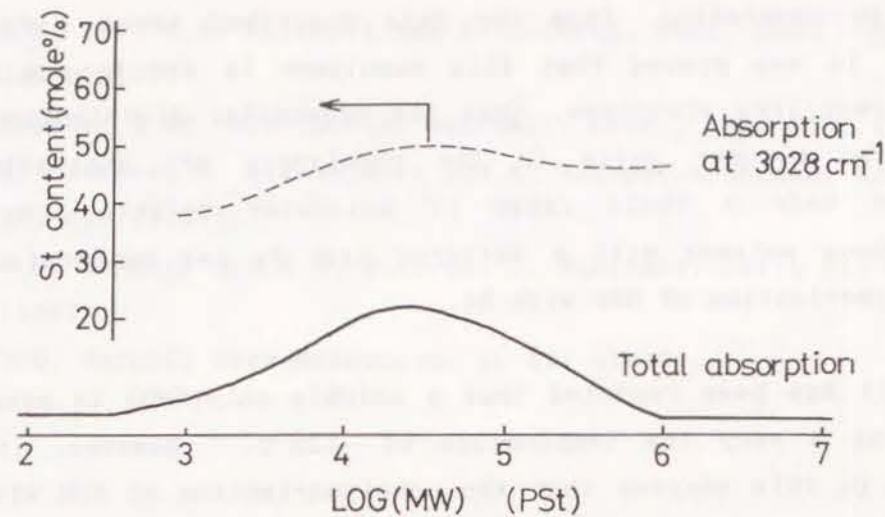
Figure 5. Distributions of MW and St-unit content of the NBD/St copolymers ([NBD]$_o$=[St]$_o$=0.5M, for other reaction conditions: see Table 1): dashed line, St-unit content calculated from the absorption at 3028 cm⁻¹; solid line, MWD calculated from the total absorption from 2800 to 3000 cm⁻¹ (see Experimental part).
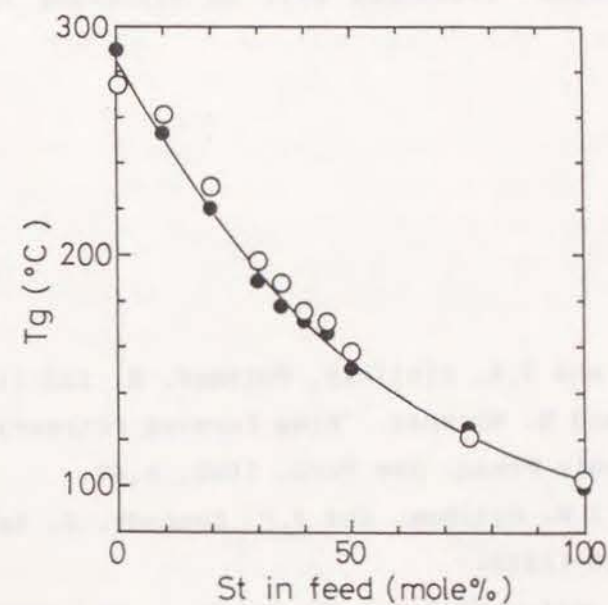
Figure 6. Tg of the copolymer as a function of St feed; ○ : whole polymer, ● : soluble fraction.

In conclusion, from the data described above (Figures 4-6), it was proved that this copolymer is far from a block copolymer-like structure, that the sequential distributions of the two monomer units in the copolymers are statistically random over a whole range of molecular weight. Thus, an amorphous polymer with a tailored high Tg was synthesized by copolymerization of NBD with St.

It has been reported that a soluble poly(NBD) is obtained only at a very low temperature of -123 ℃.[1] However, it was found in this chapter that the copolymerization of NBD with St with St content higher than 40 mole% gave a soluble copolymer of a reasonably high Tg at a relatively high temperature of -50 ℃. The effects of polymerization conditions, such as the NBD/St molar ratio, monomer or catalyst concentrations and temperature, on the polymer solubility and the "crosslinking" and "polymer linking" reactions will be discussed in the next chapter.[7]

REFERENCES

1) J.P. Kennedy and J.A. Hinlicky, Polymer, 6, 133 (1965).

2) R.J. Cotter and M. Matzner, "Ring Forming Polymerization", Part A, Academic Press, New York, 1969, p.47.

3) M.B. Roller, J.K. Gillham, and J.P. Kennedy, J. Appl. Polym. Sci., 17, 2223 (1973).

4) A. Mizuno, M. Onda and T.Sagane, Polymer, 32, 2953 (1991).

5) J.P. Kennedy, International Symp. on Macromol., Tokyo-Kyoto, I-47 (1966).

6) T.S. Lee, I.M. Kolthoff and E. Johnson, Anal. Chem., 22, 995 (1950).

7) Chapter 2 of this thesis; Makromol. Chem., 193, 2091 (1992).

8) S. Okamura, T. Higashimura and K. Takeda, Koubunshi Kagaku, 18, 389 (1961).

9) J.P. Kennedy and R.G. Squires, J. Makromol. Sci., A1, 861 (1967).

10) V.D. Mochel, Macromolecules, 2, 537 (1969).

CHAPTER 2

CATIONIC COPOLYMERIZATION OF NORBORNADIENE WITH STYRENE BY AlEtCl₂/tert-BUTYL CHLORIDE CATALYST SYSTEM: EFFECTS OF POLYMERIZATION CONDITIONS ON "CROSSLINKING" AND "POLYMER LINKING" REACTIONS

ABSTRACT

The cationic copolymerizations of norbornadiene (NBD) and styrene (St) was carried out with the $AlEtCl_2$/t-butyl chloride catalyst system under various conditions. Detailed analyses were focused on the effect of reaction conditions on the two types of intermolecular reactions, that is, the "crosslinking" reaction to form an insoluble polymer and the "polymer linking" reaction to form a soluble polymer with a molecular weight higher than that of the non-crosslinked polymer. The two types of crosslinking processes can explain the unique dependency of the polymer solubility on the the NBD/St molar ratio in the polymerization. The "polymer linking" reaction is initiated after complete consumption of the monomers and is strongly affected by the polymerization conditions. For example, longer polymerization time, lower temperature, an initial monomer concentration $[M]_o$ around $1.0 \sim 1.5$ M, a $[t\text{-BuCl}]_o/[AlEtCl_2]_o$ ratio around $0.75 \sim 1.0$, and increasing $[AlEtCl_2]_o$ are the factors that facilitate the "polymer linking".
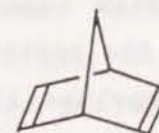
NBD

INTRODUCTION

Besides good heat resistance, relatively high-Tg amorphous polymers generally exhibit excellent physical properties (such as good transparency and low mold-shrinkage) compared with crystalline polymers and thus have a variety of applications. Poly(p-phenylene oxide), polycarbonates and poly(methyl methacrylate) are examples which belong to the category, showing glass-transition temperatures (Tg) of 209 ℃, 145 ℃ and 105 ℃, respectively.[1] Despite those excellent properties, one of their weak points is the high water absorption originating from the ether, ester, and other heteroatom-containing groups in the polymer main chains. The water absorption values (wt%, ASTM D-570)[2] of these polymers are around 0.06, 0.15 ～ 0.18, and 0.3 ～ 0.4, respectively, which are higher than those of polyethylene and polystyrene (below 0.01 and 0.03, respectively). From this view point, hydrocarbon type polymers without heteroatoms may be suitable, high-stable materials at high temperature, humidity, etc.

An example of a hydrocarbon type amorphous polymer with high Tg is the cationically prepared polymer from 2,5-norbornadiene (NBD, bicyclo[2.2.1]hepta-2,5-diene), whose Tg was determined to be 320 ℃.[3, 4, 5] Kennedy et al.[3, 4] and the author et al.[6] have independently reported that the soluble poly(NBD) is mainly composed of the nortricyclene structure I. On the other hand, poly(NBD) comprises also an insoluble part, and its structure is thought to comprise structure III formed by crosslinking reactions between the double bonds in the structure II [see eq.(1)].

(1)

NBD　　　　**I**　　　　**II**　　　　**III**
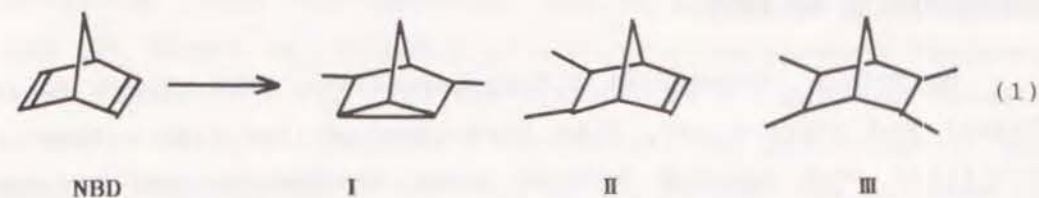
In the preceding chapter,[7] the author described that the copolymerization of NBD with 40 mole% or more of styrene (St) gave a soluble copolymer with reasonably high Tg (ca. 170 ℃ with NBD/St molar ratio of 60/40 in the polymerization), at a relatively high polymerization temperature of -50 ℃.

In the present chapter, cationic copolymerizations of NBD with St were carried out with the AlEtCl₂/tert-butyl chloride catalyst system, and the effect of polymerization conditions on "crosslinking" and "polymer linking" reactions was investigated. Here the term "crosslinking" reaction was defined as the reaction leading to insoluble polymer, whereas the "polymer linking" reaction is thought to form soluble polymers of higher molecular weight by non-extensive intermolecular reaction between two NBD repeating units (structure II).

In the first part of this chapter, the effect of NBD/St molar ratio in the polymerization on the "crosslinking" reaction is discussed, in relation to the unique dependency of polymer solubility on feed composition described in the preceding chapter.[7] In the second part, the effect of polymerization conditions, such as reaction time and monomer and catalyst concentrations, on the "polymer linking" reaction at a NBD/St molar ratio in the polymerization of 60/40 mole% was investigated in order to find factors to control the molecular weight of the polymers.

EXPERIMENTAL SECTION

Materials. Commercial 2,5-norbornadiene (NBD, Tokyo Kasei Kogyo) and styrene (St, Wako Pure Chemical Ind.) were freshly distilled over calcium hydride under atmospheric and reduced pressure, respectively. AlEtCl₂ was commercially obtained as an n-hexane solution (Tosoh Akzo) and used without further purification. CH_2Cl_2, cyclohexane and tert-butyl chloride (t-BuCl, Wako Pure Chemical Ind.) were purified by the usual method and distilled over calcium hydride before use.

Polymerization Procedures. Copolymerization was carried out under a dry nitrogen atmosphere in a baked glass reactor equipped with a stirrer and a condenser. The reaction was initiated by addition of an AlEtCl₂ solution into a monomer solution, and terminated with ammoniacal methanol. The cocatalyst (or initiator), t-BuCl, was added to a monomer solution before the addition of AlEtCl₂. Monomer conversion was determined by measuring the residual monomer concentration by gas chromatography with n-dodecane as the internal standard. The quenched polymerization mixture was sequentially washed with a dilute aqueous acid and water to remove catalyst residues. The product was recovered by precipitation of the organic layer into methanol and was dried in vacuum. Polymer yield was calculated from the recovered polymer weight on the basis of the fed monomer's weight.

Characterization of Polymers. The molecular weight distribution (MWD) of the polymers was measured by GPC on samples in o-dichlorobenzene solutions at 140 ℃ on a Waters liquid chromatograph (150-C ALC/GPC) equipped with a polystyrene gel column (TSKgel GMH-HT, 7.5mmI.D. × 60cm) and a

refractive index (RI) detector. The $\overline{M}n$ and $\overline{M}w$ were calculated from GPC curves on the basis of a polystyrene standard calibration. Viscosity (η_{sp} / c) was measured at 0.1 g/dl in decalin at 135 ℃ using a Ubbelohde's viscometer. The percentage of the boiling toluene-soluble fraction of the polymer was obtained by the Soxhlet extraction method (extraction time = 5 h). As an index of carbon-carbon double bond content in the polymer, iodine value (I.V.) was measured as previously reported (the iodine monochloride method).[8] The Tg of the polymers was measured by DSC on a Seiko DSC-20 differential scanning calorimeter on polymer samples of about 10mg under a nitrogen flow at a scanning rate of 10 ℃ per min.

RESULTS AND DISCUSSION

1. Effect of NBD/St Feed Ratio on the "Crosslinking" Reaction

The insoluble portion of NBD polymer was thought to comprise structural units of type Ⅲ, formed by the "crosslinking" reaction between polymers of structure Ⅱ.[1] The NBD/St copolymers in the present system had an unusual dependency of the content of the soluble fraction on the NBD/St molar ratio, as shown in the preceding chapter.[7] This phenomenon can not be explained only by the different content of NBD units in the copolymer, and the author thought two or more factors that might influence the solubility.

Two crosslinking processes, eqs.(2) and (3), were introduced to explain the above described phenomenon. The former is a normal cationic addition-type reaction of two polymer chains of structure Ⅱ, and the latter is a Friedel-Crafts type reaction of the structure Ⅱ with the phenyl ring of a St unit.

$$R^+ + \text{(II)} \rightarrow \text{(IV)} \xrightarrow{\text{(II)}} \qquad \qquad \qquad \qquad \quad$$

$$\rightarrow \qquad \qquad \qquad \qquad \qquad \quad (2)$$

$$R^+ + \text{(II)} \rightarrow \qquad \xrightarrow{} \qquad \qquad (3)$$
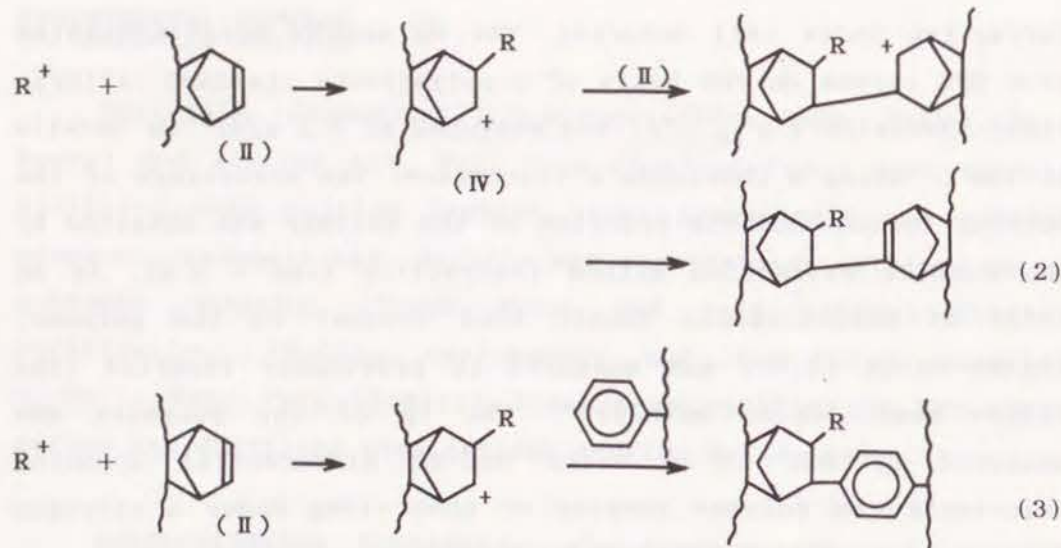
In order to estimate the probability of both reactions [eqs.(2) and (3)], the contents of carbon-carbon double bonds and St units were calculated from the iodine values (I.V.) and from the ¹H-NMR peak intensities, respectively, assuming that there are only double bonds of structure II (Table 1). Although the double bond contents listed in Table 1 do not refer to the polymer subject to the crosslinking reactions but to the recovered polymers, these values may be conveniently used for calculating reasonable probabilities as shown below.

The probabilities of occurrence of reactions (2) and (3) are given by:

(Probability of eq.(2)) $= a \times [\text{II}]^2$ (4)

(Probability of eq.(3)) $= b \times [\text{St}] \times [\text{II}]$ (5)

where [St] and [II] are the mole fraction of St unit and structure II in the copolymers, respectively, and a and b are constants. The values of $[\text{II}]^2$, $[\text{St}] \times [\text{II}]$, and the corresponding normalized values defined in eqs.(6) and (7) are also listed in Table 1.

Table 1.
Assumed structure of NBD/St copolymer (Boiling-toluene soluble fraction) a)

Monomer Ratio in Feed [NBD]/[St] (mole %)	I.V. (g-I₂/ 100g-poly.)	Soluble Fr. (wt%)	Molar Fraction of Repeating Units b)			$[\text{II}]^2$ ×10³	Normalized $[\text{II}]^2$	$[\text{St}] \times [\text{II}]$ ×10³	Normalized $[\text{St}] \times [\text{II}]$
			Styrene Unit [St]	Norbornadiene Unit b)					
				[I]+[III]	[II]				
0/100	~0	100	1.0	0	0	0	0	0	0
25/75	7.7	100	0.695	0.275	0.030	0.9	7	20.9	71
50/50	14.8	99	0.463	0.480	0.057	3.2	25	26.4	90
55/45	16.8	100	0.431	0.505	0.064	4.1	32	27.6	94
60/40	20.0	100	0.387	0.537	0.076	5.8	45	29.4	100
65/35	21.5	29	0.330	0.589	0.081	6.6	51	26.7	91
70/30	24.4	32	0.289	0.619	0.092	8.5	65	26.6	90
80/20	30.7	36	0.193	0.693	0.114	13.0	100	22.0	75
90/10	30.1	43	0.117	0.772	0.111	12.3	95	13.0	44
100/0	31.0	72	0	0.888	0.112	12.5	96	0	0

a) For reaction conditions, see Chapter 1.
b) For the structures of I, II and III, see text.

Normalized($[II]^2$) = 100 × $[II]^2$ / (maximum of $[II]^2$)   (6)

Normalized($[St] \times [II]$) = 100 × $[St] \times [II]$ / (maximum of $[St] \times [II]$)   (7)

In order to correlate the Normalized($[II]^2$) and the Normalized($[St] \times [II]$) values with the solubility of the copolymers, the solubility index (SI), defined as shown in eq.(8), was introduced as a measure of solubility of the copolymer:

SI = 200 − {Normalized($[II]^2$) + α × Normalized($[St] \times [II]$)}   (8)

Increases in Normalized($[II]^2$) and Normalized($[St] \times [II]$) mean that the reactions (2) and (3) occur with higher probability. Therefore, the larger the content of crosslinking structures in the copolymer (the smaller the content of the soluble part), the smaller the SI value. The suffix α in eq.(8) is a measure of the reactivity of the reaction shown in eq.(3) relative to that in eq.(2).

Figure 1 shows the SI value as a function of the NBD/St feed ratio in the range of α from 0.1 to 1.0. The variation of the SI value for α = 0.1 to 0.3 in Figure 1 is similar to the change of the content of soluble fraction of the copolymer shown in Table 1 (see also Figure 1 in Chapter 1), assuming that an SI value greater than 120 gives a completely soluble polymer. Therefore, one possible explanation for the unusual dependence of the copolymer solubility on the NBD/St feed ratio might be that two types of intermolecular reactions [eqs. (2) and (3)] are coexisting in the copolymerization of NBD with St, and that the contribution of the the former is major.
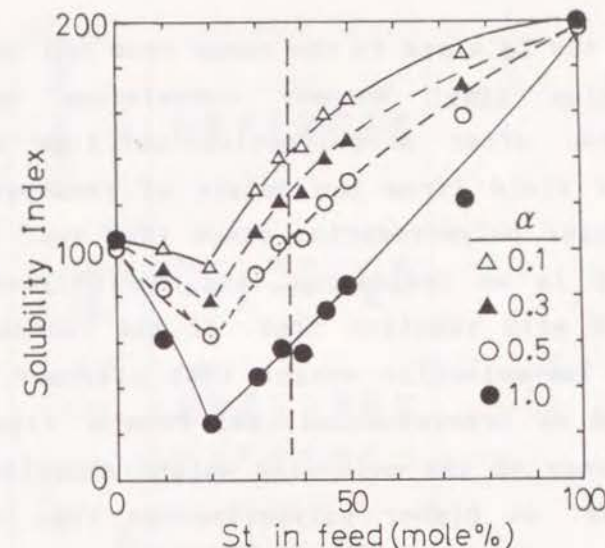
Figure 1. Solubility index (SI, see text) of the copolymer as a function of feed composition.

2. Effect of Polymerization Conditions on "Polymer Linking" Reaction

Cationic copolymerizations of NBD with St were carried out with a $[NBD]_o/[St]_o$ ratio of 60/40 mole% at −50 ℃ in CH_2Cl_2 (exceptions: Run Nos. 4 and 5 in Table 2). This monomer feed ratio was chosen because it led to a completely soluble NBD/St copolymer of highest Tg (170 ℃).[7] In this section, only the first type of the proposed reaction [eq.(2)] is considered as the "polymer linking" reaction, and the second type [eq.(3)] is neglected, because, as described in the previous section, the latter was minor.

(A) Effect of polymerization time, temperature and solvent polarity

The polymerization conditions and results were shown in Table 2. All polymers listed in Table 2 are completely soluble

in toluene, and the Tg's are in the range from 160 to 175 °C.

Polymerization time: Monomer conversions were almost quantitative even after a polymerization time of 5 min. However, polymer yield (from the weight of recovered polymer) increased at longer polymerization times (Run Nos. 1,2 and 3). This discrepancy is an indication that the polymer molecular weight increased with reaction time. At the initial stage of polymerization, low-molecular weight (MW) oligomer, which can not be recovered by precipitation, was formed. Figure 2 shows the time dependency of the molecular weight distribution (MWD) of the copolymer. At higher polymerization time the high-MW portion of the copolymer rises.

It has therefore turned out that initiation and propagation reactions in the polymerization system were already complete at the initial stage, and that the "polymer linking" reaction [for example: eq.(2)], leading to an increase in the MW of the copolymer, took place at a later reaction stage in the absence of monomers.
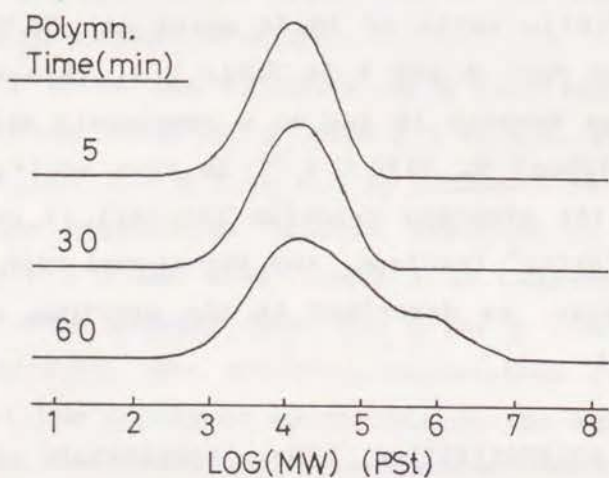
Figure 2. Effect of polymerization time on MWD of the copolymer obtained from [NBD]$_0$=0.6(M) and [St]$_0$=0.4(M), by AlEtCl$_2$/t-BuCl, in CH$_2$Cl$_2$, at -50 °C (Run Nos. 1, 2 and 3 in Table 2).

Table 2.

Copolymerization of NBD with St by AlEtCl$_2$/t-BuCl catalyst system.[a]

Run No.	[NBD]$_0$+[St]$_0$ (M)	Temp. (°C)	solvent[b]	Polymn. Time (min)	Monomer Conv.(%) NBD	Monomer Conv.(%) St	Polymer Yield (wt%)	η_{sp}/c[c] (dl/g)	$\overline{Mn}$	$\overline{Mw}/\overline{Mn}$	Polymer Conc.[d] (g/l)
1	1.0	-50	DCM	5	100	96	79	0.11	6,400	3.3	77
2	1.0	-50	DCM	30	100	98	85	0.11	6,500	3.7	82
3	1.0	-50	DCM	60	100	98	94	0.40	7,100	73	91
4	1.0	5	DCM	60	100	98	92	0.10	5,300	4.9	90
5	1.0	5	CH	60	91	97	71	0.07	4,200	6.9	69
6	0.5	-50	DCM	60	100	96	89	0.14	6,700	4.1	74
7	1.5	-50	DCM	60	100	99	96	0.42	17,100	40	141
8	2.0	-50	DCM	60	100	99	91	0.18	12,000	8.8	176

a) [NBD]$_0$/[St]$_0$ = 60/40 (mol%), [AlEtCl$_2$]$_0$=10.0mM, [t-BuCl]$_0$=5.0mM.
b) DCM : CH$_2$Cl$_2$, CH : cyclohexane.
c) Measured at 0.1 g/dl in decalin at 135 °C.
d) Polymer concentration after terminating the polymerization.

Temperature and solvent polarity: The MWD's of the copolymers obtained at various conditions are shown in Figure 3 (see also Run Nos. 3, 4, and 5 in Table 2). As temperature increased from -50 °C to 5 °C, MW ($\overline{M}n$) decreased, as usual for cationic polymerizations. For the copolymer obtained at a higher temperature (5 °C, in CH_2Cl_2), the higher-MW peak was not observed, whereas the copolymer obtained at a lower temperature (-50 °C, in CH_2Cl_2) showed this peak. This suggests that stabilization of the cation (IV), shown in eq.(2), by lowering the temperature is necessary for the "polymer linking" reaction to proceed. That is, even if the cation (IV) is formed at elevated temperature, it preferably undergoes a transfer reaction (elimination of a proton from the cation IV) to form a structure of type II.

The influence of solvent polarity was tested by using cyclohexane as nonpolar solvent in addition to the polar CH_2Cl_2. Figure 3 shows that the effect of temperature on the MWD is much stronger than that of solvent polarity.
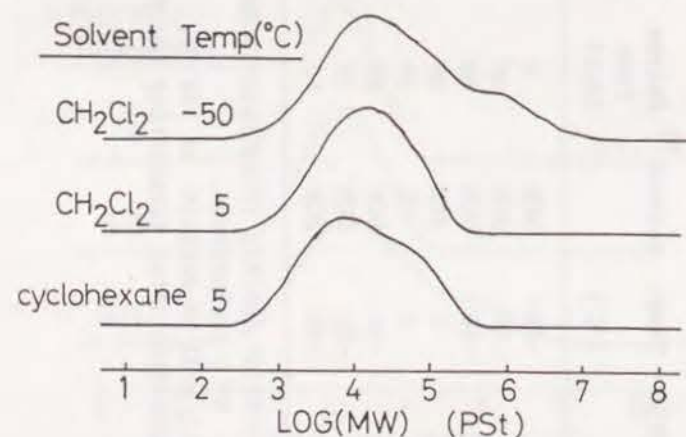
Figure 3. Effect of polymerization temp. and solvent polarity on MWD of the copolymer obtained from $[NBD]_o$=0.6 (M) and $[St]_o$=0.4 (M), by $AlEtCl_2$/t-BuCl (Run Nos. 3, 4 and 5 in Table 2).

(B)Effect of monomer concentration

As shown by the data in Table 2 (Run Nos. 6,3,7 and 8) and in Figures 4 and 5, the molecular weight ($\overline{M}n$ and η_{sp}/c) of the copolymer reached a maximum at $[M]_o$ between 1.0 and 1.5 M, and a further increase in $[M]_o$ caused a molecular weight drop. As $[M]_o$ increased from 0.5 to 1.5 M, the main peak of GPC curves shifted towards the higher-MW side and the intensity of the sub-peak at higher molecular weight increased (Figure 5). The former can be accounted for by the increasing, $[M]_o/[AlEtCl_2]_o$, whereas the latter by an increase in the concentration of double bonds in the polymer chains (II), leading to intensified "polymer linking" reaction.

However, along with the increase in $[M]_o$ from 1.5 to 2.0 M, the MW of polymer decreased and the higher-MW side peak interestingly disappeared. A possible explanation may be the depression of the "polymer linking" reaction by the higher viscosity of the polymer solution because of the higher polymer concentration.
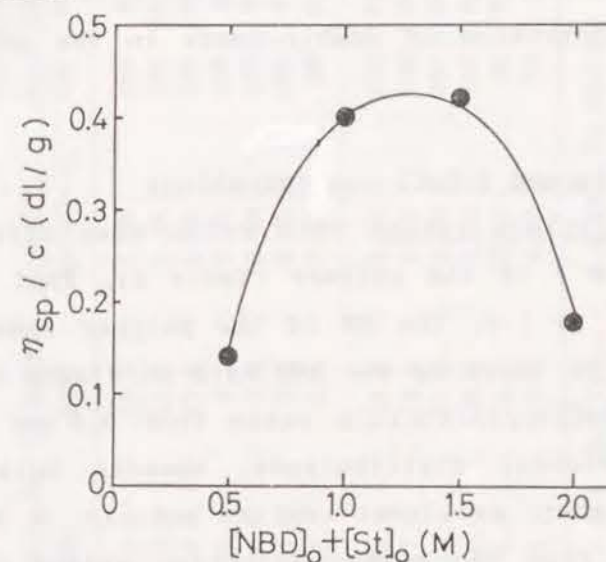
Figure 4. η_{sp}/c as a function of $[M]_o$ (Run Nos. 6, 3, 7 and 8 in Table 2).

$[M]_o(M)$
0.5
1.0
1.5
2.0

LOG(MW) (PSt)
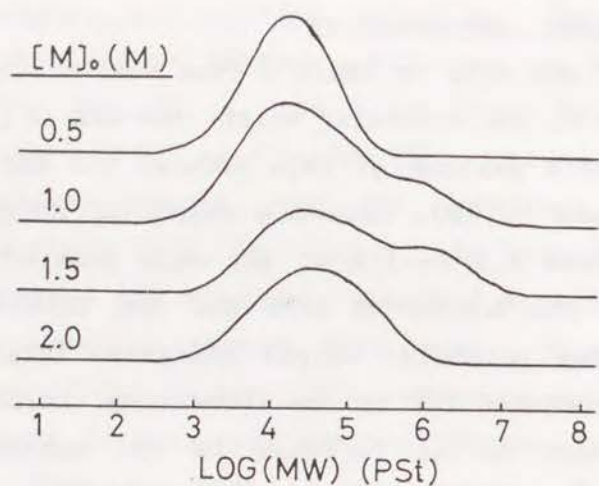
Figure 5. Effect of $[M]_o$ on MWD of the copolymer obtained from $[NBD]_o/[St]_o=60/40$, by AlEtCl$_2$/t-BuCl, in CH$_2$Cl$_2$, at -50 ℃ (Run Nos. 6, 3, 7 and 8 in Table 2).

Furthermore, the MWD of the copolymer obtained at $[M]_o$ of 0.5 M showed a monomodal distribution. This is an indication that the "polymer linking" reaction can be also depressed by lowering the concentration of double-bonds in the polymerization system.

(C)Effect of AlEtCl$_2$ and t-BuCl concentrations

[t-BuCl]$_o$/[AlEtCl$_2$]$_o$ ratio: This ratio also affected the MW ($\bar{M}n$ and η_{sp}/c) of the polymer (Table 3). That is, at a ratio around 0.75 to 1.0, the MW of the polymer came into an insoluble region. As shown by the MWD data in Figure 6, in the range of the [t-BuCl]$_o$/[AlEtCl$_2$]$_o$ ratio from 0.5 to 1.25 the copolymers gave bimodal distributions, whereas outside this range, either higher or lower ratio led to a monomodal distribution free from the higher molecular weight peak. The increase of MW, especially the increase of the higher-MW peak

Table 3.

Effect of [AlEtCl$_2$]o and [t-BuCl]o on the copolymerization of NBD with St.[a]

Run No.	[AlEtCl$_2$]o (mM)	[t-BuCl]o (mM)	[t-BuCl]o/[AlEtCl$_2$]o	Monomer Conv.(%) NBD	St	Polymer Yield (wt%)	Soluble Fraction (wt%)	η_{sp}/c [b,c] (dl/g)	$\bar{M}n$ [b,c]	$\bar{M}w/\bar{M}n$ [b,c]
9	10.0	15.0	1.50	100	97	98	100	0.14	8,600	8.4
10	10.0	12.5	1.25	100	100	98	100	0.36	12,000	62
11	10.0	10.0	1.00	100	98	98	12	(0.22)	(4,500)	(23)
12	10.0	7.5	0.75	100	98	97	33	(0.34)	(7,800)	(65)
3	10.0	5.0	0.50	100	98	94	100	0.40	7,100	73
13	10.0	2.5	0.25	100	98	90	100	0.18	9,500	7.7
14	10.0	1.0	0.10	66	58	26	100	0.09	5,500	2.6
15	20.0	10.0	0.50	100	97	97	9	(0.21)	(---)	(---)
16	17.5	8.8	0.50	100	97	97	31	(0.35)	(8,600)	(56)
17	15.0	7.5	0.50	100	97	97	100	0.46	12,000	90
3	10.0	5.0	0.50	100	98	94	100	0.40	7,100	73
18	5.0	2.5	0.50	85	90	53	98	0.11	6,500	2.7
19	1.0	0.5	0.50	12	0	2	---	---	---	---

a) [NBD]o = 0.6 (M), [St]o = 0.4 (M), in CH$_2$Cl$_2$, at -50℃, for 60 min.
b) Numbers in parentheses are taken by the soluble fractions.
c) ---: not measured.

-46-

-47-
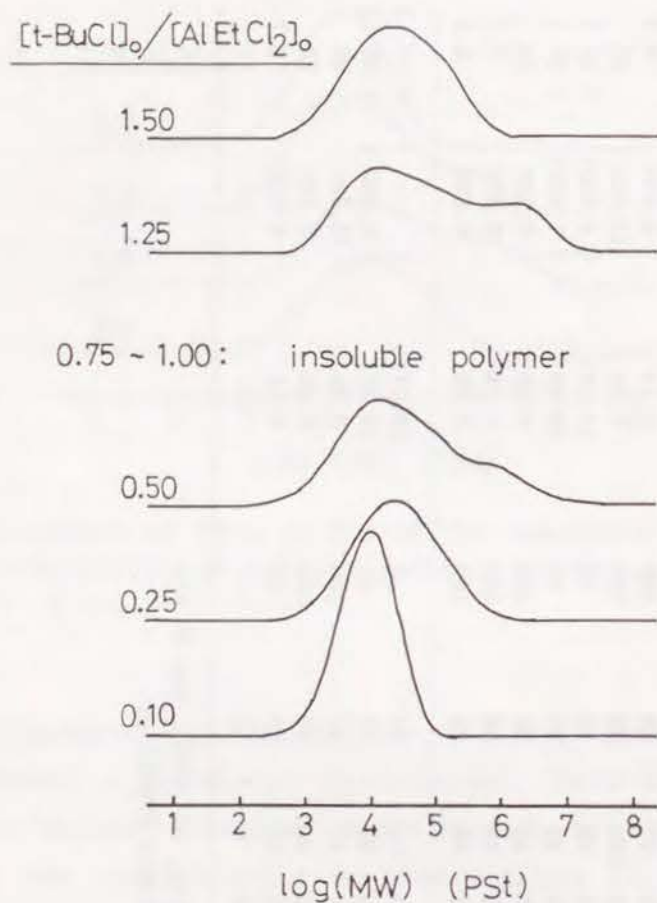
Figure 6. Effect of $[\text{t-BuCl}]_o/[\text{AlEtCl}_2]_o$ molar ratio on MWD of the copolymer obtained from $[\text{NBD}]_o=0.6(M)$ and $[\text{St}]_o=0.4(M)$, by $\text{AlEtCl}_2/\underline{t}$-BuCl, in CH_2Cl_2, at -50 ℃ (see Table 3).

intensity, on raising the catalyst ratio from 0.1 to 0.5 can be interpreted by an increase in the carbocation concentration in the system.

On the other hand, the MW drop when the catalyst ratio increased from 1.0 to 1.5 may be caused by some transfer reaction. One possible example of the transfer reaction is

shown in eq.(9), where $\underline{t}$-BuCl acts as a chain transfer agent.

$$\text{(9)}$$
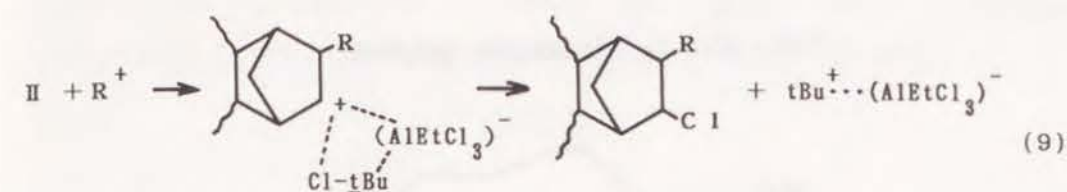
A similar behavior has been observed in the cationic polymerization of styrene by the BF_3OEt_2/H_2O system in benzene,[9] where a $[H_2O]_o/[BF_3OEt_2]_o$ ratio of 0.5 gave a maximum polymerization rate.

$[\text{AlEtCl}_2]_o$: The "polymer linking" reaction was also affected by the catalyst concentration, where $[\text{t-BuCl}]_o/[\text{AlEtCl}_2]_o = 0.5$, as shown in Table 3 and Figure 7. A lower $[\text{AlEtCl}_2]_o$ gave a soluble polymer with monomodal MWD, whereas with increasing $[\text{AlEtCl}_2]_o$, the "polymer linking" reaction became more important, and finally a higher $[\text{AlEtCl}_2]_o$ brought about the formation of an insoluble polymer by the "cross-linking" reaction.

CONCLUSION

The "crosslinking" and "polymer linking" reactions in the NBD/St cationic copolymerization were investigated. The unique dependence of the "crosslinking" reaction on the NBD/St feed ratio was interpreted by two types of intermolecular reaction processes [eqs.(2) and (3)]. The effect of the polymerization conditions on the "polymer linking" reaction is revealed in Scheme I .

The optimum polymerization conditions for preparation of soluble NBD/St copolymers, with a relatively high molecular

$$\frac{[\text{Al Et Cl}_2]_0 \text{ (mM)}}{}$$

17.5 ~ 20.0 :   insoluble polymer

15.0

10.0

5.0

1   2   3   4   5   6   7   8

log(MW) (PSt)
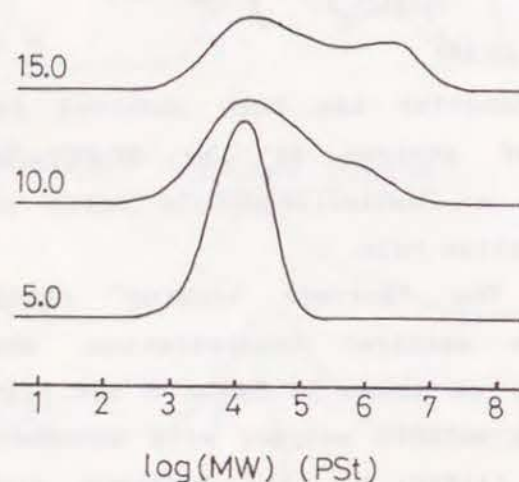
Figure 7. Effect of [AlEtCl₂]₀ on MWD of the copolymer obtained from [NBD]₀=0.6(M) and [St]₀=0.4(M), by AlEtCl₂/t-BuCl, in CH₂Cl₂, at -50 ℃ (see Table 3).

Scheme I.

FACTORS				POLYMER LINKING:
TIME	:	INCREASING	→	IS PROCEEDING
TEMP	:	LOWERING	→	IS PROCEEDING
SOLVENT POLARITY	:	INCREASING	→	IS NOT AFFECTED
[M]₀	:	1.0~1.5 (M)	→	IS MOST FREQUENTLY OCCURED
[t-BuCl]₀/[AlEtCl₂]₀	:	0.75~1.0	→	IS MOST FREQUENTLY OCCURED
[AlEtCl₂]₀	:	INCREASING	→	IS PROCEEDING

weight and a high Tg of around 170 ℃, were found to be: [M]₀ = 1.0-1.5 M, [AlEtCl₂]₀ = 10-15 mM, mole ratio [t-BuCl]₀/ [AlEtCl₂]₀ = 0.5, in CH₂Cl₂, at -50 ℃, and for 60 min.

REFERENCES

1) W.E. Lee and R.A. Rutherford, "Polymer Handbook", J. Brandrup and E.H. Immergut Ed., John Wiley & Sons, Inc., New York, 2nd Ed., 1975, p. Ⅲ -139.

2) V.A. Matonis, ibid., p. Ⅶ -1.

3) J.P. Kennedy and J.A. Hinlicky, Polymer, 6, 133(1965).

4) R.J. Cotter and M. Matzner, Ring Forming Polymerization, Part A, Academic Press, New York, 1969, p.47.

5) M.B. Roller, J.K. Gillham, and J.P. Kennedy, J. Appl. Polym. Sci., 17, 2223 (1973).

6) A. Mizuno, M. Onda and T. Sagane, Polymer, 32, 2953 (1991).

7) Chapter 1 of this thesis; Makromol. Chem., 193, 2081 (1992).

8) T.S. Lee, I.M. Kolthoff and E. Johnson, Anal. Chem., 22, 995 (1950).

9) H. Kusano, T. Masuda, T. Higashimura and S. Okamura, Polymer Letters, 9, 463 (1971).

CHAPTER 3

SYNTHESIS AND CHARACTERIZATION OF HOMO- AND CO-OLIGOMERS OF TETRACYCLO[4.4.0.1^{2,5}.1^{7,10}]DODECENE-3 BY CATIONIC POLYMERIZATION

ABSTRACT

Cationic homopolymerization of tetracyclo[4.4.0.1^{2,5}.1^{7,10}]dodecene-3 (TCD) and its copolymerization with styrene (St) were carried out with the AlEtCl$_2$/tert-butyl chloride catalyst system and the effects of temperature and TCD/St molar ratio in the polymerization, on polymer solubility, molecular weight and glass-transition temperature (Tg) were investigated. A soluble oligomer with a molecular weight of 1,000 was prepared by homopolymerization of TCD at +10 ℃ or by copolymerization with St (> 4 mole% in the feed) at -50 ℃. ^{13}C-NMR analysis of the TCD homo- and TCD/St co-polymers revealed both 3,4- and 3,11-additions or the repeat units from TCD. A polymerization mechanism including initiation, propagation, termination (deprotonation), and further crosslinking reactions is proposed. Moreover, it was demonstrated that a TCD/St copolymer with a controlled Tg in the range of 100 to 260 ℃ can be prepared by selecting the TCD/St composition.

TCD
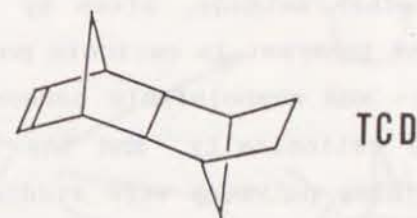
INTRODUCTION

Attention has been paid to high glass transition temperature (Tg) amorphous polymers as heat resistant thermoplastic materials with desirable characteristics such as transparency and a low mold-shrinkage. Typical examples of these materials include poly(p-phenylene oxide), poly-carbonates, and poly(methyl methacrylate), for which a number of general factors that affect glass transition temperature have been described.[1] In general, factors that increase the energy required for onset molecular motion, such as (i) inter-molecular forces, (ii) high cohesive energy density, (iii) intrachain steric hindrance, and (iv) bulky-stiff side groups, have been suggested to increase Tg. Among these factors, the author became interested in the intrachain steric hindrance and the bulky-stiff groups and have been fundamentally investigating the relationship between the structure and thermal properties of cationically synthesized polymers having alicyclic structures.[2, 3, 4]

The cationic method has been chosen from a variety of polymerization methods to introduce an alicyclic structure into a polymer chain, although the molecular weight of the polymers formed is generally low. There have been many cases where only a cationic method can generate a unique polymer structure which cannot be formed by other methods, often by the transfer and rearrangement reactions inherent in cationic polymerization.[5]

Many kinds of di- and monoolefinic norbornane derivatives have been polymerized cationically, and the structure of the alicyclic group containing polymers were studied [eqs.(1)-(3)]. 2,5-Norbornadiene (bicyclo[2.2.1]hepta-2,5-diene, I), one of the diolefinic norbornanes, was polymerized independently by Kennedy[6] and by the author[2], and the structure of the polymer

was identified [eq.(1)]. Di-endo-methylene-hexahydronaphthalene (tetracyclo[4.4.0.1$^{2, 5}$.1$^{7, 10}$]dodeca-3,8-diene, II) was also polymerized, and the polymer structure was proposed as shown in eq.(2).[7] Both polymers from I and II were proposed to form by the transannular polymerization mechanism.

$$(1)$$

$$(2)$$
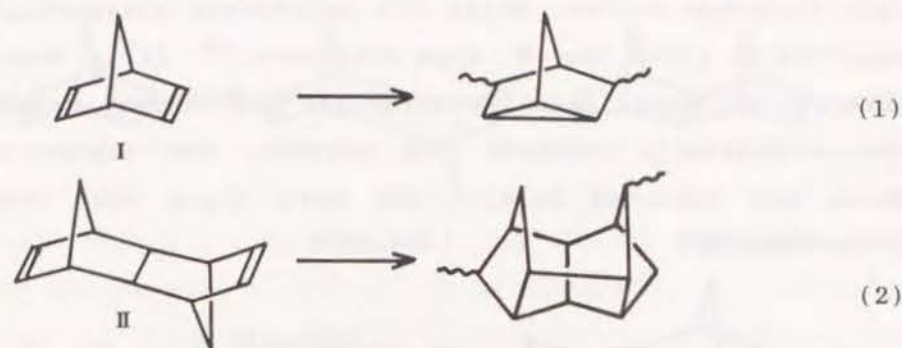
On the other hand, polymerization of norbornene (bicyclo-[2.2.1]hept-2-ene, III), the simplest form of monoolefinic norbornane, was extensively investigated [eq.(3)]. The ring-opening metathesis polymerization of III reportedly yields polymers containing cyclopentane rings and cis- and/or trans-unsaturated structure (IV).[8] In the cationic polymerization, however, Kennedy proposed two types of the polymer structures: a saturated "vinyl-type" structure (V) and a rearranged 3,7-repeat structure (VI), although the latter has not fully been identified.[9]

$$(3)$$
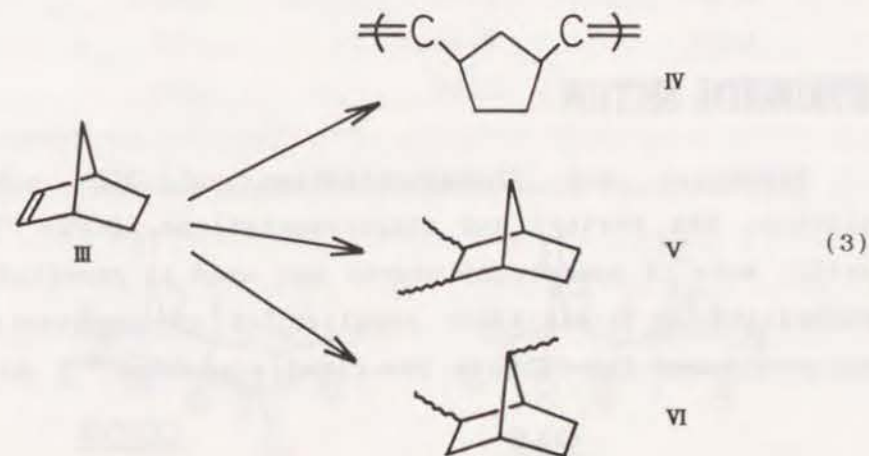
Tetracyclo[4.4.0.1^{2,5}.1^{7,10}]dodecene-3 (TCD), shown in eq.(4), has a tetracyclic structure where a bicyclic <u>norbornane</u> ring is fused to a <u>norbornene</u> structure, and its structural relation to **III** is in analogy with that of **II** to **I**. To the author's knowledge, the cationic polymerization of TCD has not been reported so far, while its metathesis polymerization was reported to yield the **IV** type structure.[10] It is therefore of interest to investigate the structure and thermal properties of the cationically produced TCD polymer, the repeat units of which are expected bulkier and more rigid than those from norbornene(**III**).

$$\xrightarrow[\text{polymerization}]{\text{cationic}} \quad ? \qquad (4)$$

TCD
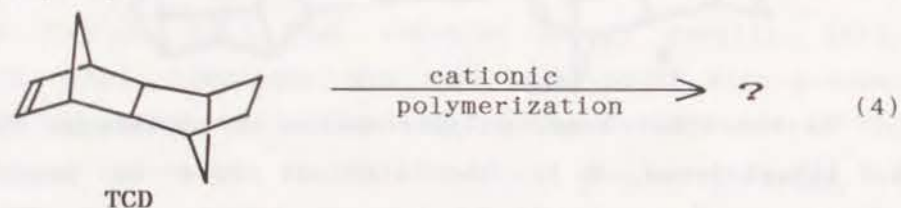
In the present chapter, TCD was synthesized by the Diels-Alder reaction of cyclopentadiene with norbornene, and its cationic homo- and co-polymerizations were carried out with the AlEtCl$_2$/<u>tert</u>-butyl chloride catalyst system in the same manner as described in the preceding chapters.[3, 4] The structure and thermal properties of the polymers were also investigated, as described below.

EXPERIMENTAL SECTION

<u>Synthesis and Characterization of TCD</u>. Norbornene (Aldrich, 98% purity) and dicyclopentadiene (DCPD) (Wako, 91% purity) were of commercial source and used as received. TCD was synthesized by Diels-Alder reaction of cyclopentadiene (CPD) and norbornene [eq.(5)] as described elsewhere;[10] molar ratio

CPD:norbornene = 1:2 at 200 ℃ for 30 min at a pressure of 10 kg/cm^2; yield 43 % after distillation (b.p. 84℃ / 6mmHg), purity 99.5 % (by GC). The purified TCD consisted the endo and exo isomers (91:9, by ^{13}C{^{1}H}-DEPT); Table 1 lists the ^{13}C-NMR chemical shifts.

$$+ \quad \longrightarrow \quad + \qquad (5)$$

TCD(endo)　　　　　　　　TCD(exo)
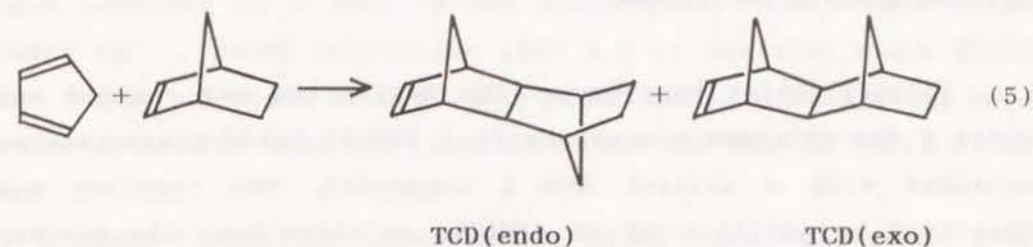
Table 1.

^{13}C chemical shifts of TCD (in CDCl$_3$)

Carbon No.[a]	Carbon Species	Chemical Shifts (ppm)	
		Endo-isomer	Exo-isomer
1, 6	CH	48.7	45.7
2, 5	CH	46.7	49.7
3, 4	CH	134.7	138.7
7, 10	CH	37.9	38.8
8, 9	CH$_2$	31.9	31.2
11	CH$_2$	52.8	42.4
12	CH$_2$	33.7	35.7

a) Numbering of carbon atoms is as follows:
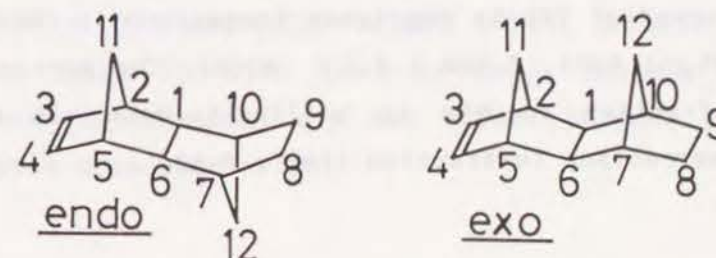
Materials. Commercial styrene (St, Wako) was freshly distilled over calcium hydride under reduced pressure. AlEtCl$_2$ was commercially obtained as solution in n-hexane (Tosoh Akzo) and used without further purification. Dichloromethane (CH$_2$Cl$_2$) and tert-butyl chloride (t-BuCl, Wako) were distilled over calcium hydride before use.

Polymerization Procedures. Polymerization was carried out under a dry-nitrogen atmosphere in a 500-ml baked glass reactor equipped with a stirrer and a condenser. The reaction was initiated by addition of an AlEtCl$_2$ solution into the monomer solution, and terminated with prechilled ammoniacal methanol. The cocatalyst (or initiator), t-BuCl, was added to the monomer solution before the addition of AlEtCl$_2$. The quenched polymerization mixture was sequentially washed with a dilute aqueous acid and water to remove catalyst residues. The product was precipitated into methanol and was dried in vacuum to give white powdery polymer. The yield of polymer was determined by gravimetry.

Characterization of Polymers. The molecular weight distribution (MWD) of the polymers was measured using gel-permeation chromatography (GPC) in o-dichlorobenzene at 140 ℃ on a Waters liquid chromatograph (150-C ALC/GPC) equipped with a polystyrene gel column (TSKgel GMH-HT, 7.5mm i.d. × 60cm) and a refractive index (RI) detector. The $\overline{Mn}$ and $\overline{Mw}$ were calculated from GPC curves on the basis of a polystyrene calibration. A dual-mode (RI and UV at 254nm) GPC detection was also applied for the proof of TCD/St copolymer formation (in CHCl$_3$, at r.t., column: PLgel 500A, 7.5mm i.d. × 60cm). The percentage of the polymer fraction soluble in boiling-toluene was obtained by Soxhlet extraction (extraction time = 5 h).

NMR samples were prepared by dissolving ca. 80 mg of the soluble fractions of the TCD homo- or copolymers (Run Nos. 1 and 8, in Table 2) at 120 ℃ in ca. 0.5 ml of hexachlorobutadiene, including ca. 0.05 ml of perdeuteriobenzene for field stabilization, in a 5 mm o.d. glass tube. ^{13}C-NMR spectra were recorded on a JOEL GX-500 spectrometer: 125.8 MHz; pulse angle 45°; pulse repetition time 5.0 s; spectral width 20000 Hz; number of scans 20,000; data point 64k. ^{1}H-NMR spectra were recorded on the same NMR instrument at 500 MHz in CDCl$_3$ at 40 ℃.

Glass-transition temperature (Tg) was measured with differential scanning calorimetry (DSC) on a Seiko DSC-20 instrument with polymer samples of about 10 mg under a nitrogen flow at a scanning rate of 10 ℃ per min.

RESULTS AND DISCUSSION

1. Polymerization

Homopolymerizations of TCD by the AlEtCl$_2$/t-BuCl catalyst system were carried out under various conditions (Run Nos. 1-4, Table 2). This catalyst system was chosen, because AlEtCl$_2$ is a strong Lewis acid and because t-BuCl is a well-known effective initiator, as described in Chapter 1.[3] Figure 1 shows the molecular weight distribution (MWD) of the polymers. The polymerization was relatively slow, reaching 5-20 % polymer yield in 60 min. The polymers obtained at +10 ℃ were completely soluble in boiling toluene but those at lower temperatures were partly insoluble. The molecular weight of the soluble polymers were in the range 700-1100 ($\overline{Mn}$, by GPC). Solvent polarity (CH$_2$Cl$_2$ versus cyclohexane) did not affect polymer yield but reduced polymer molecular weight.

Table 2.
Homopolymerization of TCD and its copolymerization with St with the AlEtCl₂/t-BuCl catalyst system a)

Run No.	[TCD]₀/[St]₀ (mole%)	Solvent	Temp. (°C)	Polymer Yield (wt%)	Soluble Fraction (wt%)	$\overline{Mn}$ b)	$\overline{Mw}/\overline{Mn}$ b)	$\overline{DPn}$ b,c)	St-unit Content (mole%)	Tg d) (°C)
1	100/ 0	CH₂Cl₂	-50	17.4	43	(840)	(1.9)	(5.3)	0	275(260)
2	100/ 0	CH₂Cl₂	-30	10.9	24	(1,070)	(1.9)	(6.7)	0	--
3	100/ 0	CH₂Cl₂	+10	5.3	100	1,060	1.8	6.6	0	269
4	100/ 0	cyclohexane	+10	4.9	100	660	1.7	4.1	0	--
5	96/ 4	CH₂Cl₂	-50	20.9	100	780	1.7	5.0	5.7	181
6	93/ 7	CH₂Cl₂	-50	22.2	100	780	2.0	5.1	10.9	166
7	70/30	CH₂Cl₂	-50	42.4	100	790	1.7	5.6	34.0	141
8	50/50	CH₂Cl₂	-50	47.0	100	870	2.0	6.6	50.8	138
9	25/75	CH₂Cl₂	-50	61.0	100	1,480	2.4	12.4	73.8	117
10	0/100	CH₂Cl₂	-50	85.5	100	23,500	4.3	226	100	98

a) Polymerization conditions: [TCD]₀ + [St]₀ = 1.0 M, [AlEtCl₂]₀/[t-BuCl]₀ = 10.0/5.0 mM, for 60 min.
b) Numbers in parentheses are for the soluble fractions in boiling toluene.
c) Calculated from $\overline{Mn}$ and TCD/St composition.
d) ---: Not measured.
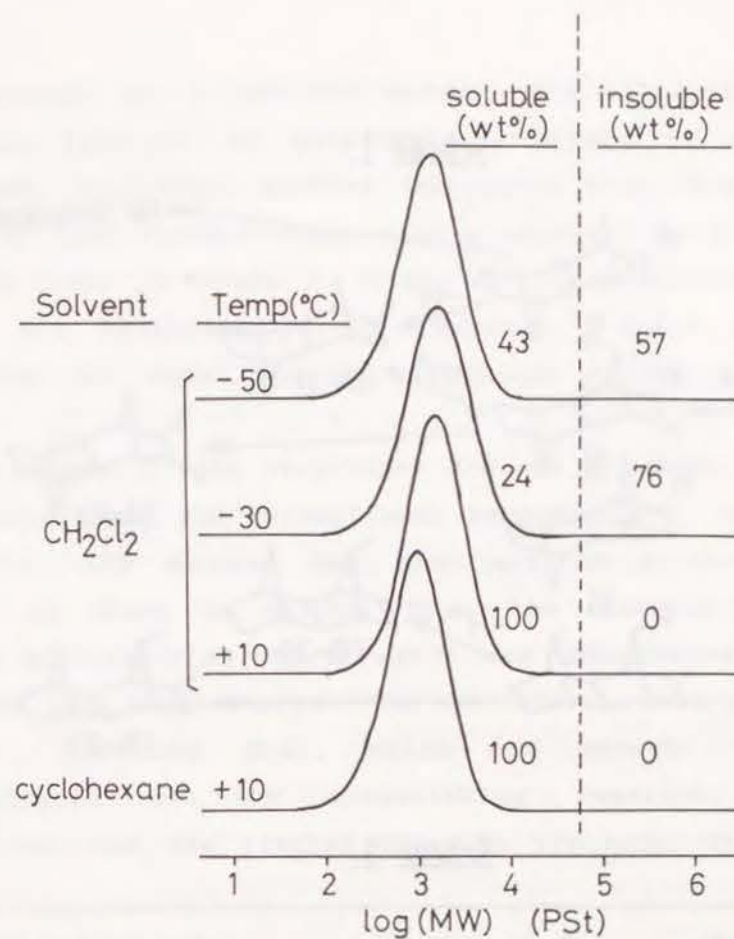
Figure 1. Effect of polymerization temperature and solvent polarity on MWD and polymer solubility of the TCD homopolymer (Run Nos. 1-4, in Table 2).

A proposed mechanism for the cationic polymerization of TCD, including initiation, propagation, and termination (deprotonation), is shown in Scheme 1, which is analogous to the mechanism for norbornene proposed by Kennedy.[5, 7] Therefore, the structures of the TCD polymer (before a polymer linking reaction occurs) could be illustrated as shown in Scheme 2 (see the structure section below). Herein and hereinafter, only the endo isomer (major isomer) was taken

Scheme 1.

TCD

$R^+ = H^+$
$\underline{t}Bu^+$
TCD^+

No propagation

(A-3)

(A-2)

(B-3)

(B-2)

Scheme 2.

Initiated Ends	Repeat Units	Terminated Ends
(A-1)	(A-2)	(A-3)
(B-1)	(B-2)	(B-3)

R = $\underline{t}$Bu or H

Scheme 3.

(A-3)

$R^+ = H^+, \underline{t}Bu^+, TCD^+$

(B-4)

(B-6)

etc.

(B-3)

(B-5)

(B-7)

etc.
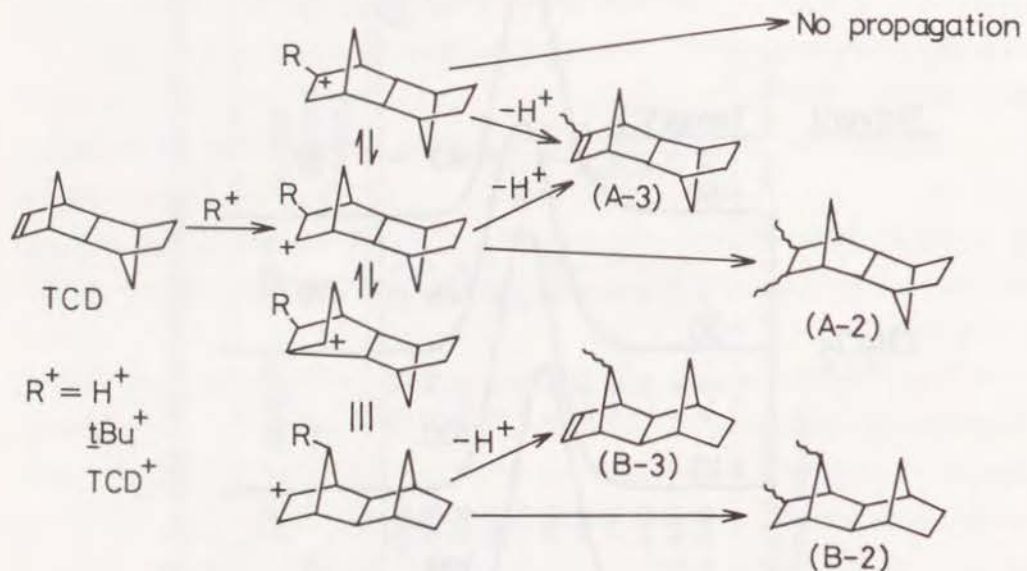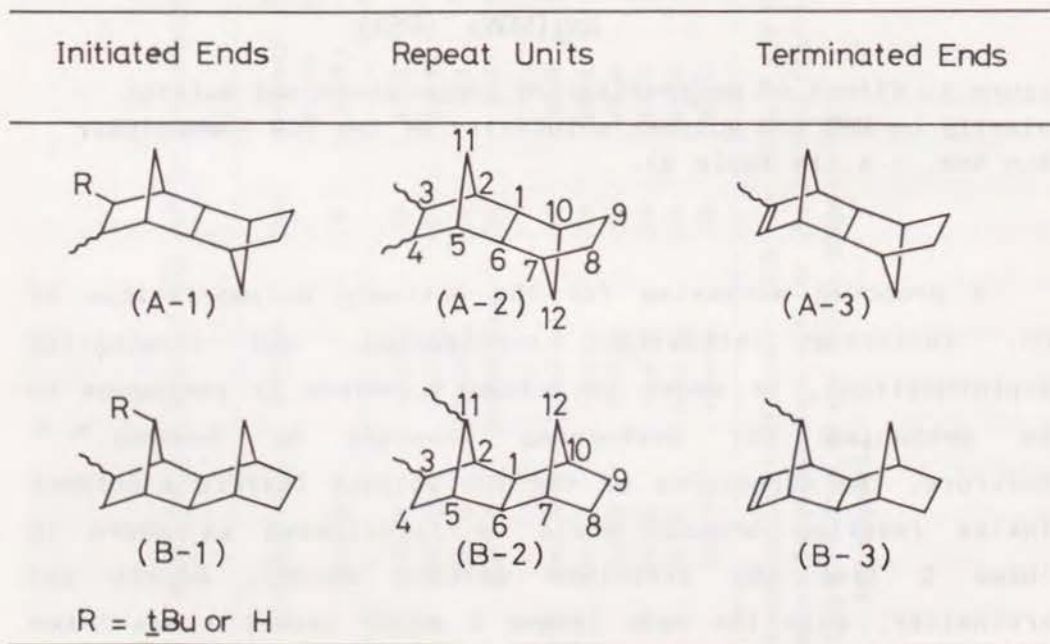
into account as a fed TCD monomer for simplicity. If the insoluble fraction of poly(TCD) is formed by crosslinking reactions, they might involve terminated ends, **A-3** and **B-3** in Scheme 2, that further react with a cation (or a proton) to form, as shown in Scheme 3, tetra- or tri-substituted TCD units (**B-6** or **B-7**, respectively). In Schemes 1, 2 and 3, **A** and **B** have designated the endo- and exo-structures of TCD unit, respectively.

In Scheme 3, the structures **A-3** and **B-3** might be regarded as trifunctional and bifunctional macromonomers, respectively. Similarly, TCD monomer may also act as a tetrafunctional monomer as shown in eq.(6). Thus, the observed decrease in polymer solubility at -50 or -30 °C was interpreted as follows: At such low temperatures, the secondary carbo-cations (for example, **B-4** and **B-5**), which are thought to be the intermediates of the crosslinking reaction, might be stabilized, and the linking reaction proceeds. The fact that
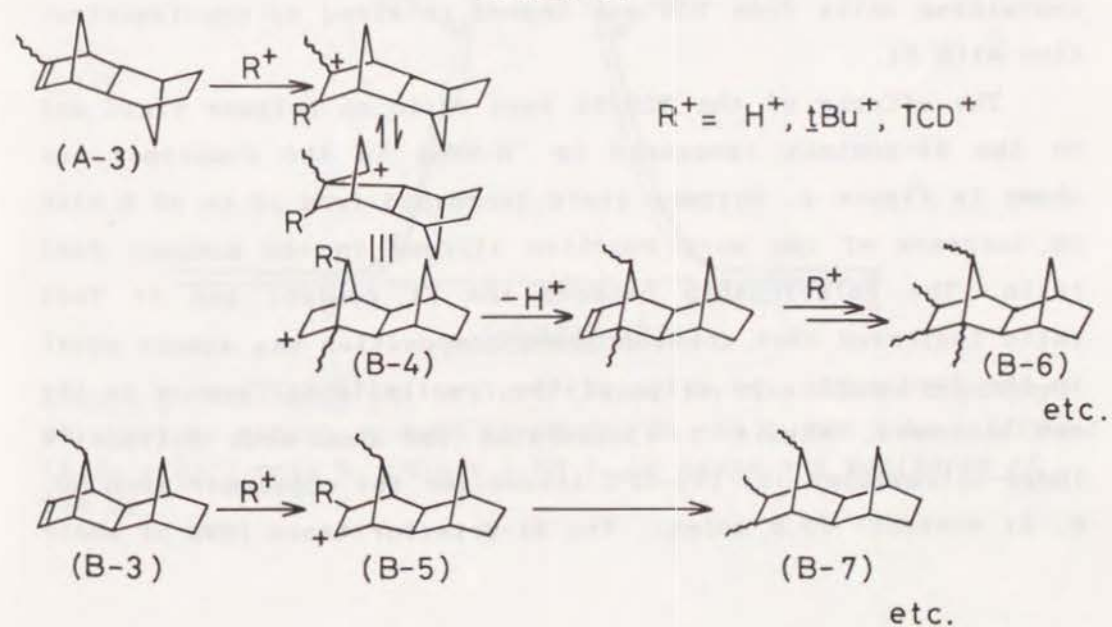
the polymer yield by gravimetry increased with decreasing temperature (Table 2) may also support the possibility of the crosslinking reaction processes (Scheme 3) in which TCD monomer is also participating as a crosslinking agent [eq.(6)].

(6)

(B-6)
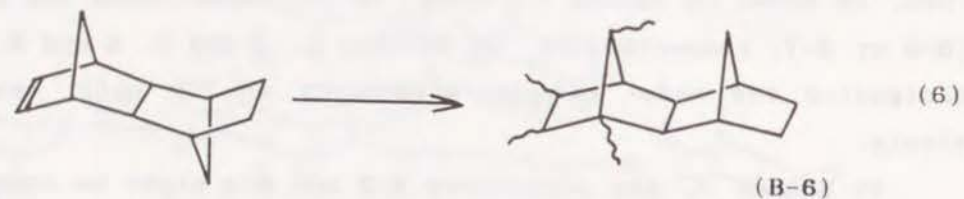
Copolymerizations of TCD with Styrene were carried out under various TCD/St feed ratios at -50°C (Run Nos. 1 and 5 ~ 10, Table 2), expecting that by incorporating St units into the TCD polymer, the insoluble fraction formed by the crosslinking reaction might decrease and that Tg could be controlled by the TCD/St feed ratio, as described in Chapter 1 of the norbornadiene/styrene system.[3] As Table 2 shows, the solubility of the polymer surprisingly increased from 43% to 100% at a very small amount of St feed ratio of 4 mole%. The reason of this solubility change is not clear, but, as expected, a soluble polymer containing units from TCD was indeed obtained by copolymerization with St.

The effects of the TCD/St feed ratio on polymer yield and on the St-content (measured by ^{1}H-NMR) in the copolymer are shown in Figure 2. Polymer yield increased from 17 to 86 % with an increase of the more reactive styrene in the monomer feed ratio. The relationship between the St content and St feed ratio indicated that the copolymer composition was almost equal to the feed ratio, in spite of the reactivity difference in the two monomers. Figure 3 illustrates the dual-mode refractive index-ultraviolet [RI-UV] GPC traces for the copolymer (Run No. 6, St content: 10.6 mole%). The RI-detector trace (MWD of whole
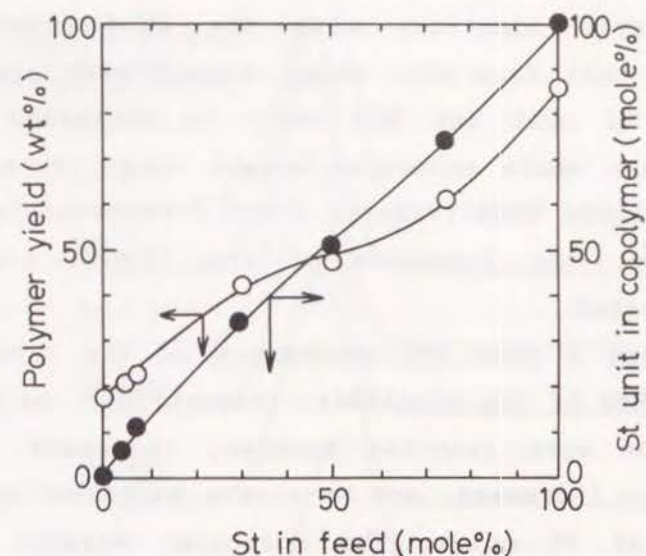
Figure 2. Monomer feed ratio dependency of polymer yield and St unit content in the TCD/St copolymer obtained at -50°C in CH_2Cl_2 for 1hr; $[TCD]_0+[St]_0 = 1.0$ M, $[AlEtCl_2]_0 = 10.0$ mM, $[\underline{t}\text{-BuCl}]_0 = 5.0$ mM.
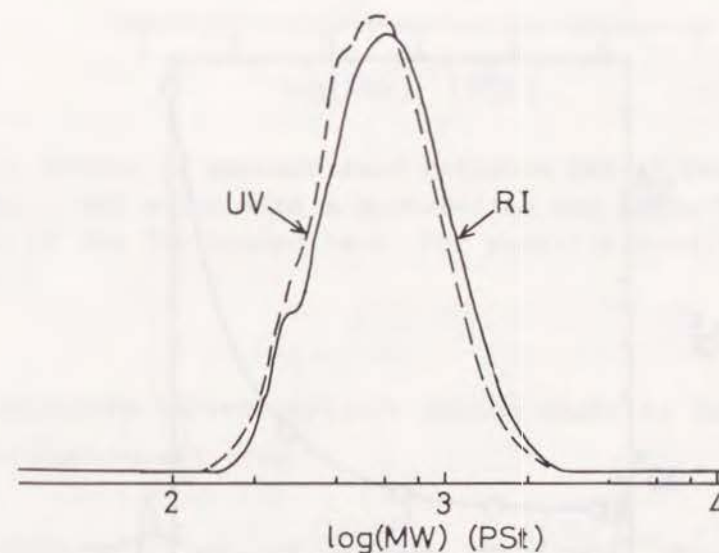
Figure 3. Dual-mode [RI-UV] GPC traces for the TCD/St copolymer obtained by $AlEtCl_2/\underline{t}$-BuCl in CH_2Cl_2 at -50 ℃ for 1 hr ($[TCD]_0/[St]_0 = 93/7$ mole %, $[M]_0 = 1.0$M). UV trace was monitored at 254 nm.

product) is nearly identical with the UV-detector trace (distribution of unit from St), which demonstrates almost the same amount of St unit (or TCD unit) is contained in the copolymer over the whole molecular weight range (from 200 to 2500). From the above data (Figures 2 and 3) together with the solubility change, the formation of true TCD-St copolymers could be demonstrated.

Figures 4 and 5 show the dependence of the TCD/St feed ratio on $\overline{M}_n$ and MWD of the copolymer, respectively. As the feed ratio of St, the more reactive monomer, increased, polymer yield continuously increased, and $\overline{M}_n$ slowly increased up to the St feed ratio of 75 mole%. The molecular weights of the copolymers were much smaller than that of the St homopolymer. As shown in eq.(7), a transfer reaction (proton elimination) from the St-TCD$^+$ propagating end and the resultant formation of
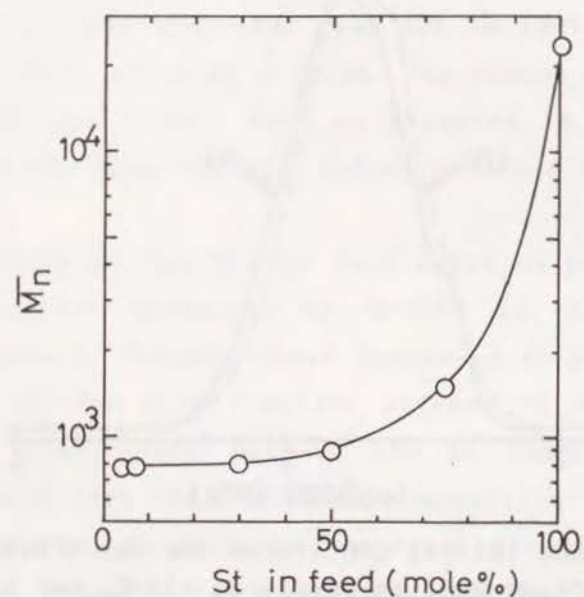
Figure 4. Effect of St feed ratio on $\overline{M}_n$ of the TCD/St copolymer (For reaction conditions, see Table 2).
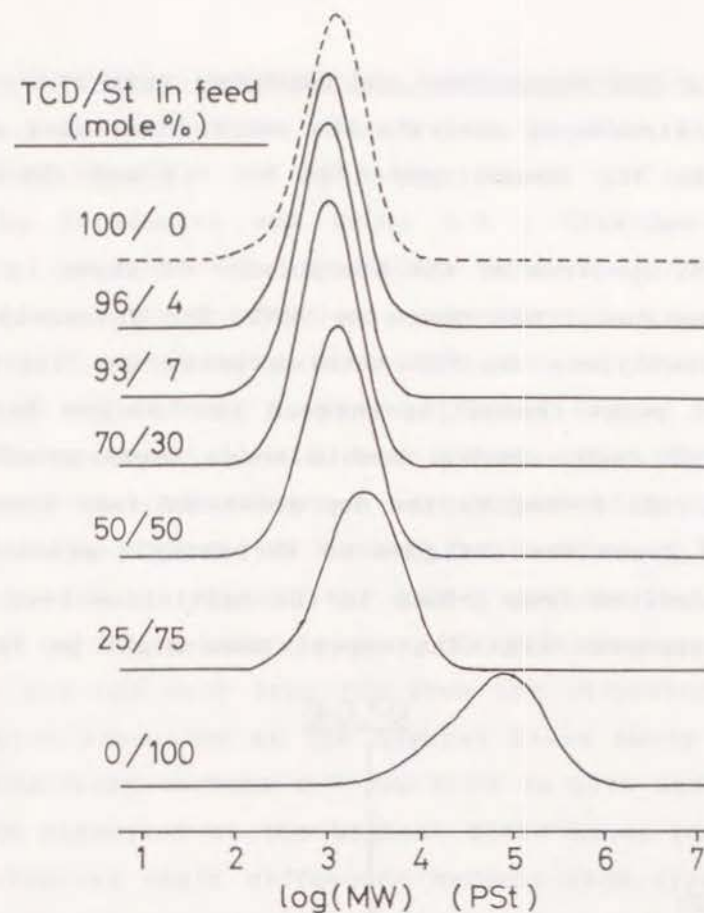
Figure 5. Effect of monomer feed ratio on MWD of the TCD/St copolymer (MWD curve with a dashed-line was taken from soluble fraction of the TCD homopolymer; For reaction conditions, see Table 2).

a less reactive buried tertiary cation might be the reason for the molecular weight drop.

(7)
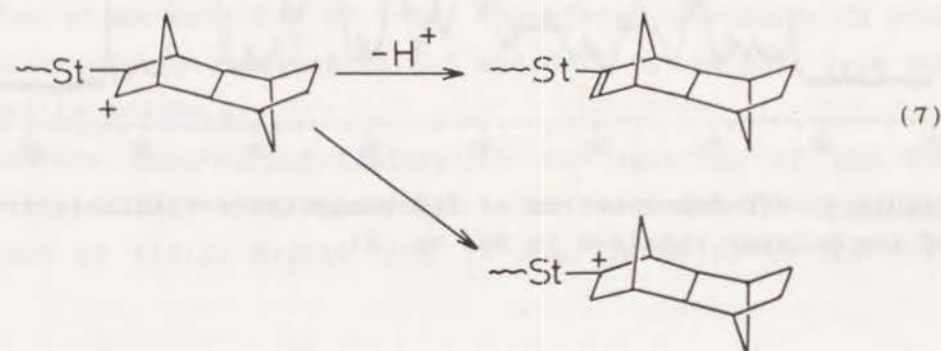
2. Structures of TCD Homopolymer and Copolymer with St

A ^{13}C-NMR structural analysis was carried out on a soluble fraction of the TCD homopolymer (Run No. 1) and the TCD/St copolymer (Run No. 8).

The ^{13}C-NMR spectrum of the homopolymer is shown in Figure 6. The peak assignment was based on DEPT. The intensity ratio of the total methylene to the methine peaks was 1:1.8. The olefinic carbon peaks resonating between 130-134 ppm indicated the existence of carbon-carbon double bonds, most probably in the terminated ends formed by the deprotonation [see Scheme 1]. The peak at 28.2 ppm was assigned to the methyl carbon of the t-butyl group derived from t-BuCl in the initiation step. These observations supported that the repeat unit might be from di-
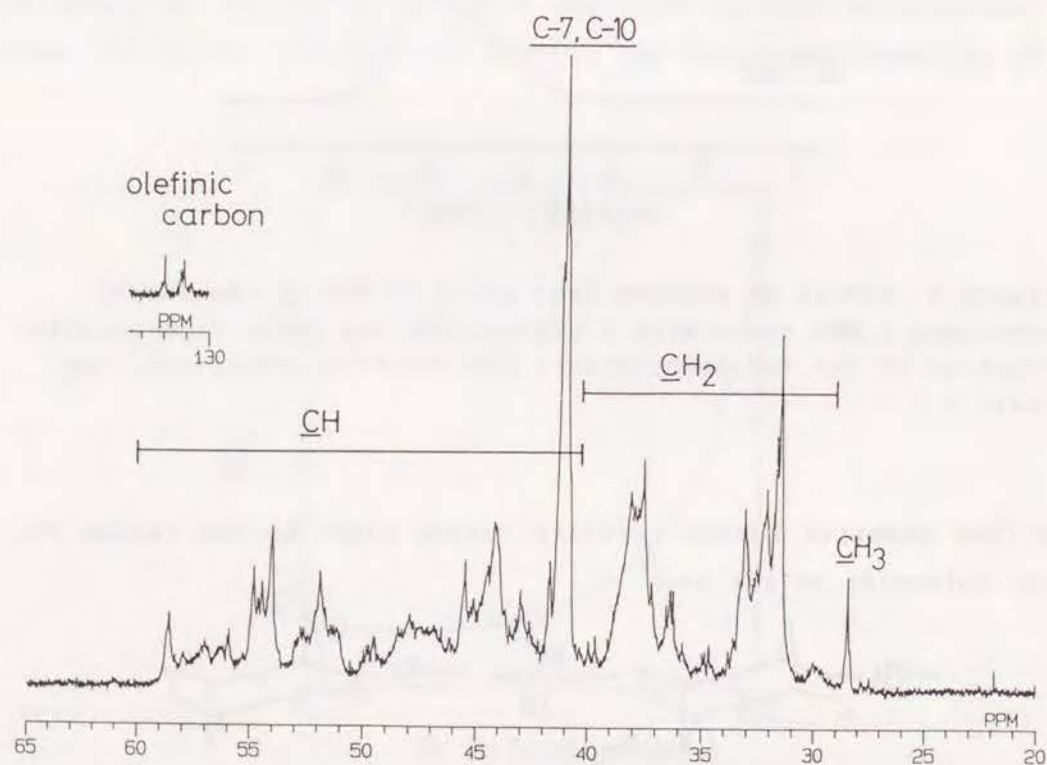
Figure 6. ^{13}C-NMR spectrum of TCD homopolymer (soluble fraction of the polymer obtained in Run No. 1).

substituted tetracyclododecane, **A-2** (calculated methylene to methine intensity ratio, CH_2:CH = 1:2), with the initial end group **A-1**(CH_2:CH = 1:2 if R=tBu, CH_2:CH = 1:1.4 if R=H) and with the terminated end group **A-3** (CH_2:CH = 1:1.5), as presumed in Scheme 2. The above consideration was likewise applicable to the B-type (exo) structure, and gave exactly the same result concerning the methylene to methine intensity ratio. If either A or B type was formed in the present system, the NMR spectrum should have shown the simpler pattern. Therefore, the formation of both types of A and B is most plausible, as proposed by Kennedy for norbornene.[5, 7]

In order to support the above speculation, attention was focussed on the relatively sharp CH peak (corresponding to two carbons per one unit from TCD from the intensity ratio) at 41 ppm, which resonated at the highest field among the CH peaks. The bridge-head carbons C-7 and C-10 in both endo- and exo-TCD monomers resonated at the highest field among the CH peaks and their chemical shift difference between endo type and exo type was very small (see Table 1). Similarly, C-7 and C-10 in the A-type polymer (model compound: TCD endo monomer) and those in B-type polymer (model compound: TCD exo monomer) were assumed to resonate closely together. Furthermore, the chemical shifts of C-7 and C-10 in the polymer were thought to be less influenced by the carbon atoms in the substituents which were attached during polymerization, resulting in the narrow peak profile, since the carbon atoms in the substituents were δ-carbon atoms from C-7 or C-10. Therefore, the sharp CH peak in concern can be assigned to C-7 and C-10 in the unit from TCD as shown in Scheme 2.

Another interesting feature of the spectrum of the TCD homopolymer (Figure 6) is that all the methylene carbons resonated at fields higher than 40 ppm, in spite of the C-11

(CH₂) peak in the TCD endo-monomer resonating at 52.8 ppm. On the basis of literature data[11] for the bridged-carbon atom from <u>norbornene</u> to 2-methyl-<u>norbornane</u>, the peak position of C-11 was reasonably assumed to shift into the range of 30-40 ppm by converting from monomer to polymer.

As shown in Figure 7(a), the whole <u>paraffinic</u> carbon resonances of the TCD/St copolymer were similar to those of the TCD homopolymer. The C-7 and C-10 peaks of the TCD units even in the copolymer were also sharp, which indicates the carbon atoms in the substituents took δ - and more remote position from C-7 or C-10, in the same manner as in the homopolymer. Unfortunately, the peaks due to the -CH₂-CH- in the unit from styrene could not be definitely assigned. From the aromatic carbon signals shown in Figure 7(b), it was confirmed that a unit from styrene was incorporated by the normal way of addition reaction. The terminal olefinic carbons were not clearly observed in this region. Probably, these peaks might be hidden in the strong aromatic resonances.

As described above, it could be concluded that the polymerization of TCD proceeded in the processes shown in Scheme 1, in both homopolymerization and copolymerization with styrene.

3. <u>Glass-Transition Temperature of Polymers</u>

As shown in Table 2, the Tg of TCD homopolymers ranged between 260 and 275 ℃, whereas norbornene polymers have been reported to have a softening point of 235 ℃ ($\overline{Mn}$=1,470).[7] The repeat units of TCD being bulkier and of more rigid structure than that of norbornene (Ⅲ), did not affect very much the melting behavior of the polymer (Tg or softening point). This may be caused by their low molecular weights, where end groups strongly affect Tg.
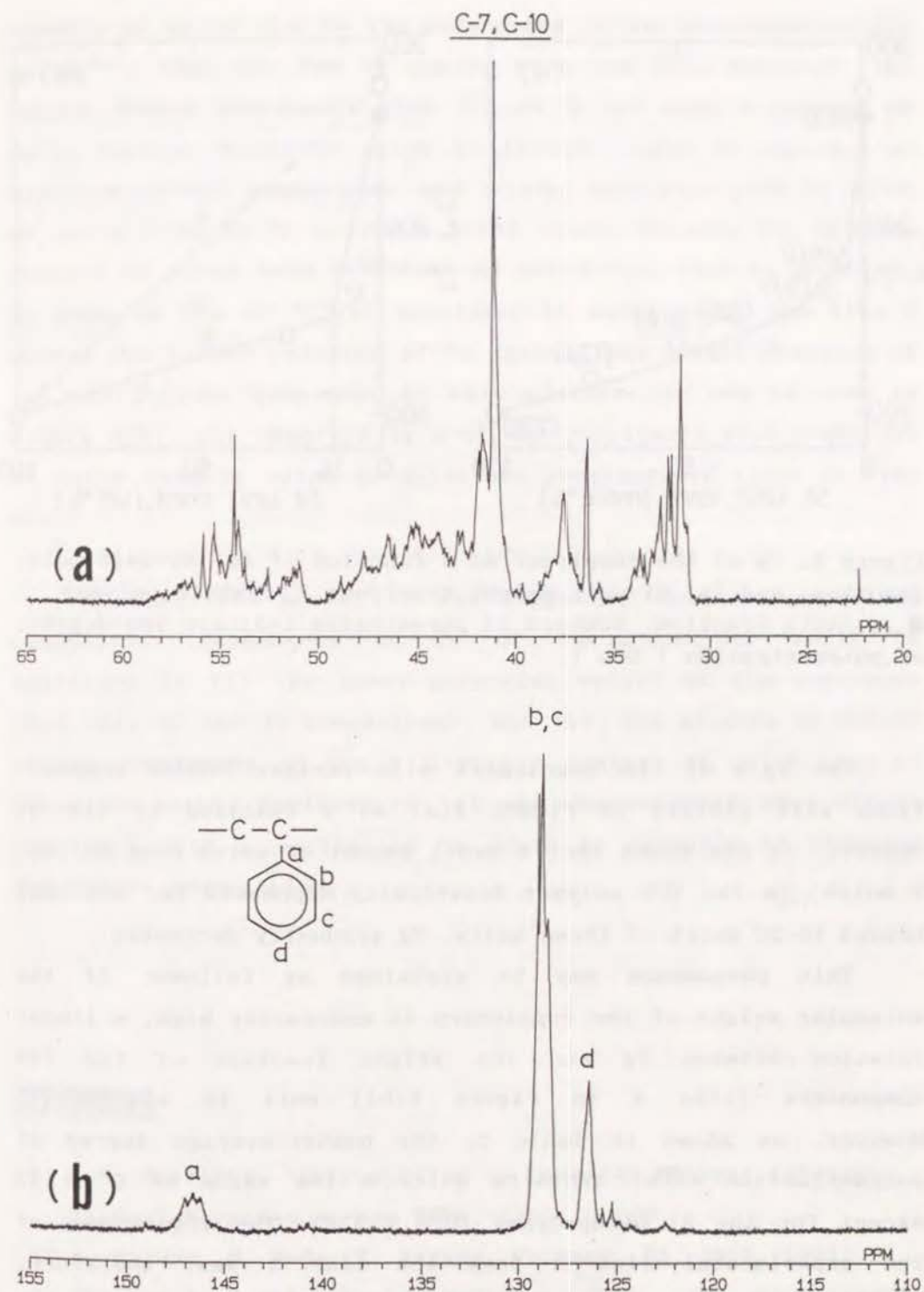
Figure 7. ¹³C-NMR spectra of (a)<u>paraffinic</u> carbon resonance region and (b) aromatic or olefinic carbon resonance region for the TCD/St copolymer (Run No.8 in Table 2).
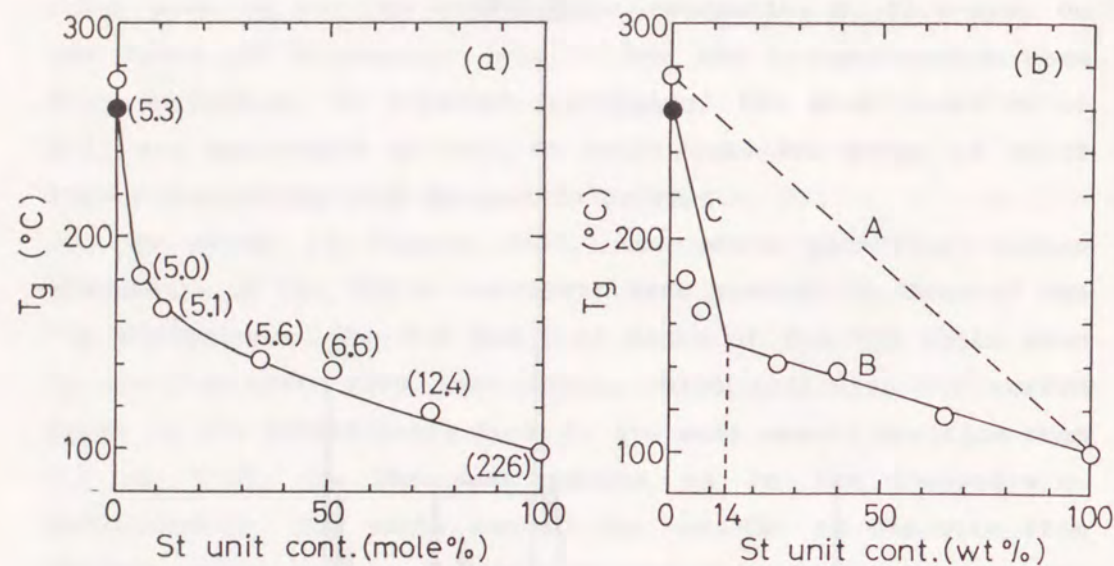
Figure 8. Tg of the copolymer as a function of (a) St-unit molar fraction, and (b) St-unit weight fraction; ○ : whole polymer, ● :soluble fraction. Numbers in parentheses indicate the degree of polymerization ($\overline{DPn}$).

The Tg's of the copolymers with various TCD/St compositions were plotted in Figure 8(a) as a function of the St content. It was found that a small amount of units from St (ca. 5 mole%) in the TCD polymer drastically depresses Tg, and that beyond 10-20 mole% of these units, Tg gradually decreases.

This phenomenon may be explained as follows: If the molecular weight of the copolymers is moderately high, a linear relation between Tg and the weight fraction of the two components [line A in Figure 8(b)] must be applied.[12] However, as shown in Table 2, the number-average degree of polymerization ($\overline{DPn}$) exhibits quite a low value of 5 to 13 except for the St homopolymer ($\overline{DPn}$ = 226). The discrepancy of the experimental line B from the line A was, therefore,

considered to be due to the dependency of the molecular weight on Tg[13], that is, low Tg coming from low $\overline{DPn}$. Moreover, the TCD/St random copolymers with $\overline{DPn}$ of 5 and with a content of units from St below 20 mole% (= 14 wt%) could be regarded as mixtures of TCD homopolymer and TCD/St copolymer with 20 mole% of units from St in a proper blend ratio. Because the minimum content of units from St should be one-fifth, that is 20 mole%, as long as $\overline{DPn}$ of TCD/St copolymer is equal to 5. The line C showed the linear relation of Tg against the weight fraction of the two polymer component in this mixture. As can be seen in Figure 8(b), the observed Tg's of the copolymers with a content of units from St below 20 mole% are considerably close to line C.

As described above, it was suggested that the anomalous composition dependency on Tg of the copolymer could be explained by (i) the lower molecular weight of the copolymer than that of the St homopolymer, and (ii) the absence of TCD/St random copolymers of $\overline{DPn}$ = 5 with a content of units from St below 20 mole%. Furthermore, it was demonstrated that TCD/St copolymer with a controlled Tg could be prepared by choosing the TCD/St composition.

REFERENCES

1) L.H. Sperling, "Introduction to Physical Polymer Science", Wiley-Interscience, New York, 1985, p.283.
2) A. Mizuno, M. Onda, T. Sagane, Polymer, 32, 2953 (1991).
3) Chapter 1 of this thesis; Makromol. Chem., 193, 2081 (1992).

4) Chapter 2 of this thesis; Makromol. Chem., 193, 2091 (1992).

5) J.P. Kennedy, Encyclop. Polym. Sci. Technol., 7, 754 (1967).

6) (a) J.P. Kennedy, J.A. Hinlicky, Polymer, 6, 133 (1965).
   (b) M.B. Roller, J.K. Gillham, J.P. Kennedy, J. Appl. Polym.
   Sci., 17, 2223 (1973).

7) J.P. Kennedy, "Cationic Polymerization of Olefins: A
   Critical Inventory", John Wiley & Sons, New York, 1975,
   p.228, and reference therein.

8) K.J. Ivin, "Ring-Opening Polymerization", Volume 1, K.J.
   Ivin and T. Saegusa, Ed., Elsevier, New York, N.Y., 1984,
   Chapter 3.

9) Ref. 7), p.220, and references therein.

10) (a) R. Ohm, C. Stein, Encyclop. Chem. Technol., 3rd. Ed., 18,
    436 (1982). (b) Fr. Demande 1,535,460 (July 1, 1968), J.
    Verge, C. Pailloux, J.-C. Muller, J.-C. Robinet (to
    Charbonages de France); U.S. Pat. 3,557,072 (Jan. 19, 1971),
    (to Charbonages de France).

11) G.C. Levy, G.L. Nelson, "Carbon-13 Nuclear Magnetic
    Resonance for Organic Chemists", Wiley-Interscience, New
    York, 1972, Chapter 3.

12) Ref. 1), p.275.

13) Ref. 1), p.272.

CHAPTER 4

SYNTHESIS AND CHARACTERIZATION OF POLY(5-ALKYL-2-NORBORNENE)S BY CATIONIC POLYMERIZATION: EFFECTS OF ALKYL SUBSTITUENTS ON MONOMER REACTIVITY, POLYMER STRUCTURE AND THERMAL PROPERTIES

ABSTRACT

Cationic polymerizations of various 5-alkyl-2-norbornenes (R-NB, where R = H, CH_3, C_2H_5, C_5H_{11}, C_7H_{15}, and $C_{10}H_{21}$) were carried out by the AlEtCl$_2$/tert-butyl chloride catalyst system, and the effects of the alkyl substituents on the monomer reactivity and polymerizability, polymer structure, and glass-transition temperature (Tg) were investigated. The introduction of an alkyl substituent into the 5-position of the norbornene ring remarkably reduced the monomer reactivity and polymerizability, although the length of alkyl group did not affect them. ^{13}C-NMR structural analysis of poly(R-NB)s revealed that not only the normal 5- or 6-alkyl-2,3-unit but also other structures such as 5- or 6-alkyl-2,7-, 4-alkyl-3,6-units, and so on were most plausible structures for the repeat units. Furthermore, the existence the 4-alkyl-3,6-repeat unit and the alkylidene type end structure indicated that the intermediate tertiary cation (5-alkyl-5-norbornyl cation), which causes the monomer's lower reactivity and polymerizability, existed during the polymerization. The Tg of the polymers at the same molecular weight range ($\overline{DPn}$=3-5) decreased in the following order:

H-NB, CH_3-NB, C_2H_5-NB > C_5H_{11}-NB > C_7H_{15}-NB > $C_{10}H_{21}$-NB.
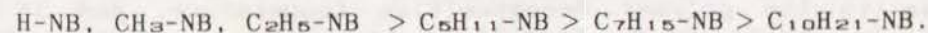
The effect of the alkyl substituent length on the Tg was discussed on the basis of the ^{13}C spin-lattice relaxation times (T_1) for the carbons in the alkyl group.

R-NB
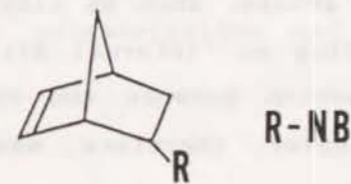
INTRODUCTION

The incorporation of bulky and stiff alicyclic structures into polymer main chains represents a useful method for increasing glass-transition temperature (Tg) of polymers, because such groups generally increase the energy required for onset molecular motion of the polymers.[1] Along this line of idea, the author has investigated the thermal properties of the cationically synthesized alicyclic structure containing polymers with high-Tg, such as the polymers from norbornadiene(I)[2, 3, 4] and from tetracyclo[4.4.0.1$^{2, 5}$.1$^{7, 10}$]dodecene-3 (II)[5], and found that the homopolymers were amorphous and with high Tg's [I, 290 ℃ ($\overline{Mn}$=4,800); II, 270 ℃ ($\overline{Mn}$=1,100)].
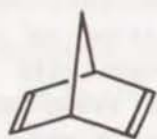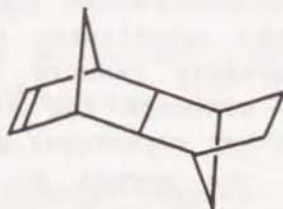
<center>I   II</center>

In the investigation[3, 5], in order that the polymers' Tg may be lowered to the moderate region (100-200 ℃), incorporation of the relatively flexible styrene unit into the alicyclic polymer chain was applied by the copolymerization of I or II with styrene, because the homopolymers' Tg are high and very close to the polymer decomposition temperature. And it was demonstrated that Tg could be controlled by the alicyclic-unit/ styrene-unit ratio in the copolymers. Concerning the controlling of Tg, except for the copolymerization, it is well-known that flexible pendant groups, such as alkyl groups, reduce the Tg of polymers by acting as "internal diluents" which lowered the frictional interaction between the chains.[6] One of the objectives of this chapter, therefore, was to investigate the effect of alkyl substituent on the Tg of the polymer. More specifically, 5-alkyl-2-norbornenes (III), which are the derivatives of norbornene and which have the potentiality to form the polymers with alicyclic structure in the main chains and with alkyl groups as side chains, were selected as monomers to investigate the effect of substituents length on the polymers' thermal properties.

<center>III C_nH_{2n+1}</center>
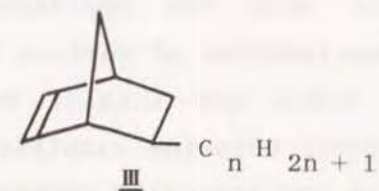
In the cationic polymerizations of norbornene[7] and II [5], the rearrangement of the carbocation formed from the monomers was reported to frequently occur. Moreover, Kennedy proposed that the relative polymerizabilities (a measure of degree of polymerization to be attained) of cycloalkenes were explained on the basis of the ability of the first-formed secondary cation to undergo a hydride shift to a nonpropagating tertiary cation.[8] We thought that 5-alkyl-2-norbornenes have the ability to form the tertiary cation (V) from the first-formed secondary cation (IV) during the polymerization, as shown in eq.(1). Their reactivity, polymerizability and polymer structures, however, might be different from those of non-substituted norbornene. The other object of this chapter, therefore, is to study the effects of the alkyl substituents and their length on the monomer reactivity and polymerizability during the cationic polymerization and the structure of the polymers.

$$(1)$$

III **IV** **V**
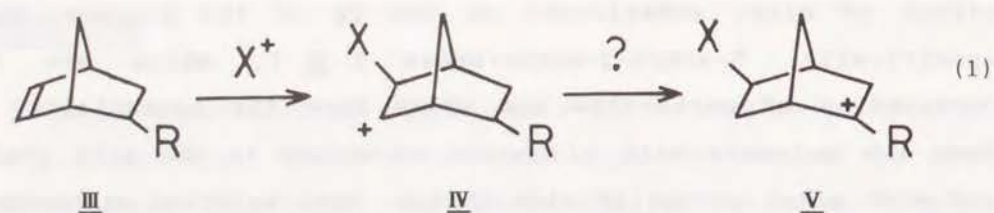
5-Alkyl-2-norbornenes (R-NB, where R = C_5H_{11}, C_7H_{15} and $C_{10}H_{21}$) were synthesized by the Diels-Alder reactions of cyclopentadiene with the corresponding 1-alkenes, and the cationic polymerizations of various R-NB (including R = H, CH_3, C_2H_5, C_5H_{11}, C_7H_{15} and $C_{10}H_{21}$) were carried out with the $AlEtCl_2$/tert-butyl chloride catalyst system in the same manner as described in the preceding chapters.[3, 4, 5] The effect of the substituent length on the monomer reactivity, polymerizability, and structure and thermal properties of the polymers were investigated, as described below.

EXPERIMENTAL SECTION

5-Alkyl-2-norbornenes. Norbornene (H-NB, Aldrich) and 5-methyl-2-norbornene (C1-NB) and 5-ethyl-2-norbornene (C2-NB) (both from Mitsui Petrochemical) were used after distillation (see Table 1). 5-Pentyl-2-norbornene (C5-NB), 5-heptyl-2-norbornene (C7-NB) and 5-decyl-2-norbornene (C10-NB) were synthesized by the Diels-Alder reactions of cyclopentadiene [CPD, formed in-situ via thermal retro Diels-Alder reaction of dicyclopentadiene (DCPD)] with the corresponding 1-alkenes (1-heptene, 1-nonene, and 1-dodecene, all from Wako Pure Chemical) as described elsewhere [eq.(2)];[5, 9] CPD:1-alkenes = 1:2 mole ratio, at 200 ℃ for 30 min at a pressure of 10 kg/cm². The purities of the R-NB's after distillation were listed in Table

1 together with other properties (boiling point, and endo/exo ratio) of R-NB's. ^{13}C chemical shifts of all R-NB's and their assignments were listed in Table 2 (measurement conditions are the same as shown below for polymers, excepting: at r.t.).

$$(2)$$

$$(n = 4,6 \text{ and } 9)$$
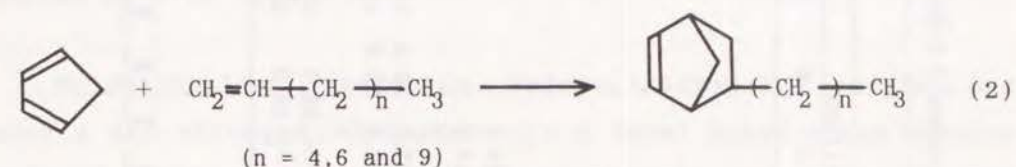
Table 1.

Properties of various 5-alkyl-2-norbornenes (R-NB)

Type of Substituent (R)	Boiling Point (℃ / mmHg)	Molar Ratio[a,b] of Endo / Exo	Purity[c] (%)
H	96 / 760	---	99.2
CH_3	115 / 760	80/20	99.1
C_2H_5	75 / 71	81/19	99.3
C_5H_{11}	68 / 3	71/29	98.7
C_7H_{15}	100 / 3	74/26	98.8
$C_{10}H_{21}$	140 / 3	75/25	97.5
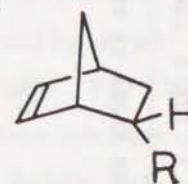
a) Endo: Exo:

b) Determined by ^{13}C-NMR.
c) Determined by GC.

Table 2

^{13}C chemical shifts (δ, ppm from TMS) of various 5-alkyl-2-norbornenes (R-NB)

Type of R-NB	Endo or Exo	Carbon No.[a] Norbornene Ring							Substituent									
		1	2	3	4	5	6	7	1	2	3	4	5	6	7	8	9	10
H-NB	---	41.9	135.2	135.2	41.9	25.3	25.3	48.5										
C1-NB	Endo	43.3	136.9	132.2	47.5	32.8	34.1	50.2	19.2									
	Exo	42.4	137.0	136.0	48.5	32.8	34.7	44.8	21.5									
C2-NB	Endo	42.6	136.9	132.3	45.2	41.0	32.3	49.6	27.7	13.1								
	Exo	41.9	137.0	136.2	46.1	41.0	33.0	45.3	29.5	13.3								
C5-NB	Endo	42.7	136.9	132.5	45.6	39.0	34.9	49.7	32.7	28.5	32.3	22.8	14.1					
	Exo	42.0	137.0	136.2	46.6	39.0	36.8	45.3	33.3	28.7	32.3	22.8	14.1					
C7-NB	Endo	42.7	136.9	132.5	45.6	39.0	34.9	49.7	32.7	28.6	30.0	29.7	32.1	22.8	14.1			
	Exo	42.0	137.0	136.2	45.6	39.0	36.8	45.3	33.3	28.8	30.0	29.7	32.1	22.8	14.1			
C10-NB	Endo	42.7	136.9	132.5	45.7	39.0	35.0	49.7	32.7	28.9	30.1	29.8	≀	29.9	29.5	32.1	22.8	14.1
	Exo	42.1	137.0	136.2	46.6	39.0	36.9	45.3	33.3	29.1	30.1	29.8	≀	29.9	29.5	32.1	22.8	14.1

a) Numbering of carbon atoms is as follows:

-80-
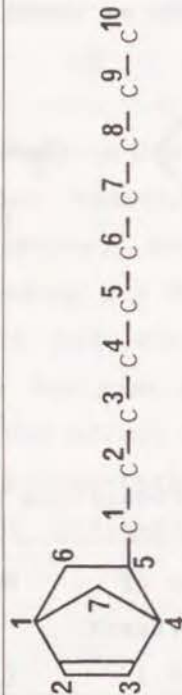
Materials. AlEtCl₂ was commercially obtained from Tosoh Akzo and used as an n-decane solution without further purification. CH₂Cl₂, tert-butyl chloride (t-BuCl, Wako) and n-heptane (the internal standard for GC analysis) were distilled over calcium hydride before use.

Polymerization Procedures. Polymerization was carried out under a dry nitrogen atmosphere in a 500ml baked glass reactor equipped with a stirrer and a condenser. The reaction was initiated by addition of an AlEtCl₂ solution into a monomer solution, and terminated with a prechilled ammoniacal methanol. The cocatalyst, t-BuCl, was added to a monomer solution before the addition of AlEtCl₂. The quenched polymerization reaction mixture was sequentially washed with a dilute aqueous acid and water to remove the initiator residues. The product was recovered by precipitation of the organic layer into methanol, and was dried in vacuum. Monomer conversion was determined by measuring the residual monomer concentration by gas chromatography with n-heptane as the internal standard. Polymer yield was determined by gravimetry.

Characterization of Polymers. The molecular weight distribution (MWD) of the polymers was measured by gel-permeation chromatography (GPC) in chloroform solutions at room temperature on a Waters liquid chromatograph (150-C ALC/GPC) equipped with a polystyrene gel column (7.5mmID × 60cm) and a refractive index (RI) detector. The $\overline{M}n$ and $\overline{M}w$ were calculated from GPC curves on the basis of a polystyrene standard calibration. As an index of carbon-carbon double bond content in the polymer, the iodine value (I.V.) was measured as previously reported (the iodine monochloride method).[10]

NMR samples were prepared by dissolving ca. 80 mg of the

-81-

polymer at 50 ℃ in ca. 0.6 ml of CDCl₃ in a 5 mm o.d. glass tube. ¹³C-NMR spectra were recorded on a JOEL GX-500 spectrometer: 125.8MHz; pulse angle 45°; pulse repetition time 5.0s; spectral width 20000Hz; number of scans 20,000; data point 64k. The ¹H decoupled ¹³C distortionless enhancement by polarization transfer (DEPT) method was also used to discriminate the carbon species. The spin-lattice relaxation time (T₁) measurement of the poly(C7-NB) was made using the inversion recovery method, which consists of the usual [180°-t-90°-acquisition(1.64s)-pulse delay(3.36s)] pulse sequence: ten different pulse separations (t); other conditions were same as shown above.

Glass-transition temperature (Tg) was measured by differential scanning calorimetry (DSC) on a Seiko DSC-220C instrument with polymer samples of about 10mg under a nitrogen flow at a scanning rate of 10 ℃ per min.

RESULTS AND DISCUSSION

1. Polymerizations of Various R-NB's

Polymerizations of R-NB's with the AlEtCl₂/t-BuCl catalyst system[3] in CH₂Cl₂ were carried out under various conditions (Table 3). All polymers listed in Table 3 were completely soluble in toluene.

(A) Monomer Reactivity and Polymerizability

The time-conversion curves for various R-NB's are shown in Figure 1. Monomer conversions after 3 h reached around 70% for H-NB but as low as 10% for other alkyl-substituted norbornenes irrespective of the alkyl substituents' length. Therefore, the introduction of alkyl groups, even the shortest methyl group,

Table 3.

Cationic Polymerization of Various 5-alkyl-2-norbornenes (R-NB) by AlEtCl₂/t-BuCl in CH₂Cl₂.[a]

Run No.	Type of R	[M]₀ (M)	Temp. (℃)	Monomer Conv. (%)	Polymer Yield (wt%)	I.V. (g-l₂/100g-poly.)	$\overline{Mn}$[b]	$\overline{Mw/Mn}$[b] (GPC)	$\overline{DPn}$[c]	$\overline{Mn}$[d] (I.V.)	Pysical[e] Appearance at 23℃	Tg[f] (℃)
1	H	1.0	-50	69.8	56.7	48.5	410	1.7	4.4	520	transparent colorless glassy solid	+27
2	H	1.0	-78	54.7	38.6	32.7	730	1.7	7.7	730	white powder	+155
3	H	3.0	-78	41.6	29.1	24.6	1170	2.0	12.4	970	white powder	+231
4	CH₃	1.0	-50	10.6	8.6	69.9	330	1.4	3.1	360	transparent yellow glassy solid	+36
5	CH₃	3.0	-78	5.8	2.3	49.5	600	1.3	5.5	550	white powder	+124
6	C₂H₅	1.0	-50	8.1	5.8	65.1	360	1.4	3.0	390	transparent yellow glassy solid	+22
7	C₂H₅	3.0	-78	4.5	1.1	56.8	650	1.3	5.3	550	transparent yellow glassy solid	+94
8	C₅H₁₁	1.0	-50	8.6	5.2	55.2	540	1.3	3.3	460	yellow viscous liquid	-6
9	C₇H₁₅	1.0	-50	9.3	3.3	43.0	580	1.4	3.0	590	yellow viscous liquid	-25
10	C₁₀H₂₁	1.0	-50	10.3	6.3	44.5	720	1.3	3.1	570	yellow viscous liquid	-51

a) Other polymerization conditions: [AlEtCl₂]₀/[t-BuCl]₀ = 30.0/15.0 mM, for 180 min.
b) Calculated from GPC data (Polystyrene standard calibration).
c) $\overline{DPn}$ = ($\overline{Mn}$ by GPC)/(MW of R-NB).
d) Calculated from I.V. data, assuming each polymer chain contains one C=C bond at a terminated end.
e) Visually observed at 23℃ after the polymer was dried at 130℃ for 12 hr.
f) Taken from the DSC data at the 2nd heating cycle.
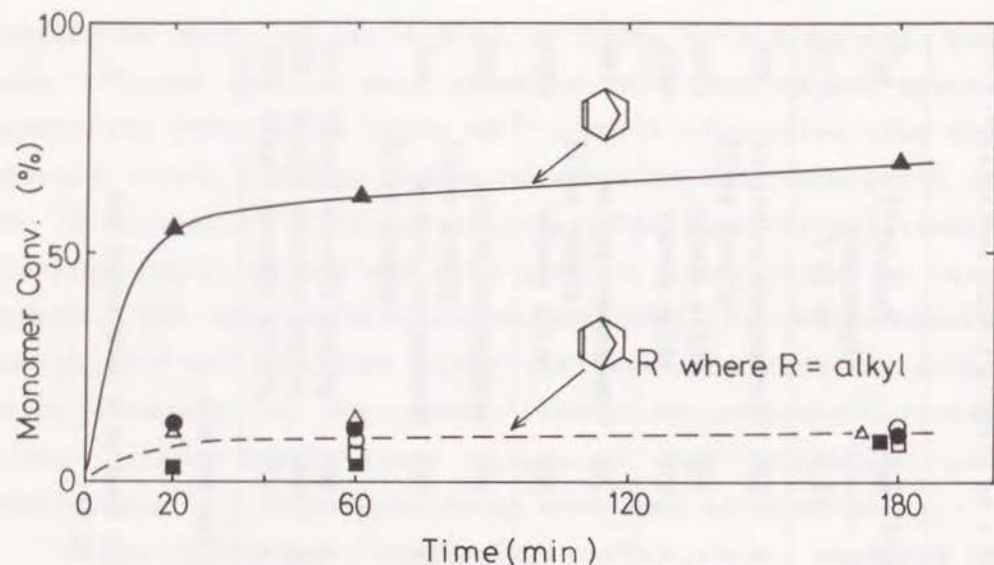
Figure 1. Time-conversion curves for the polymerization of various R-NB's in CH_2Cl_2 at -50 ℃ by $AlEtCl_2/t$-BuCl (= 30/10 mM) and $[M]_0$=1.0M. Type of R-NB: (▲) H-NB; (△) C1-NB; (■) C2-NB; (□) C5-NB; (●) C7-NB; (○) C10-NB.

into the 5-position of the norbornene ring remarkably reduced the monomer reactivity in cationic polymerization, while their length did not affect the reactivity.

Figures 2 and 3, respectively, show the molecular weight distributions (MWD) and the number-average of degree of poly-merization ($\overline{DP}n$) of the various poly(5-alkyl-2-norbornene)s obtained at -50 ℃ with the initial monomer concentration of 1.0 M. Although the MWD (Figure 2) did not clearly display the difference between the type of monomers, the $\overline{DP}n$ data (Figure 3) revealed that the polymerizability was decreased by the incorporation of alkyl groups, in a similar manner to the monomer reactivity. Therefore, it could be concluded that H-NB had a higher reactivity and polymerizability than those of the alkylnorbornenes.
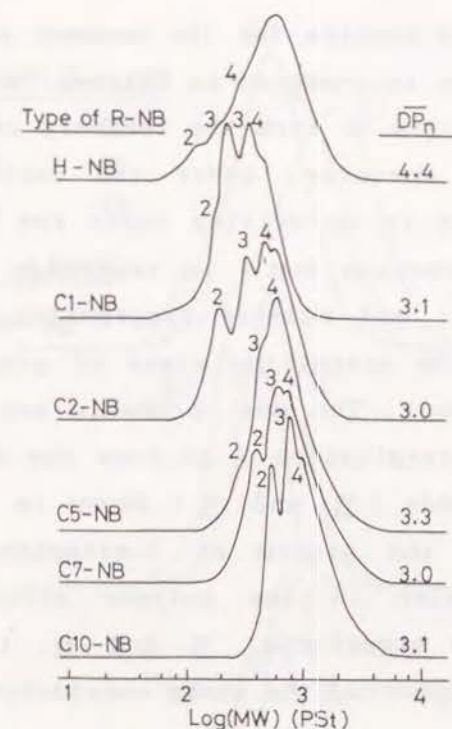
Figure 2. MWD's of poly(R-NB)s obtained in CH_2Cl_2 at -50 ℃. Type of R-NB and $\overline{DP}n$ as indicated: see Table 3 for the $\overline{M}n$ data and reaction conditions.
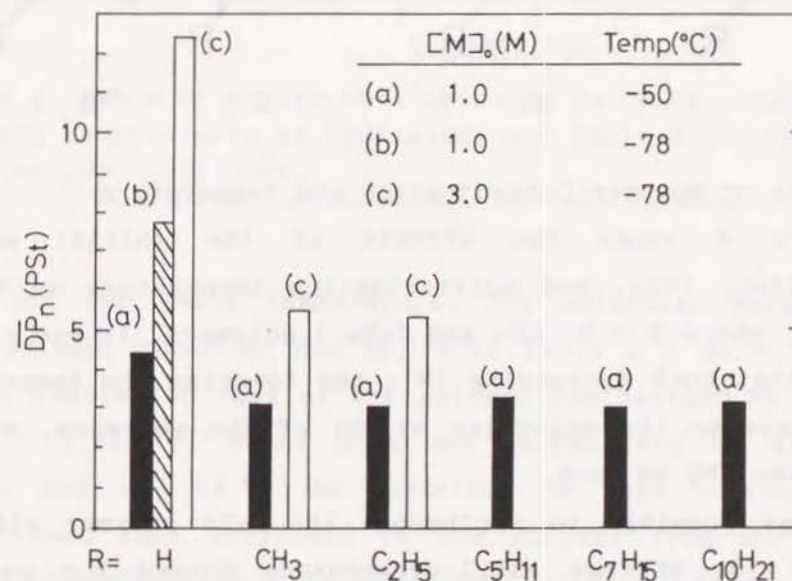
Figure 3. $\overline{DP}n$'s of poly(R-NB)s obtained in CH_2Cl_2. $[M]_0$ and temperatures as indicated: see Table 3 for the $\overline{M}n$ data and reaction conditions.

The observed results for the monomer reactivity and poly-merizability were interpreted as follows: 5-Alkyl-2-norbornenes have the possibility to form the tertiary cation ($\underline{V}$), whereas H-NB does not. Moreover, under the cationic polymerization conditions there is no driving force for the tertiary cation ($\underline{V}$, "buried carbenium ion") to rearrange to the less stable secondary cation, and neither propagation (because of steric compression in the transition state of propagation) nor rear-rangement can occur. The most probable process, therefore, is deprotonation (termination) to form the double-bond contain-ing terminated ends ($\underline{VI}$ and $\underline{VII}$) shown in eq.(3), as reported by Kennedy for the system of 2-methylene norbornane.[8] As discussed in later in the polymer structure section, the existence of the structures, $\underline{VI}$ and $\underline{VII}$, in the poly(5-alkyl-2-norbornene)s supported the above consideration.

$$\underline{V} \qquad \underline{VI} \qquad \underline{VII} \qquad (3)$$
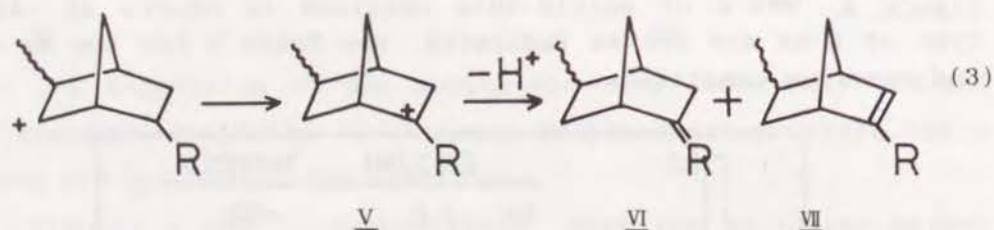
(B) Effects of Monomer Concentration and Temperature

Figure 4 shows the effects of the initial monomer concentration, $[M]_0$, and polymerization temperature on MWD of the R-NB (where R = H, CH₃ and C₂H₅) polymers. It was clearly observed that both increasing $[M]_0$ and lowering the temperature led to increase the molecular weight of the polymers, without changing the MWD so much.

It was possible to synthesize the H-NB polymer with the $\overline{DP}n$ above 10, whereas alkyl-norbornenes formed the polymers with $\overline{DP}n$ of at most 5.5, even in the conditions of the higher

	$[M]_0$(M)	Temp(°C)
(a)	1.0	-50
(b)	1.0	-78
(c)	3.0	-78
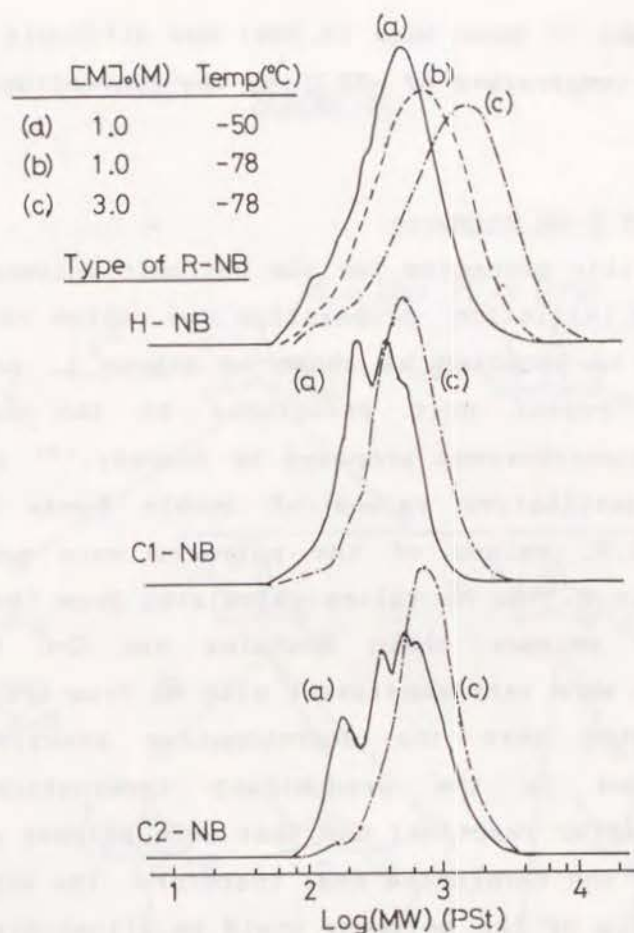
Figure 4. MWD's of poly(R-NB)s obtained in CH₂Cl₂. Type of R-NB, $[M]_0$ and temperatures as indicated: see Table 3 for the $\overline{M}n$ data and reaction conditions.

$[M]_0$ and the lower temperature. The molecular weight of the H-NB polymer shown by Run No. 3 in Table 3 ($\overline{M}n = 1,170$) is almost similar to that of the polymer synthesized by Kennedy[11] ($\overline{M}n = 1,480$), where H-NB was polymerized by AlEtCl₂, in C₂H₅Cl and at -78 °C. As described in this section, it was reconfirmed that synthesis of the polymer from norbornene or its alkyl-substituted derivatives with a moderately high

molecular weight (= more than 10,000) was difficult to achieve even at a low temperature of -78 ℃ by the conventional cationic method.

2. Structure of R-NB Polymers

The plausible mechanism for the cationic polymerization of R-NB including initiation, propagation and cation rearrangement reactions can be proposed as shown in Scheme 1, according to the probable repeat unit structures in the cationically polymerized polynorbornene proposed by Kennedy.[12] In order to obtain the quantitative values of double bonds in polymer chains, the I.V. values of the polymers were measured and listed in Table 3. The $\overline{Mn}$ values calculated from the I.V. data assuming each polymer chain contains one C=C bond at a terminated end were very consistent with $\overline{Mn}$ from GPC data. This result indicated that the deprotonation reaction of the propagating end is the predominant termination reaction (strictly, transfer reaction) and that each polymer chain has a double bond at the terminated end. Therefore, the structures of the repeat units of the polymers could be illustrated as shown in Scheme 2.

In order to investigate the structure of the norbornene-type polymer obtained by this cationic system, ^{13}C-NMR analysis on the C2-NB polymer sample (Run No.6) was carried out. The reason for the selection of alkyl norbornene polymer as a sample was as follows: By introducing the alkyl group into the polymer structure, the structure would be more easily analyzed than that of the H-NB polymer using the clue of ^{13}C chemical shifts of carbons in the alkyl groups and olefinic carbons to which the alkyl groups were attached.

The ^{13}C-NMR spectrum of the paraffinic carbon region [poly(C2-NB), Run No.6] was shown in Figure 5. The carbon

Scheme 1.

Scheme 2.

Type	Initiated Ends	Repeat Units	Terminated Ends

X = tBu or H
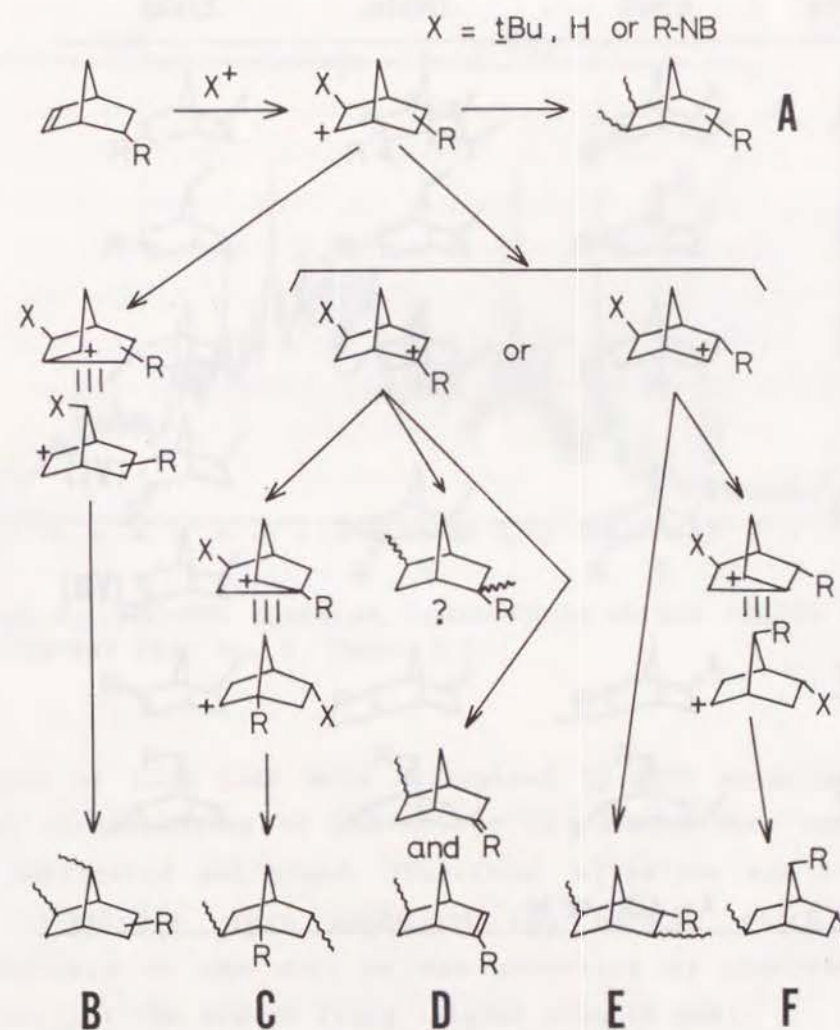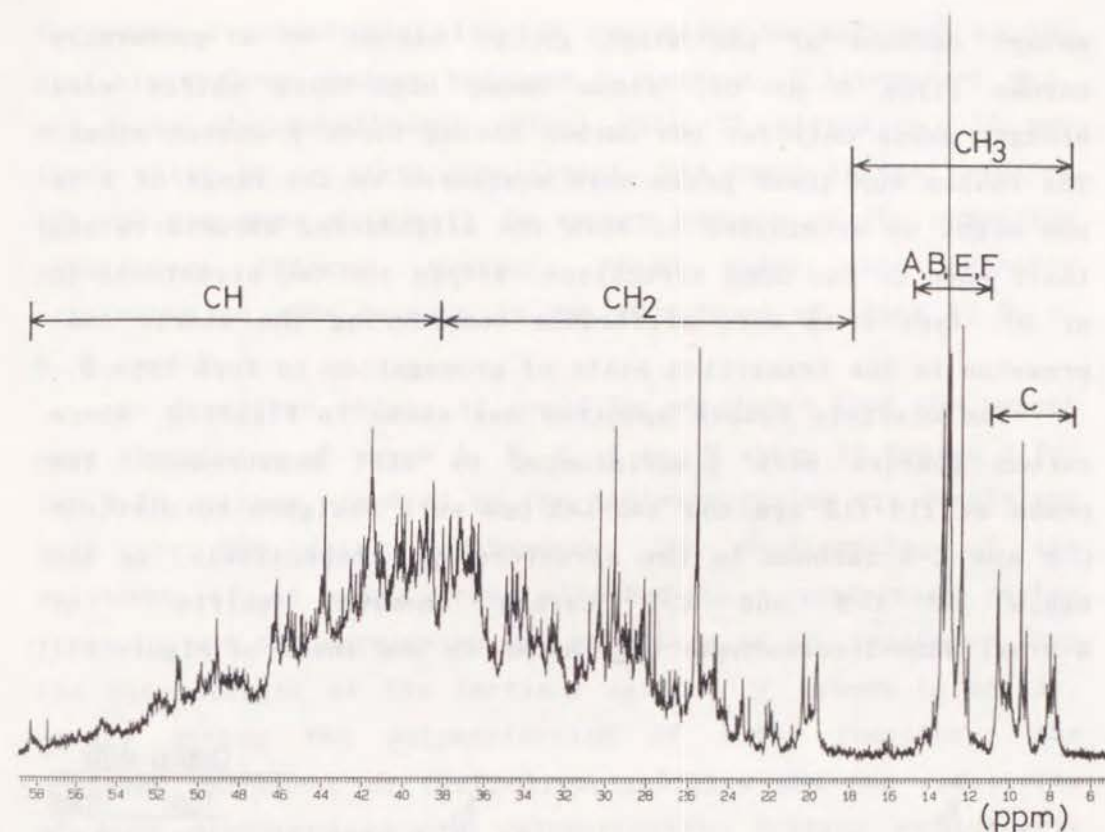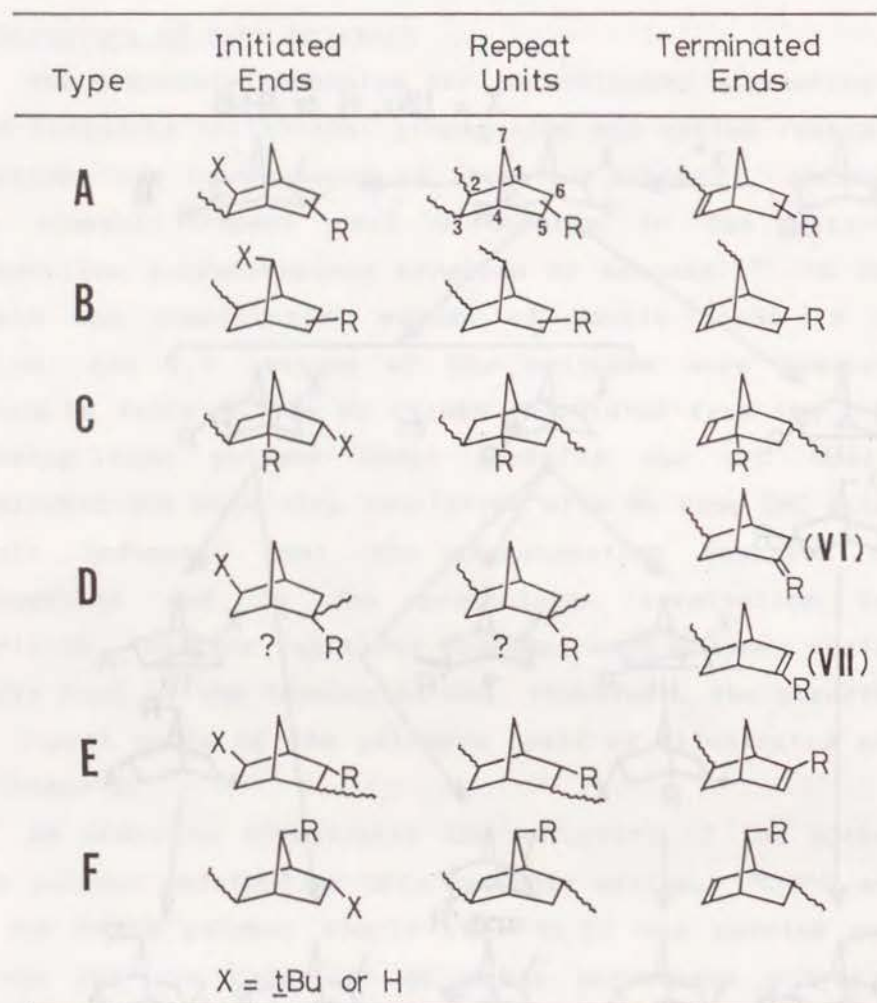
Figure 5. ^{13}C-NMR spectrum (paraffinic carbon region) of the poly(C2-NB) [Run No. 6, Table 3].

species of each peak were determined by DEPT measurement. The peaks corresponding to the CH₂ or CH carbons were observed to be complicated and broad. Therefore, attention was focused on the relatively sharp peaks of CH₃ carbon, which is less susceptible to the endo or exo structure as observed in the monomer, at the higher field (higher than 15 ppm).

The peaks of 12-14 ppm were assigned to the methyl carbons of the ethyl groups attached to types A, B, E, and F units, because the chemical shifts of the methyl carbons were expected not to change very much from those in C2-NB monomer. Other peaks of 9-11 ppm and around 8 ppm might be assigned to the

methyl carbons of the ethyl groups bonded to a quaternary carbon (type C or D), since these high-field shifts were brought about only for the carbon having three γ-carbon atoms. The reason why these peaks were scattered in the range of 8-11 ppm might be attributed to both the neighboring structures and their endo or exo bond directions. Within the two structures (C or D), type C is more preferable considering the steric compression in the transition state of propagation to form type D.

The olefinic carbon spectrum was shown in Figure 6, where carbon species were discriminated by DEPT measurement. The peaks at 110-112 ppm and 140-142 ppm were assigned to olefinic C-8 and C-5 carbons in the structure Ⅵ, respectively, on the basis of C-8 and C-5 carbon chemical shifts[13] of 5-ethylidene-2-norbornene (Ⅷ, shown in the inset of Figure 6).

	Chemical shifts	
	(cis)	(trans)
C-5 :	141.96	141.34
C-8 :	112.68	113.09
		(ppm)
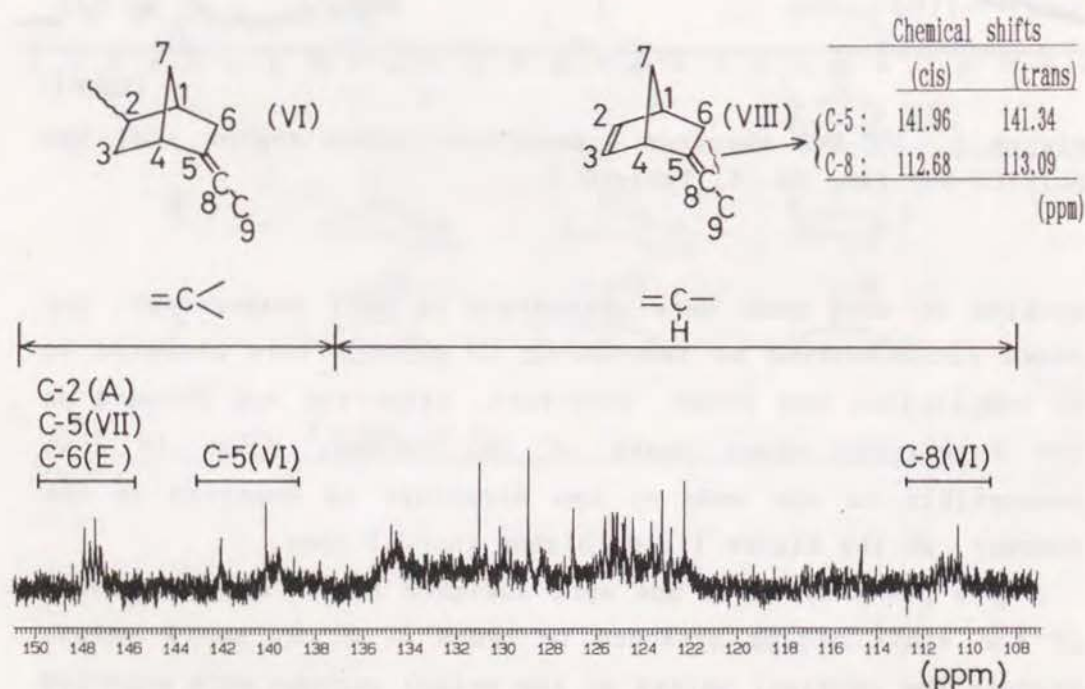
Figure 6. ^{13}C-NMR spectrum (olefinic carbon region) of the poly(C2-NB) [Run No. 6, Table 3].

The peaks resonating at 146-148 ppm might be assigned to the olefinic carbons without hydrogen in types A, D (structure Ⅶ), and E by the substituent effect rule,[14] giving ca. 10 ppm lower shift by an alkyl substituent. The peaks in the range of 122-136 ppm were difficult to assign because of the competing substituent effects. However, these peaks were probably attributed to -CH= carbons in the structures of types A, B, C, D, E, and F.

As described above, it could be concluded that the repeat unit structures of types A, B, C, E and F shown in Scheme 2 for the R-NB polymer prepared by the cationic system are consistent with the NMR data. Furthermore, the confirmation of the existence of an alkyl group attached to a quaternary carbon (type C) and the terminated end structure of Ⅵ indicated that the intermediate of the tertiary cation, Ⅴ, shown in eq.(3), exists during the polymerization of R-NB. Therefore, the observed phenomena on the polymerizability and the reactivity of R-NB discussed in the polymerization section was clearly interpreted by the existence of the cation Ⅴ.

3. Tg of Polymers

Tg and physical appearance at 23 ℃ of all polymers were shown in Table 3. The molecular weight dependency of Tg for various alkyl-substituted norbornene polymers ($\overline{DPn}$ vs. Tg) was also shown in Figure 7. Tg drastically increased with increase of $\overline{DPn}$ in this oligomer region ($\overline{DPn}$: below 12.4), and the longer substituent reduced the Tg. Interestingly, the Tg of C1-NB and C2-NB polymers were found to be almost the same level of that of non-substituent H-NB polymer in the similar $\overline{DPn}$ region. That is, the Tg of the polymers at the same $\overline{DPn}$ (= 3 ~ 4) decrease in the following order:

H-NB, C1-NB, C2-NB > C5-NB > C7-NB > C10-NB.
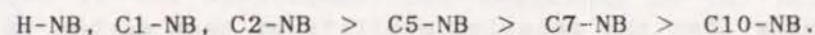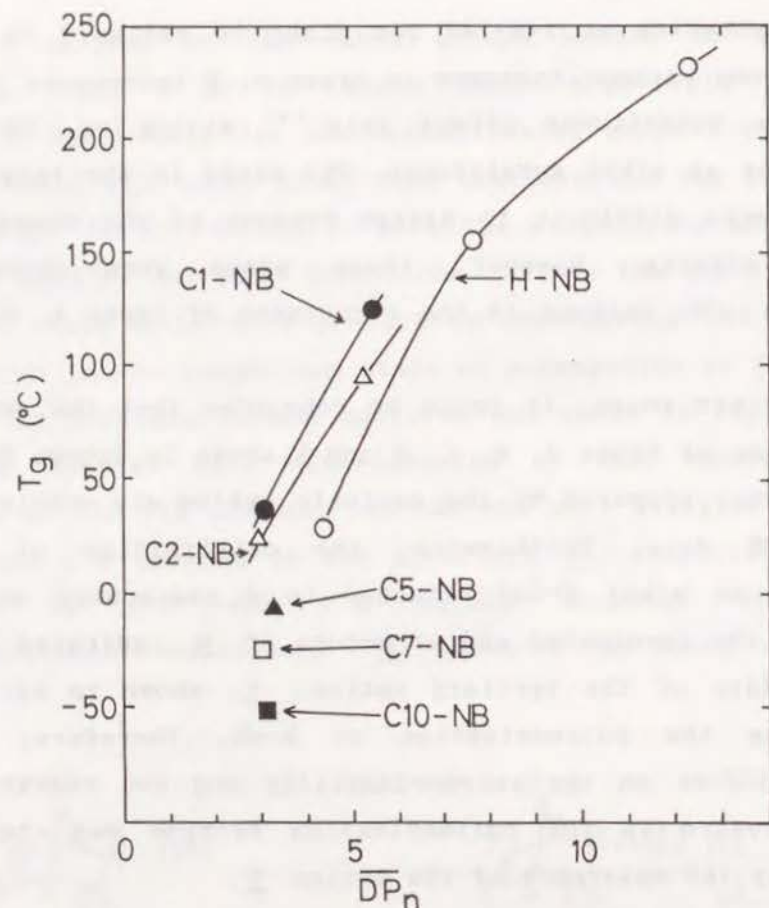
Figure 7. Tg of poly(R-NB)s as a function of $\overline{DP}_n$ (by GPC). Type of R-NB as indicated.

In order to explain the effect of the length of alkyl substituent on the polymer's Tg, an attempt was made to determine the atomic mobility of each carbon in the substituent through their relaxation times (T_1) measured by the inversion recovery method.[15] Although Tg of a polymer basically reflects a molecular motion at a glass-rubber transition in a solid state, we measured the relaxation time, as an alternative measure of atomic motion, in a solution state for convenience sake, assuming that the relative mobility of each carbon in the alkyl substituent at a solid state is in parallel with that in

solution state.

Figure 8 shows the ^{13}C-NMR spectra of poly(C7-NB) [Run No. 9] measured by the inversion recovery method with different pulse separations (t). The relaxation time (T_1) calculated from eq.(4) for each carbon in the alkyl substituent was listed in Table 4.

$$M(t) = M_0 \times [1 - 2e^{-(t/T_1)}] \qquad (4)$$

where $M(t)$: peak intensity at t

M_0 : peak intensity at $t = \infty$

T_1 : relaxation time

The dipole-dipole mechanism generally dominates ^{13}C relaxation behavior. Therefore, if the number of hydrogen atoms attached to a carbon is the same, the relation between T_1 and the rotational correlation time (τ_c) shown in eq.(5) can be applied.[16]

$$T_1 \propto 1 / \tau_c \qquad (5)$$

That is, T_1 is inversely proportional to the τ_c, where τ_c represents an average time during which an atom stays at the same place. In other words, the faster the motion of a carbon atom is, the larger T_1 becomes.

As shown in Table 4, T_1's of carbons consisted of the alicyclic structure in the main chain are almost in the same range as those of C-1 and C-2 carbons in the alkyl side chain $(T_1 = 0.14 - 0.43)$. On the other hand, T_1's of carbons from C-3 to C-7 in the alkyl side chain becomes larger with being more remote from the main chain. Therefore, it could be concluded that the decrease of the Tg with increasing the number of carbons in the substituent was explained on the basis of the
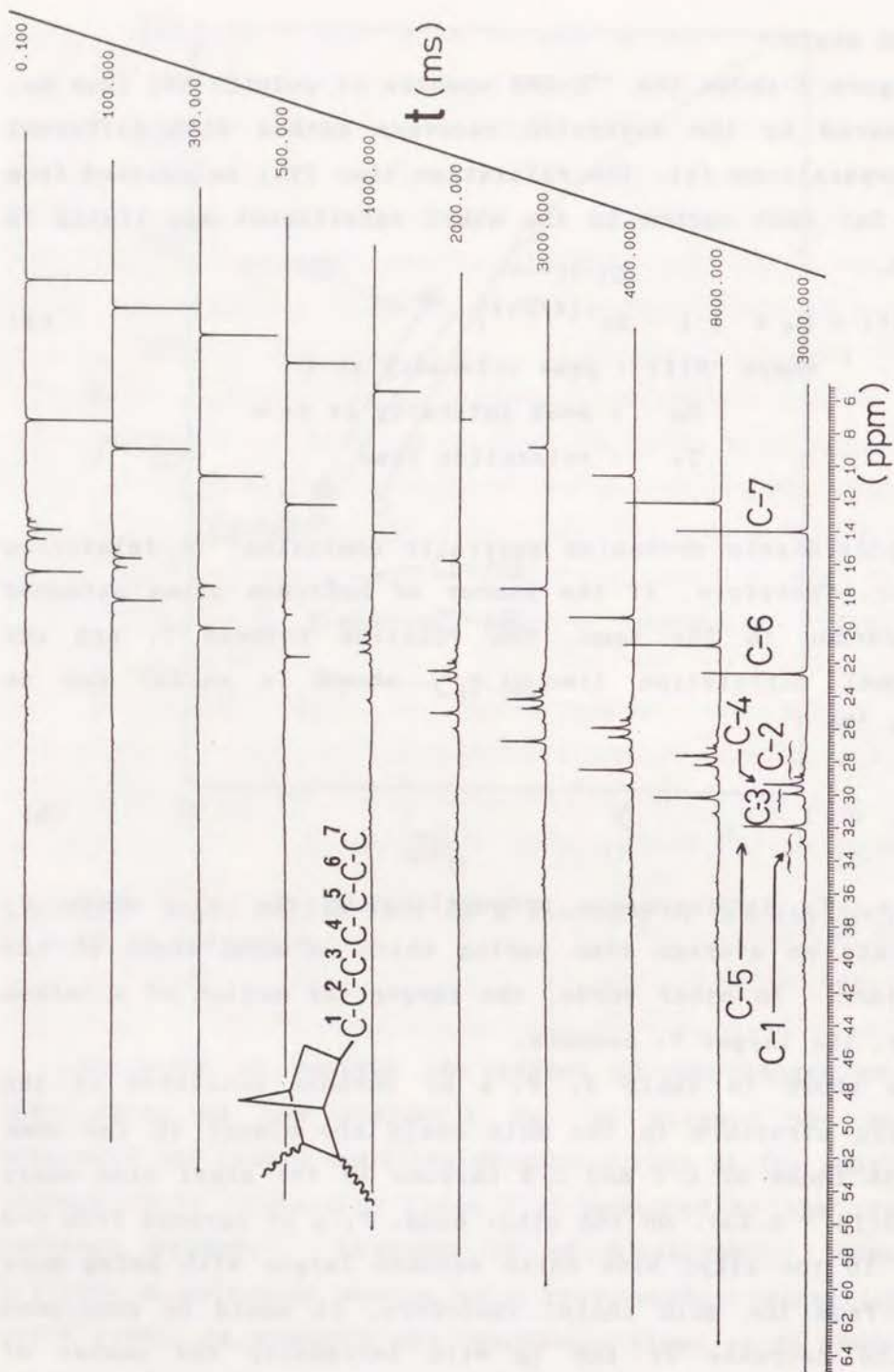
Figure 8. ^{13}C-NMR spectra of the poly(C7-NB) [Run No. 9, Table 3] obtained by the inversion recovery method at 50 °C in CDCl₃ with different pulse separations (t).

Table 4.

Spin-lattice relaxation time of carbons in the C7-NB polymer[a)]

Type of Carbon	Relaxation Time (T_1) (sec)
Substituent	
C-1	0.29
C-2	0.43
C-3	0.58
C-4	1.01
C-5	1.44
C-6	2.31
C-7	3.46
Carbons in main chain alicyclic structure	0.14-0.29

a) For numbering of carbons; see Figure 8.

mobility of the substituent in the polymer as an internal diluent. Moreover, the fact that the Tg's of C1-NB and C2-NB polymers were almost in the same level of that of non-substituent H-NB polymer could be interpreted by the smaller values of T_1 for C-1 and C-2 carbons in the alkyl group, which were equivalent to those of carbons in the alicyclic main chain structure.

REFERENCES AND NOTES

1) L.H. Sperling, "Introduction to Physical Polymer Science", Wiley-Interscience, New York, 1985, Chapter 6.

2) A. Mizuno, M. Onda, T. Sagane, Polymer, 32, 2953 (1991).

3) Chapter 1 of this thesis; Makromol. Chem., 193, 2081 (1992).

4) Chapter 2 of this thesis; Makromol. Chem., 193, 2091 (1992).

5) Chapter 3 of this thesis; Makromol. Chem., in press.

6) Polymethacrylates [S.S. Rogers, L. Mandelkern, J. Phys. Chem., 61, 985 (1957)]; poly-p-alkyl-styrenes [W.G. Barb, J. Polym. Sci., 37, 515 (1959)]; poly- α -olefins [M.L. Dannis, J. Appl. Polym. Sci., 1, 121 (1959); K.R. Dunham, J. Vandenbergh, J.W.H. Farber, L.E. Contois, J. Polym. Sci., 1A, 751 (1963)]; and polyacrylates [J.A. Shetter, Polym. Lett., 1, 209 (1963)].

7) J.P. Kennedy, "Cationic Polymerization of Olefins: A Critical Inventory", John Wiley & Sons, New York, 1975, p. 228, and reference therein.

8) J.P. Kennedy, H.S. Makowski, J. Polym. Sci., Part C, No.22, 247 (1968).

9) (a) R. Ohm, C. Stein, Encyclop. Chem. Technol., 3rd. Ed., 18, 436 (1982). (b) Fr. Demande 1,535,460 (July 1, 1968), J. Verge, C. Pailloux, J.-C. Muller, J.-C. Robinet (to Charbonages de France); U.S. Pat. 3,557,072 (Jan. 19, 1971) (to Charbonages de France).

10) T.S. Lee, I.M. Kolthoff, E. Johnson, Anal. Chem., 22, 995 (1950).

11) J.P. Kennedy, H.S. Makowski, J. Macromol. Sci., (Chem.), A1, 345 (1967).

12) J.P. Kennedy, Encyclop. Polym. Sci. Technol., 7, 754 (1967).

13) W. Bremser, L. Ernst, B. Franke, R. Gerhards, A. Hardt, P.M.E. Lewis, "Carbon-13 NMR Spectral Data", 4th Ed., Verlag Chemie, Weinheim, 1987, References 32907 and 32913.

14) G.C. Levy, G.L. Nelson, "Carbon-13 Nuclear Magnetic Resonance for Organic Chemists", Wiley-Interscience, New York, 1972, Chapter 3.

15) Ref. 14), Chapter 9.

16) F.W. Wehrli, T. Wirthlin, "Interpretation of Carbon-13 NMR Spectra", Heyden, London, 1978, Chapter 4.

PART II

SYNTHESIS OF POLY(VINYL ETHER)S
WITH RIGID AROMATIC PENDANT STRUCTURES:
CONTROL OF LIQUID CRYSTALLINITY

CHAPTER 5

EFFECTS OF MOLECULAR WEIGHT DISTRIBUTION ON THERMAL PROPERTIES OF SIDE-CHAIN LIQUID CRYSTALLINE POLY(VINYL ETHER)S WITH PENDANT BIPHENYL MESOGENIC GROUPS

ABSTRACT

Three biphenyl-containing vinyl ether monomers: 2-(4-biphenyloxy)ethyl vinyl ether (I), 2-(4-biphenylcarboxy)ethyl vinyl ether (II), and 2-(4'-methoxy-4-biphenyloxy)ethyl vinyl ether (III), were cationically polymerized with the hydrogen iodide/iodine (HI/I$_2$) initiator system to form living polymers with narrow molecular weight distributions. The thermal properties of the polymers were determined by DSC and by visual observations of samples placed on a hot stage on a polarizing microscope. Polymer I and Polymer II formed only isotropic melts, but Polymer III showed enantiotropic, liquid crystalline (LC) behavior, and formed both smectic and nematic phases after one heating and cooling cycle. For comparison, polymers were also prepared with boron trifluoride etherate (BF$_3$OEt$_2$) as the initiator. Polymer III obtained with this initiator had a much broader molecular weight distribution and formed only a nematic phase. At approximately the same molecular weight, this sample also had a much higher isotropization temperature than the narrow distribution sample of Polymer III.
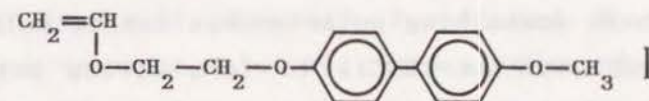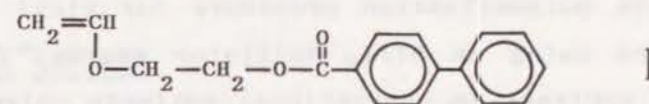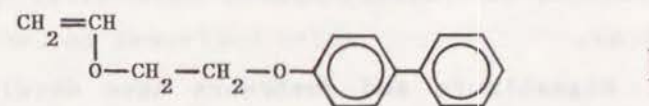
INTRODUCTION

Liquid-crystalline polymers (LCP) can contain mesogenic units either in the main chain or in the side chain, and both types are of theoretical and practical interest.[1] In contrast to the main chain LCP, the liquid-crystalline order of side chain LCP is generally closely related to that of the monomer,[2] so side chain LCP are of value for investigations on the relationship between mesogenic unit structure and mesophase type in polymers as compared to low molecular weight mesogens.

Side-chain LCP can be prepared by three different routes including addition polymerization, condensation polymerization and post-reactions of polymers.[2] Among the three methods, the most convenient approach is to introduce the mesogenic unit beforehand into a reactive monomer capable of undergoing addition or chain-growth polymerization.[2] However, for the most part, the side chain LCP prepared by chain-growth polymerization have been limited to polymethacrylates,[3] polyacrylates,[3] and polystyrene derivatives,[4] and very few of these investigations were concerned with the control and effect of molecular weight distribution on the properties of the LCP. One example of such control is the preparation of polymethacrylates by group-transfer polymerization,[5] but the molecular weight distributions of these polymers were still quite broad ($\overline{Mw}/\overline{Mn} = 1.2-1.8$).

Recently, Higashimura and coworkers have developed a new living cationic polymerization procedure for vinyl ethers and propenyl ethers using an HI/I_2 initiator system.[6-8] By this technique, in contrast to conventional cationic polymerization, even vinyl ethers containing polar groups can be polymerized in a polar solvent such as CH_2Cl_2 to form living polymers. The author's goal, therefore, was to prepare side chain LC poly-(vinyl ether)s with controlled molecular weight distributions by using this type of living cationic technique. If polymers with narrow distributions could be made in this manner, the effect of molecular weight on thermal properties could be determined without the undue influence of the component low and high molecular weight fractions. For this purpose, poly(vinyl ether)s were prepared by the living cationic polymerization of monomers containing biphenyl groups, including I, II, and III below:
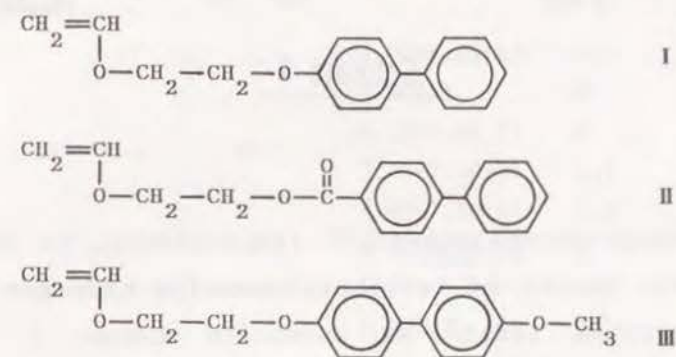
The cationic polymerization reactions of I and III[9] initiated with conventional Lewis acids were previously reported, and as expected, these reactions yielded polymers with broad molecular weight distributions. Living cationic polymerization reactions of I, II, and III, which were carried out in the present chapter, gave narrow molecular weight distributions, as described below.

EXPERIMENTAL SECTION

Monomer Synthesis. Monomers I, II, and III were prepared by the phase transfer-catalyzed condensation of 2-chloroethyl vinyl ether with 4-phenylphenol,[9] sodium-4-phenylbenzoate,[10]
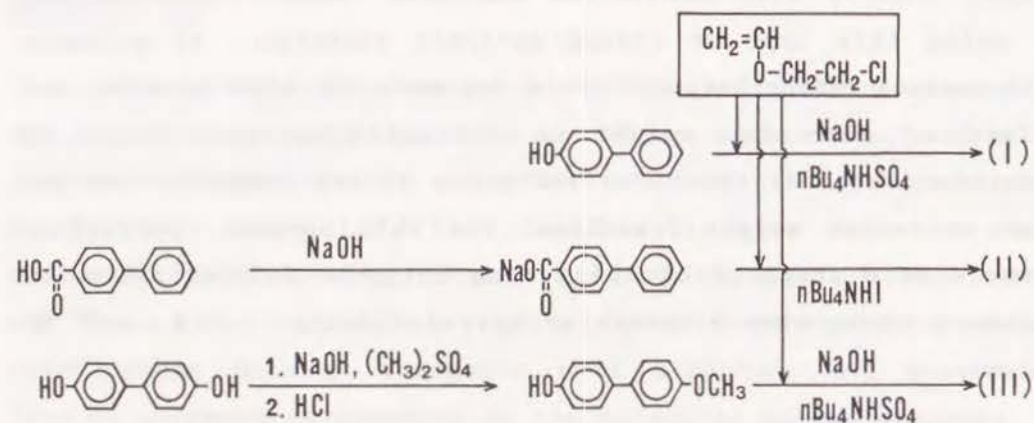
Scheme 1

and 4-(4'methoxy-phenyl)phenol,[9] respectively, in the presence
of a catalytic amount of tetrabutylammonium hydrogen sulfate or
tetrabutylammonium iodide as shown in Scheme 1. The three
monomers were purified by recrystallization from methanol, and
the melting points and the chemical shifts of the ^{1}H-NMR
spectra of the monomers are summarized in Table 1.

Materials. The hydrogen iodide (HI), iodine (I_2), and
boron trifluoride etherate (BF_3OEt_2) initiators and the
solvents (toluene, dichloromethane, and n-hexane) were purified
and used as previously reported.[6]

Polymerization Procedures. Cationic polymerization reac-
tions were carried out in predried Schlenk tubes equipped with
a three-way stopcock under a dry nitrogen atmosphere after the
solid monomers were degassed. The reactions with BF_3OEt_2 were
carried out by adding the initiator solution to the monomer
solution, but for the HI/I_2 initiator, an HI solution in

Table 1.

Characterization of the monomers

Monomer	Tm[a]	Td[b]	Tc[b]	^{1}H-NMR chemical shift		
	(℃)			δ (ppm)	Proton[c]	Ratio
I	79	-	63	3.90-4.40(m)	a,c,d	6
				6.55 (d of d)	b	1
				6.95-7.10(m)	e	2
				7.25-7.70(m)	f,g,h,i	7
II	76	-	37	4.05-4.25(m)	a,c	4
				4.60(m)	d	2
				6.53(d of d)	b	1
				7.35-7.50(m)	h,i	3
				7.60-7.70(m)	f,g	4
				8.10-8.15(m)	e	2
III	121	109[d]	105[d]	3.82(s)	i	3
				3.90-4.35(m)	a,c,d	6
				6.55(d of d)	b	1
				6.85-7.05(m)	h,e	4
				7.40-7.55(m)	f,g	4

a) Determined by DSC (taken from the 2nd heating cycle thermogram).

b) Determined by DSC (taken from the 1st cooling cycle thermogram).
   Td, deisotropization temp.; Tc, recrystallization temp.

c)
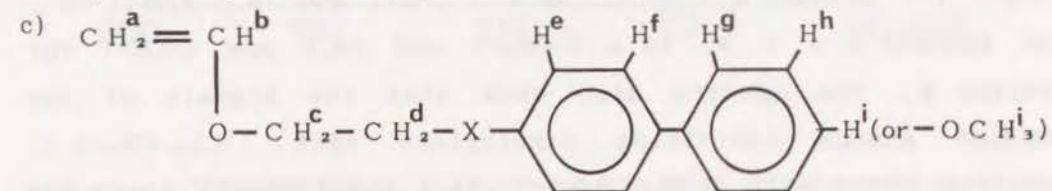
I, X = O; II, X = OC(=O); III, X = O.

d) Monotropic liquid crystalline phase was identified with the polarizing
   microscope (mosaic texture characteristic of smectic phase was observed).

n-hexane was added to the monomer solution, and an iodine solution was then added to this mixture to initiate polymerization. The reactions were terminated with cold ammoniacal methanol. The quenched polymerization solution was washed as previously reported,[7] and the conversion of monomer was determined by gel permeation chromatography (GPC, see conditions shown below). All polymers were purified by precipitation from CH_2Cl_2 solutions into methanol and were dried in vacuum.

Characterization of Monomers and Polymers. The molecular weight distribution of the polymer was measured by GPC on samples in $CHCl_3$ solutions on Waters liquid chromatograph equipped with five polystyrene gel columns (8mm × 23cm each) and a refractive index (RI) detector. The number-average molecular weight ($\overline{Mn}$) and weight-average molecular weight ($\overline{Mw}$) were calculated with the use of a polystyrene calibration curve. ^{1}H- and ^{13}C-NMR spectra were obtained with Varian XL-200 and XL-300 spectrometers in $CDCl_3$ at room temperature. In the ^{13}C-NMR spectra of polymers (see Figures 1, 2, and 3), the absorptions of the methylene ($-CH_2-$) and the methine ($-CH-$) carbons in the main chain structure appears at 40.9, 39.2 ($-CH_2-$) and 74.9 ppm ($-CH-$) for polymer I ; 40.6, 39.2 ($-CH_2-$) and 74.1 ppm ($-CH-$) for polymer II ; 41.4, 40.8 ($-CH_2-$) and 74.1 ppm ($-CH-$) for polymer III. The spectra also show that the signals of the pendant groups containing oxyethylene unit [$-CH_2-CH_2-O-$], ethylene ester unit [$-CH_2-CH_2-O-C(=O)-$] and biphenyl group are exactly the same as those of corresponding monomers. All polymers also showed the expected ^{1}H-NMR spectra.

Thermal analysis was carried out on a Perkin-Elmer DSC-2 instrument with polymer samples of about 10 mg under a nitrogen flow at a scanning rate of 10 ℃/min. Indium and naphthalene
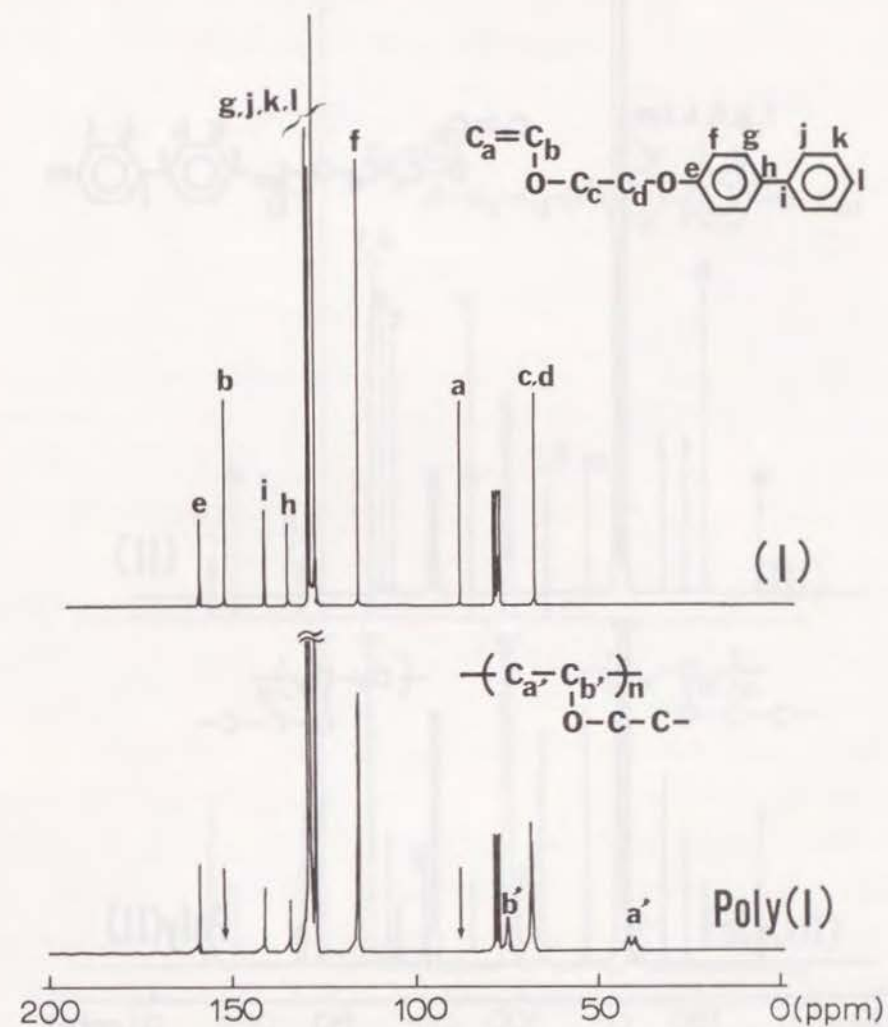
Figure 1. ^{13}C-NMR spectra of I and poly I obtained with HI/I_2 in CH_2Cl_2 (Run No. 4 of Table 2).
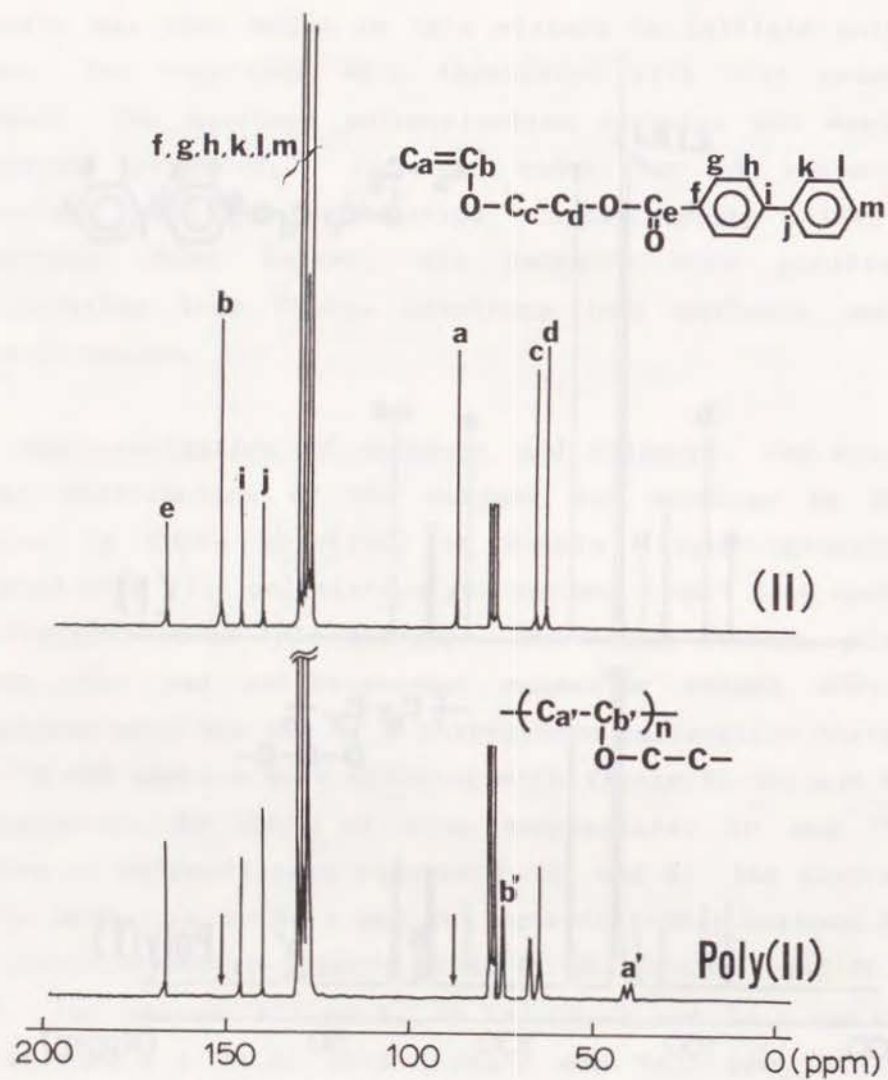
Figure 2. ^{13}C-NMR spectra of II and poly II obtained with HI/I$_2$ in CH$_2$Cl$_2$ (Run No. 6 of Table 2).
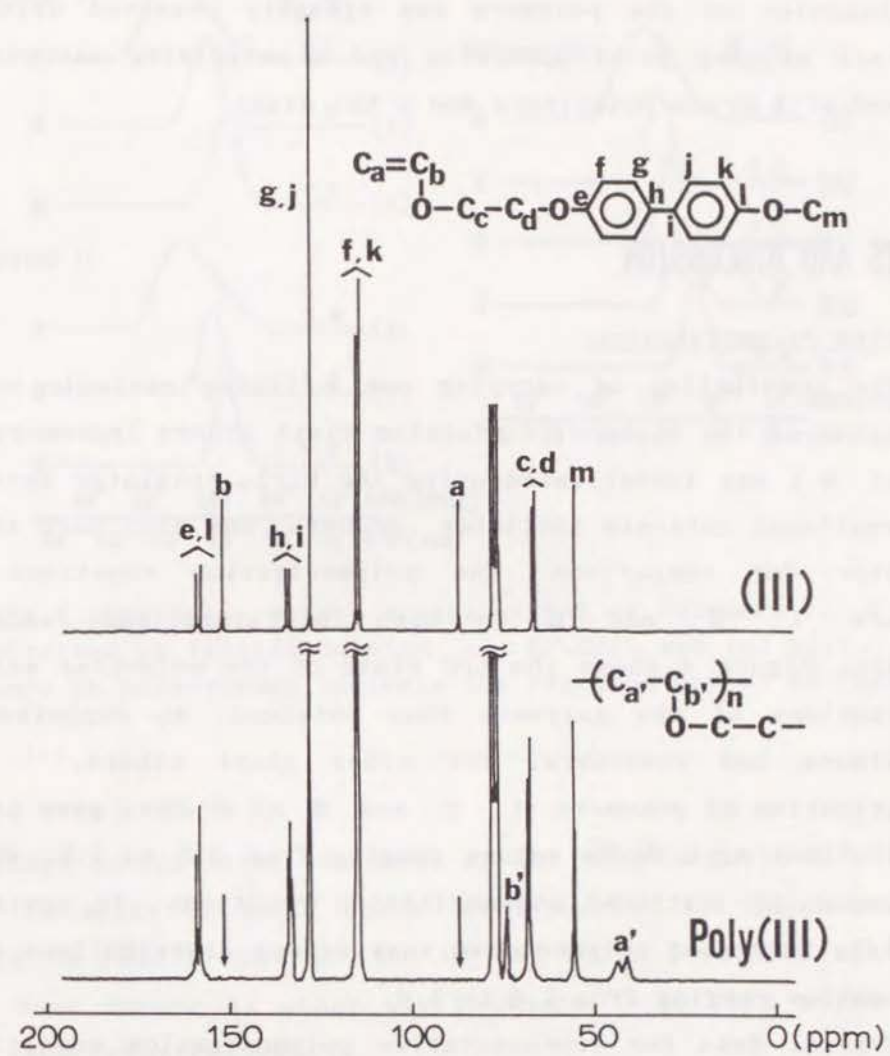
Figure 3. ^{13}C-NMR spectra of III and poly III obtained with HI/I$_2$ in CH$_2$Cl$_2$ (Run No. 10 of Table 2).

were used for the calibration of the temperature scale. The melt behavior of the polymers was visually observed using a capillary melting point apparatus and a polarizing microscope equipped with cross-polarizers and a hot stage.

RESULTS AND DISCUSSION

1. Living Polymerization

The possibility of carrying out a living cationic polymerization of the biphenyl-containing vinyl ethers [monomers I, II, and III] was investigated using the HI/I_2 initiator system. A conventional cationic initiator, BF_3OEt_2, was also used as an initiator for comparison. The polymerization reactions of monomers I, II, and III by both initiators gave soluble polymers. Figure 4 shows the GPC plots of the molecular weight distributions of the polymers thus obtained. As reported by Higashimura and coworkers, for other vinyl ethers,[11] the polymerization of monomers I, II, and III by BF_3OEt_2 gave broad distributions with $\overline{M}_w/\overline{M}_n$ values ranging from 2.5 to 3.0, which are normal for cationic polymerization reactions. In contrast the HI/I_2 initiated polymers had very narrow distributions with $\overline{M}_w/\overline{M}_n$ ratios ranging from 1.2 to 1.4.

Typical data for representative polymerization conditions and molecular weights of the polymers obtained are summarized in Table 2. The living character of the polymerization reactions of I, II, and III initiated by the HI/I_2 system was indicated not only by the narrow distributions shown in Figure 4, but also by the relationship between polymerization reactants and $\overline{M}_n$ in many cases and the observation that $\overline{M}_n$ of the polymers increased proportionally to the monomer-to-initiator feed molar ratio $([M]_0/[HI]_0)$ and to the molar ratio of monomer
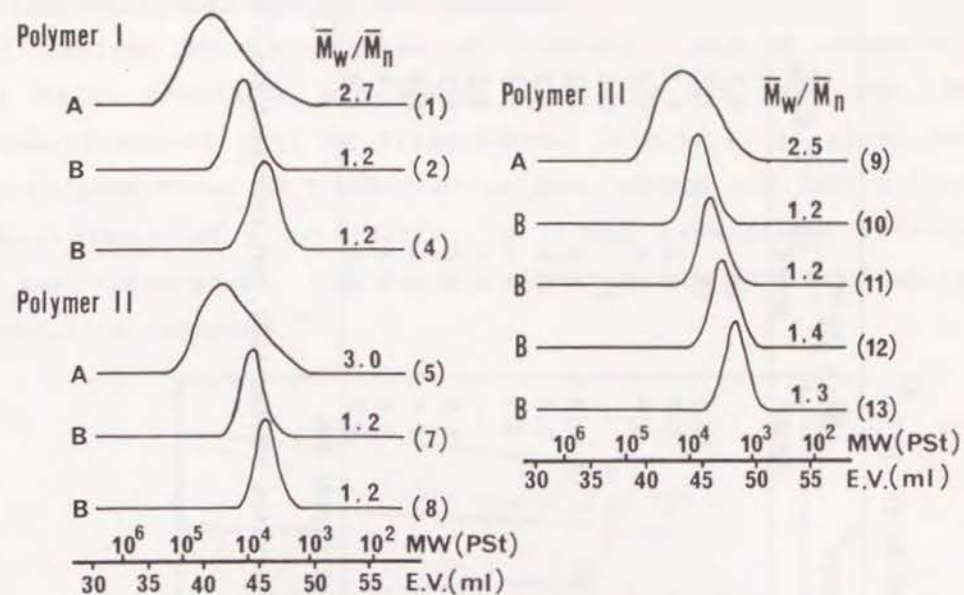
Figure 4. Molecular weight distributions of Polymers I, II, and III obtained by initiation with: (A) BF_3OEt_2 and (B) HI/I_2; numbers in parentheses indicate the reaction number in Table 2.

consumed-to-initiator, as shown by the data in Table 2.

In spite of their bulky substituents, all three monomers could be readily polymerized by the HI/I_2 initiator system in the same manner as other vinyl ethers[11] to form polymers of the expected structure:

$$\begin{array}{c} +CH_2-CH \xrightarrow{}_n \\ O-CH_2-CH_2-X-\bigcirc-\bigcirc-Y \end{array} \quad (-X-: -O- \text{ or } -O-\underset{\underset{O}{\|}}{C}-, -Y: -H \text{ or } -OCH_3)$$

-112-

-113-
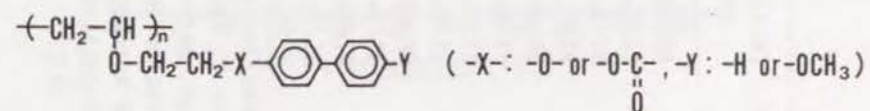
Table 2.

Cationic polymerization of I, II, and III at −15°C [a]

Reaction No.	Monomer	Initiator (concn, mM)	Solvent [b]	[M]o (M)	Reaction time [c] (hr)	$\overline{Mn} \times 10^{-3}$ Calcd [d]	Obsvd [e]	$\overline{Mw}/\overline{Mn}$
(1)	I	BF₃OEt₂ (10.0)	T	0.17	1.5	–	18	2.7
(2)	I	HI/I₂ (5.9/0.2)	D	0.25	48	10.2	12	1.2
(3)	I	HI/I₂ (8.4/10.0)	T	0.20	18	5.7	6.5	1.2
(4)	I	HI/I₂ (10.3/0.2)	D	0.21	2	4.9	5.4	1.2
(5)	II	BF₃OEt₂ (2.5)	T	0.15	3	–	11	3.0
(6)	II	HI/I₂ (8.9/0.2)	D	0.21	70	6.3	8.5	1.3
(7)	II	HI/I₂ (10.0/10.0)	T	0.21	48	5.6	7.6	1.2
(8)	II	HI/I₂ (20.0/20.0)	T	0.21	48	2.9	4.8	1.2
(9)	III	BF₃OEt₂ (2.5)	T	0.06	3	–	6.7	2.5
(10)	III	HI/I₂ (4.3/0.2)	D	0.11	162	6.9	6.0	1.2
(11)	III	HI/I₂ (2.9/3.0)	T	0.06	408	4.8	4.3	1.2
(12)[f]	III	HI/I₂ (10.3/0.2)	D	0.11	3	2.9	2.4	1.4
(13)[f]	III	HI/I₂ (13.1/10.0)	T	0.11	24	2.3	1.8	1.3

a) All reaction conversion were close to 100% except for reaction 11, which was 85%.

b) Reaction solvents: T, toluene, D, dichloromethane.

c) These values do not necessary indicate the time when the monomer conversion reaches 100%, but represent the time between the initiation and the termination.

d) Calcd $\overline{Mn}$ = (MW of monomer) X ([M]consumed/[HI]o).

e) Determined by GPC calibrated with standard polystyrene samples.

f) Reactions run at −5°C.

2. Thermal Properties of the Polymers

Typical DSC thermograms of Polymers I and II obtained by the HI/I₂ initiator are shown in Figure 5(A) and (B). Both polymers showed only Tg transitions; Polymer I at about 56 °C and Polymer II at 32 °C. Neither polymer showed any indication of the presence of a crystalline or liquid crystalline endotherm in the thermograms. The Tg of Polymer I was the same as that previously reported.[9]
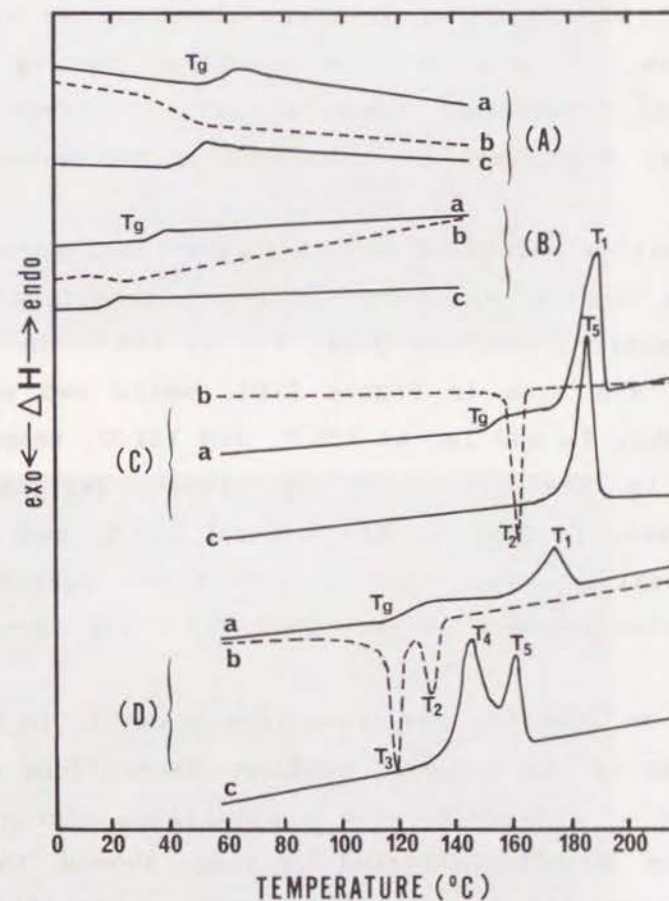
Figure 5. DSC thermograms of (A) Polymer I by HI/I₂, (B) Polymer II by HI/I₂, (C) Polymer III by BF₃OEt₂, and (D) Polymer III by HI/I₂. [(A) No. 4, (B) No. 6, (C) No. 9, (D) No. 11, in Table 2; a) the first heating cycle, b) the first cooling cycle, c) the second heating cycle.]

In contrast, the thermograms of all samples of Polymer Ⅲ showed at least one endotherm and in some cases two, as seen in Figure 5(C) and (D) for the DSC thermograms of Polymer Ⅲ obtained by initiation with BF_3OEt_2 and HI/I_2, respectively. The thermal transition data and calculated data for thermodynamic properties for all samples of Polymer Ⅲ are collected together in Table 3. The BF_3OEt_2-initiated polymer showed a glass transition at 157 ℃ and an endothermic transition peak, T_1, at 190 ℃ in the first heating cycle and an exothermic transition peak, T_2, at 160 ℃ in the first cooling cycle in Figure 5(C). An endothermic transition peak, designated T_5 in Figure 5(C), at 185 ℃ was also observed in the second heating cycle.

The transition values of the HI/I_2-initiated polymers were different from those of the former. A glass transition at 134 ℃ and an endothermic transition peak, T_1, at 174 ℃ in the first heating cycle are seen in Figure 5(D), while two exothermic transition peaks, T_2 and T_3, at 133 ℃ and 121 ℃, respectively, are evident in the first cooling cycle. Two endothermic transition peaks, T_4 and T_5, are seen at 145 ℃ and 160 ℃ in the second heating cycle. After the first heating cycle, subsequent cycles on each polymer gave virtually identical DSC thermograms.

In order to identify the transition peaks T_1 to T_5 in the DSC thermograms of the polymer, texture observations were made of all samples of Polymer Ⅲ with a polarizing microscope. The sample of the BF_3OEt_2-initiated polymer showed thread-like textures characteristic of the nematic phase[12] at the temperature just below T_2 in the cooling cycle and just below T_5 (or T_1) in the heating cycle, as shown in the photomicrographs in Figure 6. On the other hand, Polymer Ⅲ samples obtained with HI/I_2 showed both nematic, thread-like textures

(B)

(A)

$: 100 \mu$
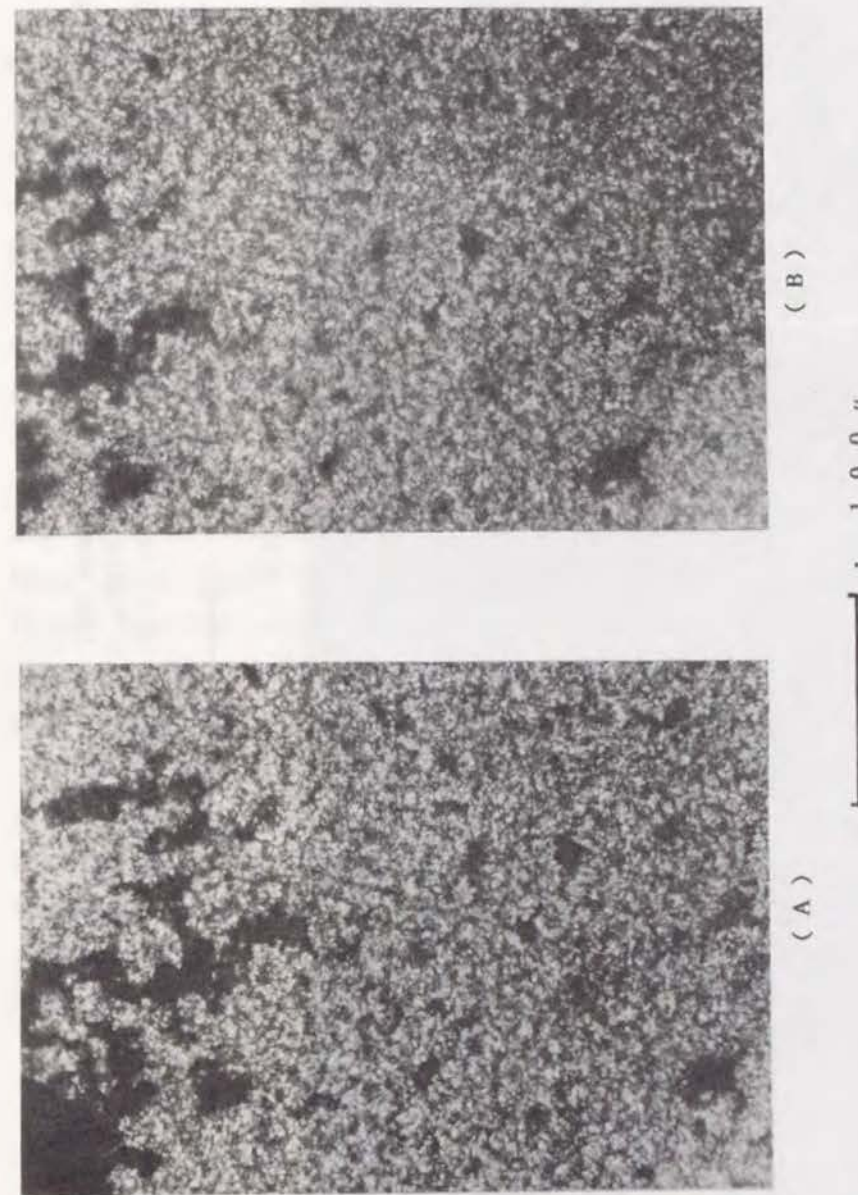
Figure 6. Micrographs of the nematic texture exhibited by Polymer Ⅲ obtained by BF_3OEt_2 (No.9 in Table 2) in the first cooling cycle. (A) at 155 ℃ (just below T_{i-n}). (B) after 30 min at the same temperature; original magnification is 320 ×.

(C)

(B)

⊢——⊣ : 100 μ

(A)
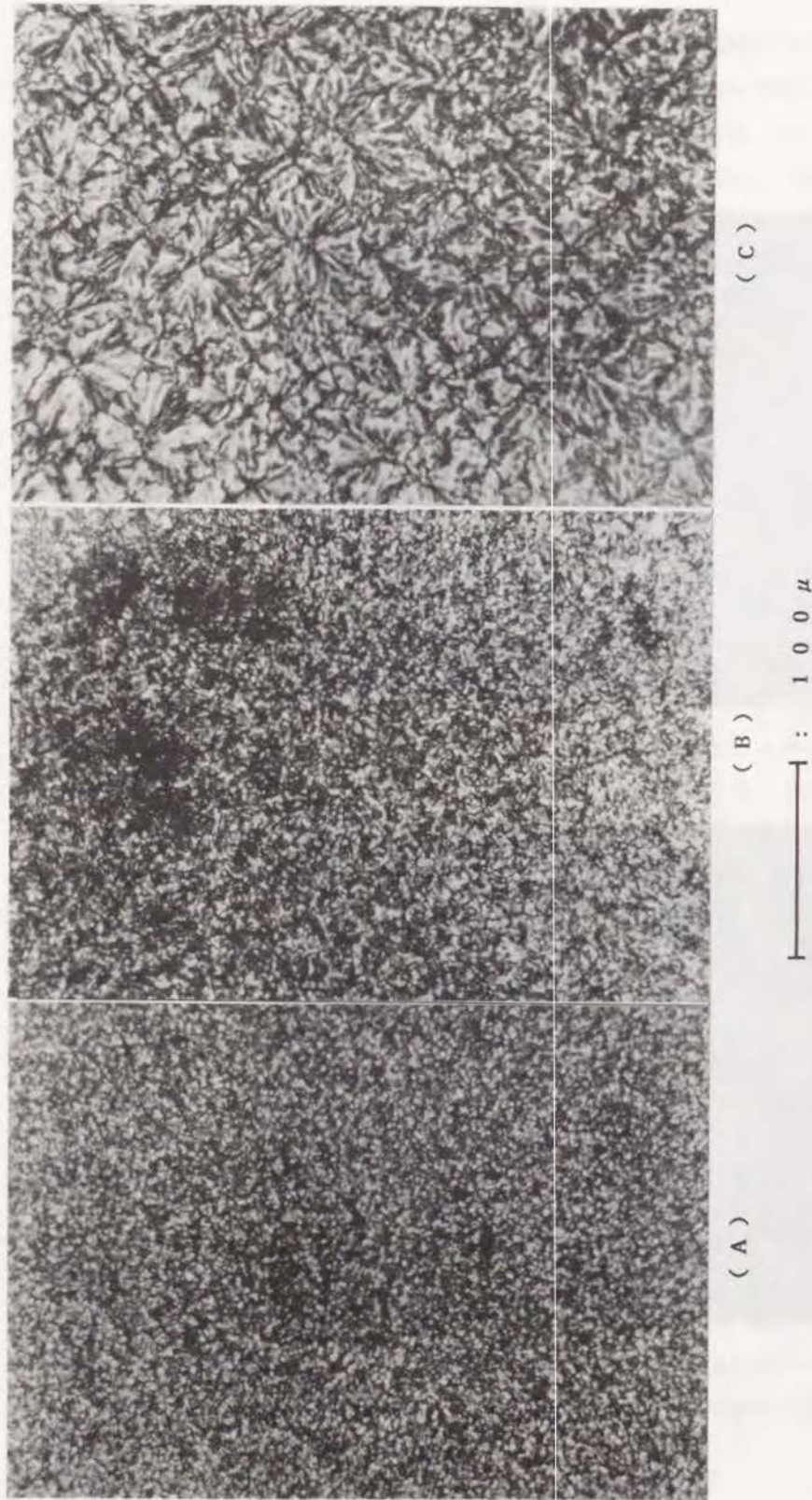
Figure 7. Micrographs of the nematic texture [(A),(B)] and the smectic texture [(C)] of Polymer III obtained with the HI/I₂ initiator (No. 11 in Table 2) in the first cooling cycle. (A) at 130 °C (between Ti-n and Tn-s), (B) after 30 min at the same temperature. (C) at 118 °C (just below Tn-s); original magnification is 320 ×.

between T_2 and T_3 (also between T_4 and T_5, and just below T_1) and focal-conic textures characteristic of the smectic phase[12] at temperatures just below T_3 (or T_4), as shown in the photomicrographs in Figure 7.

None of the samples of Polymer III obtained with either BF_3OEt_2 or HI/I_2 showed glass transitions in the DSC thermograms after the first heating cycle. The virgin polymers, which were obtained by precipitation from solution, were the only samples which showed a Tg. The Tg transition may overlap with the T_2 (or T_5) transition in the BF_3OEt_2-initiated samples and with the T_3 (or T_4) in the HI/I_2-initiated samples after one heating cycle. That is, the Tg transition may have shifted to a higher temperature after the first heating and cooling cycle possible because the glassy state so formed differed from that of the virgin polymer. The virgin polymer as precipitated may have had either a poorly ordered nematic structure, or may have even been isotropic, while the glass formed after the first heating and cooling cycle may have been in an ordered nematic state (the BF_3OEt_2-initiated samples) or in a smectic state (the HI/I_2-initiated samples).

Each transition peak, and each phase before and after the peak, could be identified, and the transitions are represented in Figure 8, in which Tx-y indicates the transition temperature from the x-phase to y-phase. The assigned transitions are also indicated in Table 3. Observations on a capillary melting point apparatus gave the same results.

Broad MWD Polymer III by BF$_3$OEt$_2$

Virgin Polymer: Nematic Glass (less ordered) —Tg→ Nematic LC —T$_1$(=Tn-i)→ Isotropic

Nematic Glass (more ordered) ←T$_2$(=Ti-n)— Isotropic

T$_5$(=Tn-i)

Narrow MWD Polymer III by HI/I$_2$

Virgin Polymer: Nematic Glass (less ordered) —Tg→ Nematic LC —T$_1$(=Tn-i)→ Isotropic

Smectic Glass —T$_3$(=Tn-s)⇄ Nematic LC —T$_2$(=Ti-n)⇄ Isotropic

T$_4$(=Ts-n) ⇄ T$_5$(=Tn-i)
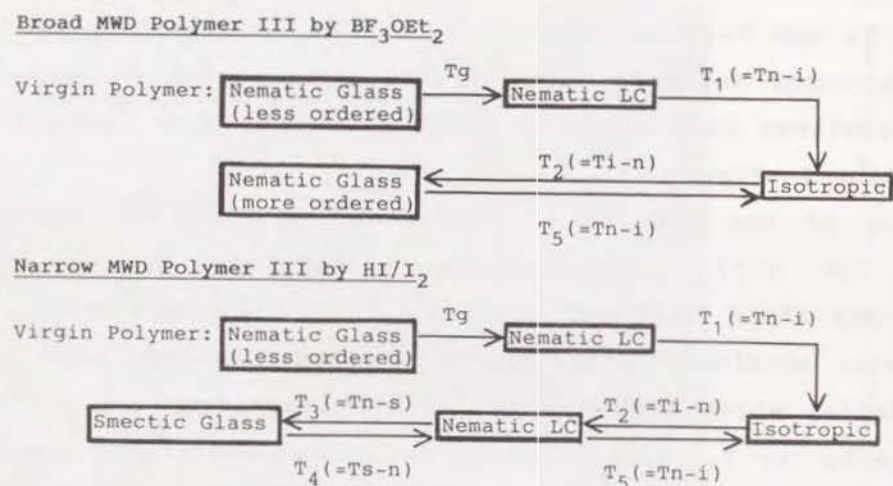
Figure 8. Schematic representations of the comparative thermal transitions of the broad and narrow distribution polymers.

3. Molecular Weight Dependency

The molecular weight ($\overline{Mn}$) dependencies of the thermal transitions of Polymer III are shown by the data in Table 3. The narrow MWD samples of Polymer III in the molecular weight range of 1,800 to 6,000 showed only a slight effect of $\overline{Mn}$ on Tg, Ts-n, and Ti-n. Thus, Tg and Ts-n increased and, surprisingly, Ti-n decreased with increasing $\overline{Mn}$, but Tn-i and Tn-s were not affected by this molecular weight variation.

The data in Table 3 also indicates that there is some molecular weight dependency on the thermodynamic parameters, ΔH and ΔS. That is, ΔHs-n and ΔSs-n decreased and ΔHn-i and ΔSn-i increased with increasing the $\overline{Mn}$, but the summations of ΔHs-n + ΔHn-i and ΔSs-n + ΔSn-i were not affected by changes in $\overline{Mn}$.

For the broad distribution sample of III, Polymer 9, obtained with the BF₃OEt₂ initiator, all of the observed transition temperatures were higher than those for the narrow

Table 3. Thermal properties of broad (9) and narrow (10–13) distribution samples of polymer III

Reaction No.	Thermal transitions (°C) [a]					Thermodynamic parameters [c]					
	Heating cycle [a]			Cooling cycle [b]		ΔH (cal/g)			ΔS × 10² (cal/g·K)		
	Tg	Ts-n	Tn-i	Ti-n	Tn-s	ΔHs-n	ΔHn-i	ΔHs-n+ΔHn-i	ΔSs-n	ΔSn-i	ΔSs-n+ΔSn-i
(9)	157	---	190 (185)	160	---	---	11.9	11.9	---	2.6	2.6
(10)	138	--- (149)	171 (161)	130	123	5.3	6.9	12.2	1.3	1.6	2.8
(11)	134	--- (145)	174 (160)	133	121	7.4	4.6	12.0	1.8	1.1	2.8
(12)	130	--- (143)	169 (159)	138	123	8.1	3.9	12.0	1.9	0.9	2.8
(13)	128	--- (140)	170 (160)	140	122	8.3	4.1	12.4	2.0	0.9	3.0

a) Taken from the first heating cycle; numbers in parentheses indicate the transition temperatures taken from the second heating cycle.
b) Taken from the first cooling cycle.
c) Taken from the second heating cycle.

distribution sample, but the ΔH and ΔS values for the transitions of the nematic glass phase to isotropic phase were almost the same level as the values of $\Delta Hs-n + \Delta Hn-i$ and $\Delta Ss-n + \Delta Sn-i$, respectively, of the former. Possibly the Tg and Tn-i values are more strongly affected by the higher molecular weight fraction of the broad distribution samples, and considering the inverse relationship for the narrow fraction polymers, perhaps Ti-n is affected more by the lower molecular weight fraction of the broad distribution. In contrast, the sum of the ΔH and ΔS value from the smectic to nematic to isotropic phases was not affected by the molecular weight of the polymer, as seen in the results for the narrow distribution polymer samples in Table 3.

The possible sensitivity of the Tg transition of the broad distribution sample of polymer 9 to the high molecular weight fraction may be responsible for the observation that it did not show a smectic phase. That is, the glass transition temperature of the nematic mesophase may be above the Ts-n temperature for this polymer so that on cooling the polymer becomes immobile before it can rearrange to form the smectic phase. Hence, the presence of a higher molecular weight fraction may cause the resulting increase of the Tg of the nematic phase preventing the formation of the smectic mesophase. If so, this polymer would have a monotropic smectic phase relative to Tg. Percec and coworkers reported[9] that their sample of polymer III, which was obtained with the BF_3OEt_2 initiator, showed a smectic texture below its isotropization temperature of 173 ℃, but they did not observe a Tg for their polymer, and they did not report a molecular weight for their sample.

REFERENCES

1) (a) A.C. Griffin and J.F. Johnson, Ed., "Liquid Crystals and Ordered Fluids," Vol. 4, Plenum, New York, 1984.
(b) L.L. Chapoy, Ed., "Recent Advances in Liquid Crystalline Polymers," Elsevier, New York, 1985.

2) H. Finkelmann, in "Polymer Liquid Crystals," A. Ciferri, W.R. Krinbaum and R.B. Meyer, Ed., Academic Press, New York, 1982, Chapter 2.

3) (a) H. Finkelmann and G. Rehage, Adv. Polym. Sci., 60/61, 99 (1984). (b) V.P. Shibaev and N.A. Plate, Adv. Polym. Sci., 60/61, 173 (1984).

4) V. Percec, J.M. Rodriguez-Parada and C. Ericsson, Polym. Bull., 17, 347 (1984).

5) W. Kreuder and O.W. Webster, Macromol. Chem., Rapid Commun., 7, 5 (1986).

6) M. Miyamoto, M. Sawamoto and T. Higashimura, Macromolecules, 17, 265 (1984).

7) T. Enoki, M. Sawamoto and T. Higashimura, J. Polym. Sci., Polym. Chem. Ed., 24, 2261 (1986).

8) (a) T. Higashimura, A. Tanizaki and M. Sawamoto, J. Polym. Sci., Polym. Chem. Ed., 22, 3173 (1984).
(b) T. Higashimura, M. Miyamoto and M. Sawamoto, Macromolecules, 18, 611 (1984).
(c) T. Higashimura and M. Sawamoto, Makromol. Chem., Suppl., 12, 153 (1985).

9) J.M. Rodriguez-Parada and V. Percec, J. Polym. Sci., Polym. Chem. Ed., 24, 1363 (1986).

10) (a) K. Kato, T. Ichijo and M. Hasegawa, J. Polym. Sci., A-1, 9, 2109 (1971).
(b) S. Watanabe and K. Kato, J. Polym. Sci., Polym. Chem. Ed., 22, 2801 (1984).

11) (a) S. Aoshima, O. Hasegawa and T. Higashimura, Polym. Bull., 13, 229 (1985).

   (b) S. Aoshima, O. Hasegawa and T. Higashimura, Polym. Bull., 14, 417 (1985).

   (c) T. Nakamura, S. Aoshima and T. Higashimura, Polym. Bull., 14, 515 (1985).

12) D. Demus and L. Richter, "Textures of Liquid Crystals," Verlag Chemie, New York, 1978.

CHAPTER 6

MOLECULAR WEIGHT EFFECTS ON THERMAL PROPERTIES OF SIDE-CHAIN LIQUID CRYSTALLINE POLY(VINYL ETHER)S WITH PENDANT CYANOBIPHENYL MESOGENIC GROUPS

ABSTRACT

A vinyl ether monomer containing a cyanobiphenyl group, 2-(4'-cyano-4-biphenyloxy)ethyl vinyl ether (CBPVE), was cationically polymerized with the hydrogen iodide/iodine (HI/I_2) initiator system and with the hydrogen iodide/zinc iodide (HI/ZnI_2) initiator system to form narrow molecular weight distribution (MWD) polymers. Both of these initiators have been shown to yield "living polymer" polymerization reactions. The thermal properties of the poly(CBPVE) were determined by DSC and by visual observations of samples placed on a hot stage on a polarizing microscope. Polymer samples which had $\overline{M}n$ values less than 2,600 and a narrow MWD ($\overline{M}w/\overline{M}n$ = 1.02-1.1) showed enantiotropic liquid-crystalline behavior and formed a smectic phase after one heating cycle. In contrast, the polymer sample having $\overline{M}n$ values greater than 2,600 and a reasonably narrow MWD ($\overline{M}w/\overline{M}n$ = 1.2-1.3) prepared with these initiators, and also polymers prepared with a boron trifluoride etherate (BF_3OEt_2) initiator which had a broad MWD ($\overline{M}w/\overline{M}n$ = 2.1, $\overline{M}n$=4,400), formed only isotropic melts. These molecular weight effects on the thermal properties of poly(CBPVE) are discussed.

CBPVE
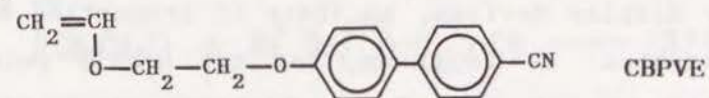
INTRODUCTION

Side-chain liquid-crystalline polymers, LCP, are of interest for a variety of applications, especially in the field of electrooptics.[1] Although it has been long known that molecular weight and molecular weight distribution are important factors that affect the thermal properties of LCP,[2] there have been very few reports on this effect.

Chapter 5 of this thesis described the differences in thermal properties of LCP with both narrow and broad molecular weight distributions, MWDs, which were prepared from 2-(4'-methoxy-4-biphenyloxy)ethyl vinyl ether by both a living and a conventional cationic polymerization reactions.[3] In that chapter, the author described the properties of a poly(vinyl ether) with a mesogen (I) having an electron-donating group, the methoxy group (OCH₃), at the terminal position of the side chain. In this chapter a polymer with a mesogen (II) having an electron-withdrawing group, the cyano group (CN), at the terminal position was prepared.

$$-O-\bigcirc-\bigcirc-OCH_3 \qquad -O-\bigcirc-\bigcirc-CN$$
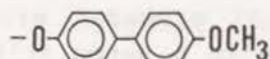
I   II

Cyanobiphenyl-containing low molecular weight LC compounds are used for display devices, so their LC properties have been thoroughly studied. It is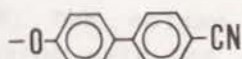 known that the highly polar cyano group attached to one end of the biphenyl group causes the formation of an antiparallel, near-neighbor pairing.[4, 5] It is of interest, therefore, to find out what occurs when a mesogen (II) with a cyano group at its terminal position is attached to a polymer backbone as a side chain. In that type of structure, it may be less likely to form the antiparallel pairing and more likely to show a normal smectic ordering.[4] Moreover, from the author's previous study,[3] it will be important to determine if the phase-transition phenomena of the cyanobiphenyl group containing polymers are also effected by their molecular weight distribution.

For this purpose, a series of poly(vinyl ether)s containing a pendant cyanobiphenyl group but having different MWDs were prepared by both a living cationic polymerization reaction and a normal cationic polymerization reaction of 2-(4'-cyano-4-biphenyloxy)ethyl vinyl ether (CBPVE). The thermal properties of the polymers so formed were examined in relation to their molecular weight and MWD.

$$CH_2=CH$$
$$O\,CH_2CH_2O-\bigcirc-\bigcirc-CN \qquad CBPVE$$
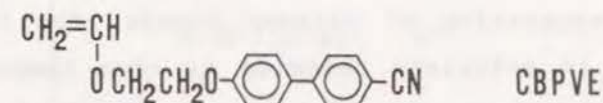
EXPERIMENTAL SECTION

Materials. 2-(4'-Cyano-4-biphenyloxy)ethyl vinyl ether (CBPVE) was prepared by the phase-transfer-catalyzed condensation of 2-chloroethyl vinyl ether with sodium salt of 4-(4-cyanophenyl)phenol in the presence of a catalytic amount of tetrabutylammonium hydrogen sulfate,[6] as shown below:

$$CH_2=CH$$
$$O\,CH_2CH_2Cl + Na^+\,{}^-O-\bigcirc-\bigcirc-CN \longrightarrow CBPVE$$
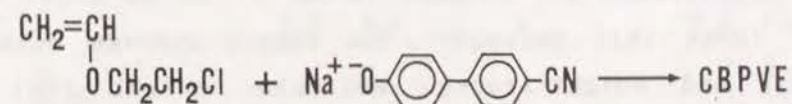
CBPVE was purified by recrystallization from methanol, mp 105 ℃ (by DSC). The hydrogen iodide (HI), iodine (I₂), zinc iodide (ZnI₂), and boron trifluoride etherate (BF₃OEt₂) initiators and the solvents (methylene chloride, n-hexane, and diethyl ether) were purified and used as previously reported.[7, 8]

Polymerization Procedures. Cationic polymerization reactions were carried out as previously reported.[3,8,9] All polymers were purified by precipitation from CH_2Cl_2 solutions into methanol and were dried under vacuum.

Fractionation and Blending Procedures. Fractionation of polymer B of Table 2 and Figure 7 was carried out using a methanol/acetone (2/1 v/v%) mixture solvent at room temperature at a concentration of 100 mg of polymer in 10 ml of solvent. The insoluble fraction, designated B-H, was recovered by filtration, and the soluble fraction, B-L, was recovered by evaporation of the solvent.

For the preparation of polymer blends, the two polymers were dissolved in methylene chloride at room temperature at a concentration of 100 mg of total polymer in 10 ml of solvent. In this manner, blends of polymers B and D of Table 2 and Figure 7 were prepared. The polymer blend was recovered by precipitation from solution into methanol and dried under vacuum before characterization.

Characterization of Monomers and Polymers. The molecular weight distribution of the polymer was measured by GPC in $CHCl_3$ on a Waters Associates, Inc., liquid chromatograph equipped with five polystyrene gel columns (8 mm × 23 cm each) and a refractive index (RI) detector. The number-average molecular weight ($\overline{Mn}$) and weight-average molecular weight ($\overline{Mw}$) were calculated with the use of a polystyrene calibration curve. ^{1}H- and ^{13}C-NMR spectra were obtained with Varian XL-200 and XL-300 spectrometers in $CDCl_3$ at room temperature. The chemical shifts of the ^{1}H- and ^{13}C-NMR spectra of the monomer (CBPVE) and the polymers are summarized in Table 1.

Table 1.

^{1}H and ^{13}C-NMR chemical shifts for the monomer and the polymer[a]

	^{1}H-NMR		^{13}C-NMR	
	δ (ppm)	proton	δ (ppm)	carbon
Monomer				
	4.00~4.40(m)	a,c,d	67.0, 67.3	c,d
			87.9	a
	6.55(d of d)	b	111.0	l
			116.0	f
	6.95~7.20(m)	f	118.8	m
			127.8, 129.1	j,g
	7.40~7.80(m)	g,j,k	132.7	h
			133.3	k
			145.9	i
			152.3	b
			160.0	e
Polymer	1.0 ~ 2.0	a'	39.6, 41.8	a'
			74.3	b'
	3.4 ~ 4.3	b',c,d	The signals of the	
	6.6 ~ 7.1	f	pendant group(R) are	
			at the same position as	
	7.1 ~ 7.9	g,j,k	those of the monomer.	

a) Chemical shifts are given in ppm relative to TMS.

Thermal analyses were carried out on a Perkin-Elmer DSC-2 instrument on polymer or monomer samples of 5-10 mg under a nitrogen flow at a scanning rate of 10 ℃ /min. Indium and naphthalene were used for the calibration of the temperature scale. The melt behavior of the polymers was also visually observed by using a polarizing microscope equipped with cross-polarizer and a hot stage.

RESULTS AND DISCUSSION

1. Polymerization of CBPVE

Cationic polymerization of CBPVE was carried out using the HI/I_2 or the HI/ZnI_2 initiator system for the preparation of narrow MWD samples and the boron trifluoride etherate (BF_3OEt_2) initiator, a conventional cationic initiator, for the preparation of broad MWD samples. All three initiator systems gave soluble polymers with the expected structures as shown by the NMR results in Table 1. The polymerization conditions used and the molecular weights of the polymers so obtained are summarized in Table 2. Figure 1 contains the GPC chromatograms, which were used to calculate $\overline{Mn}$ and $\overline{Mw}$ for evaluating the MWDs of the polymers.

As shown by the data in Table 2 and Figure 1, both the HI/I_2 initiator and the HI/ZnI_2 initiator gave living polymers having narrow distributions with $\overline{Mw}/\overline{Mn}$ ratios ranging from 1.04 to 1.2, in the same manner as for other vinyl ethers,[10] even though the monomer had a highly polar cyano group. In contrast, the BF_3OEt_2 initiator gave a polymer with a broad MWD and an $\overline{Mw}/\overline{Mn}$ ratio of 2.1.

Table 2.

Cationic polymerization of CBPVE in CH_2Cl_2 at -5 ℃

Polymer	Initiator (concn, mM)	[M]$_0$ (M)	Reaction time [a] (hr)	$\overline{Mn} \times 10^{-3}$ Calcd [b]	Obsvd [c]	$\overline{Mw}/\overline{Mn}$	$\overline{DPn}$
A	HI/ZnI$_2$ (11.9/0.2)	0.05	91	1.1	1.3	1.04	4.9
B	HI/I$_2$ (12.2/0.2)	0.11	20	2.4	2.1	1.1	7.9
C	HI/I$_2$ (7.2/0.2)	0.11	20	3.9	3.5	1.2	13.2
D	HI/ZnI$_2$ (3.1/0.2)	0.09	115	7.7	7.3	1.2	27.5
E	BF$_3$OEt$_2$ (2.5)	0.05	24	---	4.4	2.1	16.6

a) All reaction conversions were close to 100%.
b) Calcd $\overline{Mn}$ = (fractional conversion) × ([M]$_0$/[HI]$_0$) / (MW of monomer).
c) Determined by GPC calibrated with standard polystyrene samples.
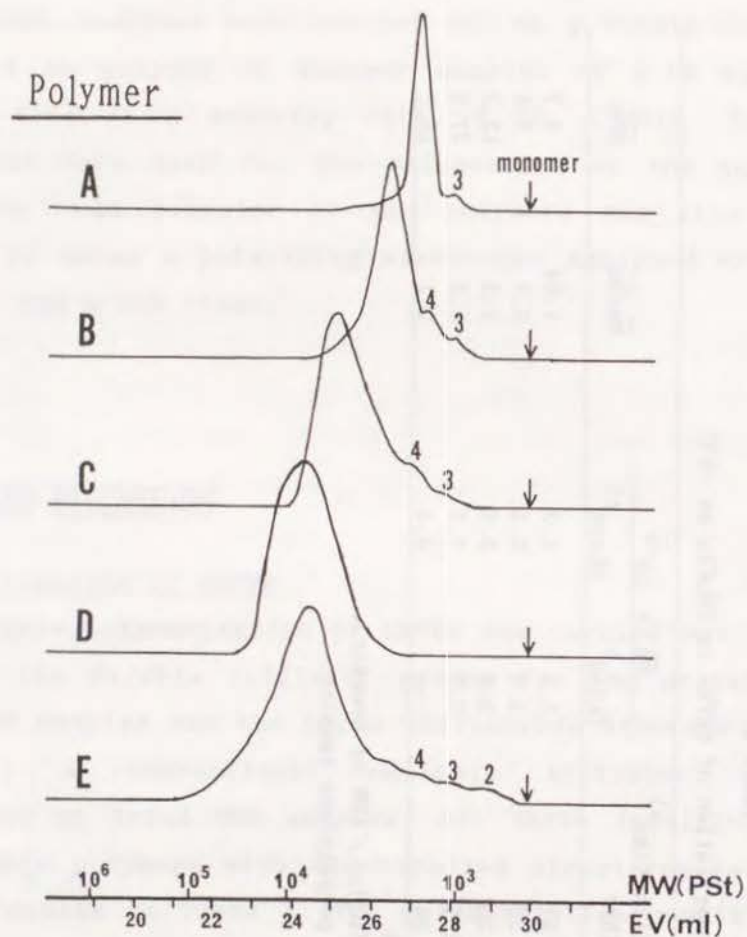
Figure 1. Molecular weight distribution of CBPVE polymers; see Table 2 for reaction conditions. Numbers indicate the degree of polymerization.

2. Thermal Properties of Polymers

Typical DSC thermograms for the polymers obtained by HI/ I_2, polymers B and C, and by BF_3OEt_2, polymer E, are shown in Figure 2. The HI/I_2-initiated polymer with a low molecular weight and a narrow molecular weight distribution, polymer B,
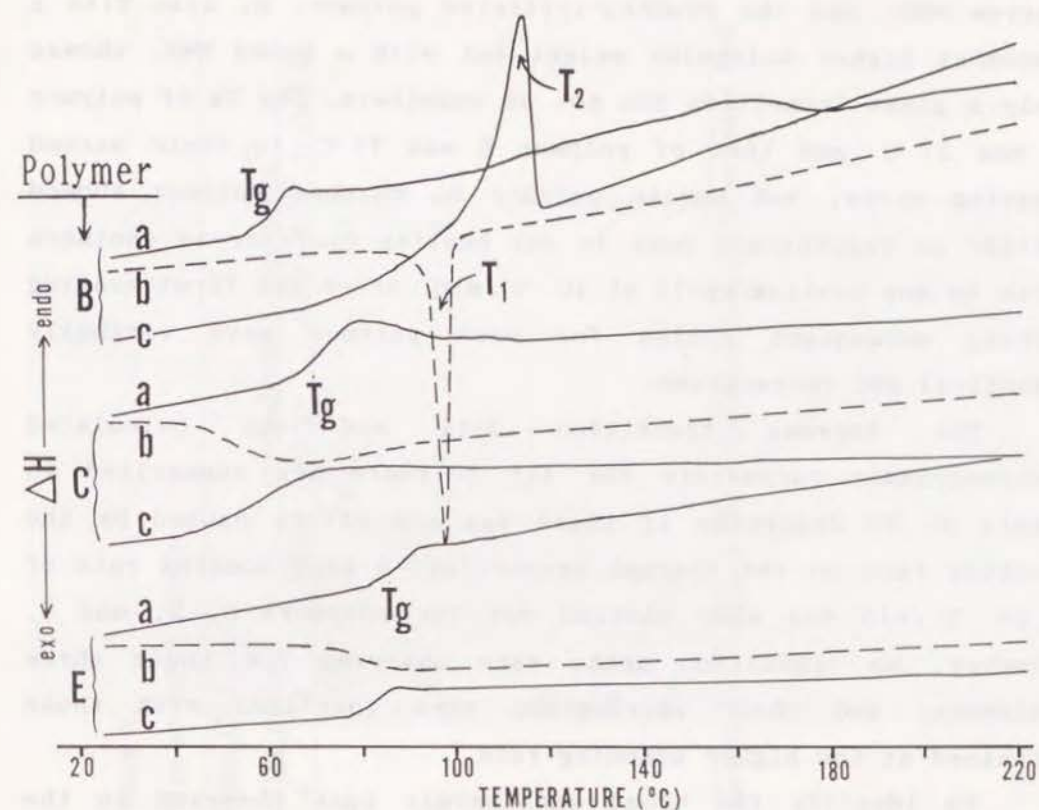
Figure 2. DSC thermograms of CBPVE polymers B, C, and E: (a) the first heating cycle, (b) the first cooling cycle, (c) the second heating cycle.

showed a glass transition at 59 ℃ and a broad endothermic peak from 100 to 180 ℃ in the first heating cycle. An exothermic transition peak, T_1, at 96 ℃ in the first cooling cycle and an endothermic transition peak, T_2, at 115 ℃ in the second heating cycle were also observed. The DSC thermogram for polymer A was essentially identical with that of polymer B.

In contrast, the HI/I_2-initiated polymer, C, which has a somewhat higher molecular weight than that of B but also a

narrow MWD, and the BF₃OEt₂-initiated polymer, E, also with a somewhat higher molecular weight but with a broad MWD, showed only a glass transition but not an endotherm. The Tg of polymer C was 57 ℃ and that of polymer E was 77 ℃ in their second heating cycle, but unlike polymer B, neither polymer showed either an endothermic peak in any heating cycle or an exotherm peak in any cooling cycle at 10 ℃/min. After the first heating cycle, subsequent cycles for each polymer gave virtually identical DSC thermograms.

The thermal transition data and the calculated thermodynamic parameters for all polymers are summarized in Table 3. To determine if there was any effect caused by the cooling rate on the thermal properties, a slow cooling rate of 1.25 ℃/min was also carried out for polymers C, D, and E. However, no transition peaks were observed for these three polymers, and their thermograms were identical with those obtained at the higher scanning rate.

To identify the broad endothermic peak observed in the first heating cycle, the exothermic transition peak, T₁, of the cooling cycle, and the endothermic transition peak, T₂, of the second heating cycle, texture observations of polymers A and B were made on samples placed on a hot stage of a polarizing microscope. Polymers A and B showed both threadlike textures and dark region, indicative of the coexistence of a nematic phase and an isotropic phase, above their Tg in the first heating cycle, as shown in Figure 3, with an isotropization temperature at about 150 ℃. The fan-shaped textures, which are characteristic of a smectic phase, were observed at a temperature just below T₁ in the first cooling cycle, as shown in Figure 4. In contrast, polymers C, D, and E showed no texture, and even after the sample close to Tg in the cooling cycle was annealed for 12 h, no birefringence was observed.

Table 3.

Thermal properties of CBPVE polymers

Polymer	$\overline{Mn} \times 10^{-3}$	$\overline{Mw}/\overline{Mn}$	heating cycle a) Tg	heating cycle a) Ts-i	cooling cycle b) Ti-s	cooling cycle b) Tg	ΔHs-i (cal/g)	ΔSs-i $\times 10^2$ (cal/g·K)
A	1.3	1.04	60 (--)e)	--d) (115)	96	--e)	8.1	2.1
B	2.1	1.1	59 (--)e)	--d) (116)	97	--e)	5.1	1.3
C	3.5	1.2	72 (57)	--	--	66		
D	7.3	1.2	78 (72)	--	--	65		
E	4.4	2.1	83 (77)	--	--	76		

a) Taken from the first DSC heating cycle, numbers in parentheses indicate the transition temperatures taken from the second heating cycle.
b) Taken from the first DSC cooling cycle.
c) Taken from the second DSC heating cycle.
d) A broad unkown peak from 100 to 180℃ was observed.
e) Tg may overlap with Ts-i or Ti-s; see text.
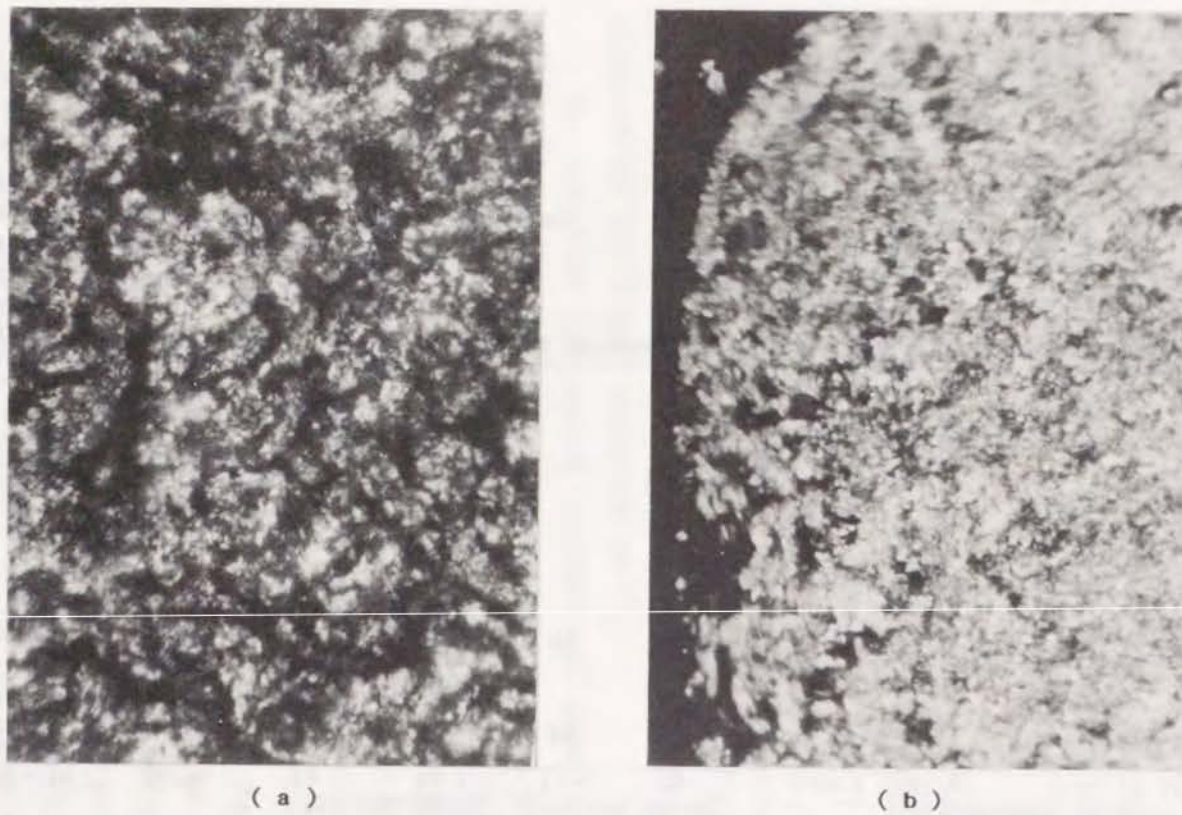
(a)   (b)

├───────────┤ : 1 0 0 μ

Figure 3. Photomicrographs of the nematic threadlike texture shown by polymer B in the first heating cycle, (a) at 75 ℃ and (b) at 95 ℃ ; at these temperatures, both are above Tg; original magnification is 320 × .
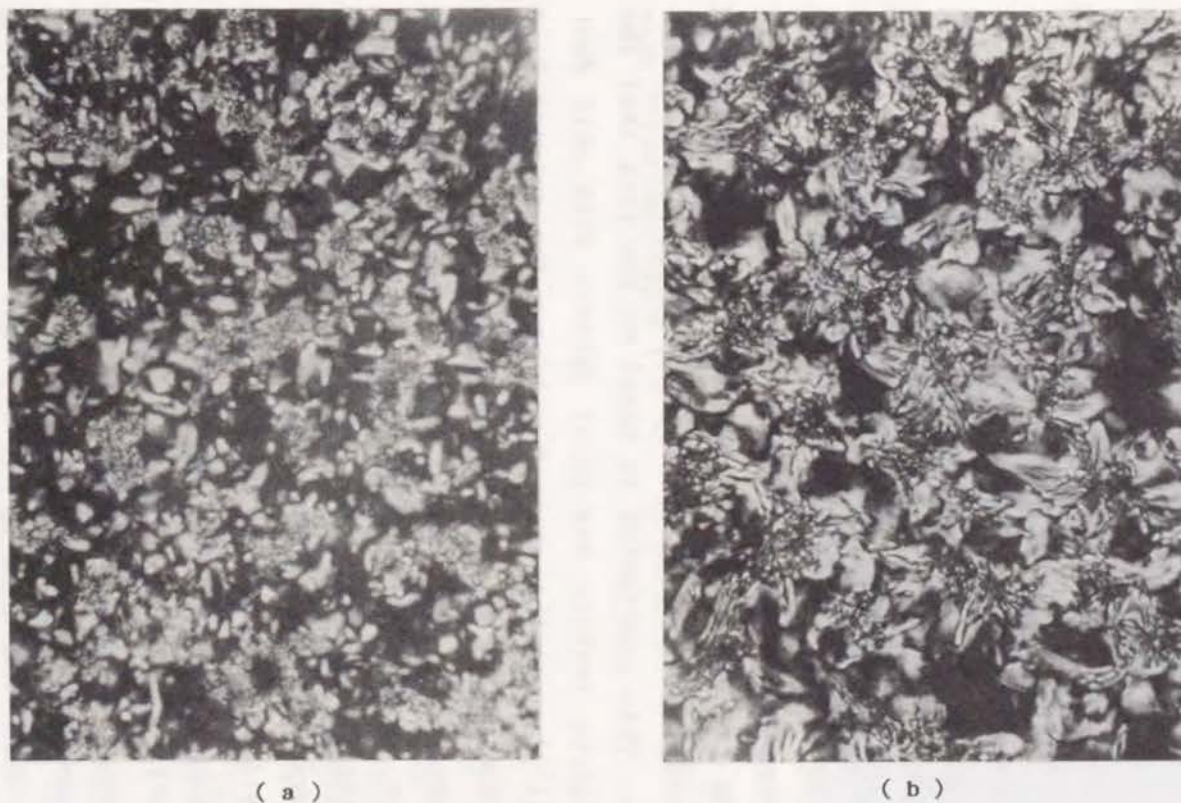
(a)   (b)

├───────────┤ : 1 0 0 μ

Figure 4. Photomicrographs of the smectic textures shown by the CBPVE polymer obtained by initiation with HI/I₂, polymer B in Table 2, in the first cooling cycle: (a) at 90 ℃, just below the Ti-s, batonnets with focal-conic texture, and (b) after 10 min at the same temperature, focal-conic texture; original magnification is 320 × .

These observations indicate that the broad transition peak in the first heating cycle of polymers A and B, as obtained directly by precipitation from their solution, can be considered to be a transition from the nematic to the isotropic state. Subsequently, the transitions represented by peaks T_1 and T_2 are assigned to the phase transition from the isotropic state to the smectic state (Ti-s) and from the smectic state back to isotropic liquid (Ts-i), respectively. A related compound containing the cyanobiphenyl mesogen **II**, 4-(n-octyl-oxy)-4'-cyanobiphenyl[4], and a related polymer, the poly-acrylate having mesogen **II**[5], were both reported to show the smectic phase too.

Further observations of the textures of polymer A and B in thin-film sample revealed that the phase below T_1 in the first cooling cycle and below T_2 in the second heating cycle is the smectic C phase. This conclusion is based on the fact that the smectic C schlieren texture has point defects with only four brushes $(s= \pm 1)$[11], and this texture is seen for polymer B in Figure 5. In contrast, the smectic A phase does not show a schlieren texture.

The virgin samples of polymers A and B showed a Tg transition in the first heating cycles, but neither showed a Tg in subsequent cooling and heating cycles, most likely because their Tg transitions overlapped either the T_1 (Ti-s) or T_2 (Ts-i) transition after the first heating cycle, as was previously observed for LC polymers from 2-(4'-methoxy-4-biphenyloxy)ethyl vinyl ether.[3] That is, the Tg transition of the smectic glass appears to be higher than that of the nematic glass of the virgin polymer.

⊢――――――――――⊣ : 100μ

Figure 5. Smectic C schlieren textures shown by polymer B in the first cooling cycle at 96 ℃, close to Ti-s (Original magnification: 320 ×).

The phase transitions of both low and high molecular weight poly(CBPVE)s are summarized in Figure 6. For low molecular weight polymers A and B, the virgin polymers appeared to exist at least partially as a nematic glass, but after one heating cycle through the Tg into the isotropic liquid state and subsequent cooling, they formed the more ordered smectic phase, which was then frozen at the Tg transition; that is, the nematic state becomes monotropic ralative to the Tg of the smectic state.[3] In that manner, the LC properties of poly-(CBPVE) after the first heating cycle were dependent on the molecular weight (MW) and MWD because the lower MW and narrower MWD polymers, polymer A and B, had an accessible transition

Polymers A and B: low MW and narrow MWD polymers

Virgin Polymer : [Nematic Glass] $\xrightarrow{T_g}$ [Nematic LC]

$\downarrow$ endothermic peak

[Smectic Glass] $\underset{T_{s-i}(=T_2)}{\overset{T_{i-s}(=T_1)}{\rightleftharpoons}}$ [Isotropic Liquid]
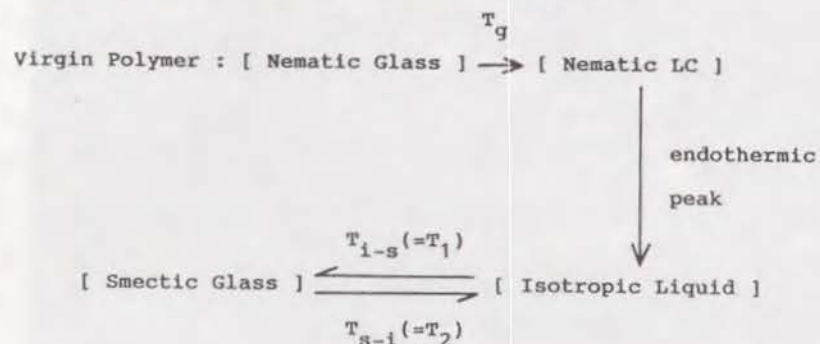
Polymers C, D, and E: high MW and broad MWD polymers

Virgin Polymer:

[Amorphous Glass] $\overset{T_g}{\rightleftharpoons}$ [Isotropic Liquid]

Figure 6. Schematic representation of phase transitions for the different CBPVE polymers.

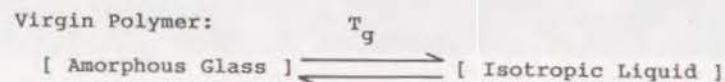from the smectic to the isotropic states while the higher MW and broader MWD polymers, polymers C, D, and E, had their Tg above the isotropic to smectic transition temperature. Hence, the latter polymers formed only an amorphous glass on cooling from the isotropic liquid as shown in Figure 6.

3. Molecular Weight Dependency of the Thermal Properties

In order to reconfirm this interpretation that the relatively lower MW and narrower MWD poly(CBPVE) could show a smectic phase while the relatively higher MW polymer could form only an isotropic phase after the first heating cycle, two experiments were carried out, including (1) fractionation of the broader MWD polymer and (2) blending of the broader and narrower MWD polymers as follows:

(1) Fractionation. Because both polymers A and B contain small amounts of very low MW fractions, this fraction could show a plasticizing effect, which could explain why the overall Tg was depressed and the smectic phase would form. For this reason, the fractionation of polymer B to high and low MW components was carried out, and the thermal properties of each fraction were determined.

(2) Blending. Because the thermal properties of polymers B and C in Table 3 differed so greatly with increasing $\overline{Mn}$ from 2,100 to 3,500, then by adding a small amount of the higher MW polymer, which does not show a smectic phase, to the low MW polymer, which does, it should be possible to change the thermal properties of the latter. Therefore, the thermal properties of a blend of these two polymers were determined.

Figure 7 shows the MWD of the CBPVE polymers before and after fractionation and blending, and the thermal properties of these samples are summarized in Table 4. Two conclusion can be drawn from the data in Table 4:

(1) Both the higher MW and the lower MW portions of polymer B exhibited a smectic phase, so the reason that polymer B forms a smectic phase cannot be attributed only to the presence of the low MW portion of the sample;

(2) By adding only 25% by weight of the higher MW polymer, polymer D, which did not show any mesophase, to the lower MW polymer, polymer B, which did, the thermal properties of B were changed dramatically, and the properties of the blend were dominated by that of the higher MW polymer.

The thermal properties of poly(CBPVE) as a function of $\overline{Mw}$ are summarized in Figure 8. Because $\overline{Mw}$ is particularly sensitive to the higher MW portion, this property is an appropriate one to use to discuss the MW dependency of the

Table 4. Thermal properties of CBPVE polymers after Fractionation and after Blending

Polymer	$\bar{M}_n \times 10^{-3}$ [d]	$\bar{M}_w/\bar{M}_n$	thermal transitions (°C)				thermodynamic parameters [g]	
			heating cycle [e]		cooling cycle [f]			
			Tg	Ts-i	Ti-s	Tg	ΔH_{s-i} (cal/g)	$\Delta S_{s-i} \times 10^2$ (cal/g·K)
B-L [a]	2.1	1.02	58 (--)[i]	--[h] (106)[i]	90	--[i]	4.9	1.3
B-H [b]	2.6	1.03	67 (--)[i]	--[h] (111)[i]	85	--[i]	3.5	0.9
F [c]	2.6	1.3	75 (63)	-- (--)	--	65		

a) Low molecular weight fraction of polymer B.
b) High molecular weight fraction of polymer B.
c) Blend of 75 wt% polymer B with 25 wt% polymer D.
d) Determined by GPC relative to polystyrene standards.
e) Taken from the first DSC heating cycle; numbers in parentheses indicate the transition temperatures taken from the second heating cycle.
f) Taken from the first cooling cycle.
g) Taken from the second heating cycle.
h) A broad unknown peak from 100 to 200 °C was observed.
i) Tg may overlap with Ts-i or Ti-s; see text.
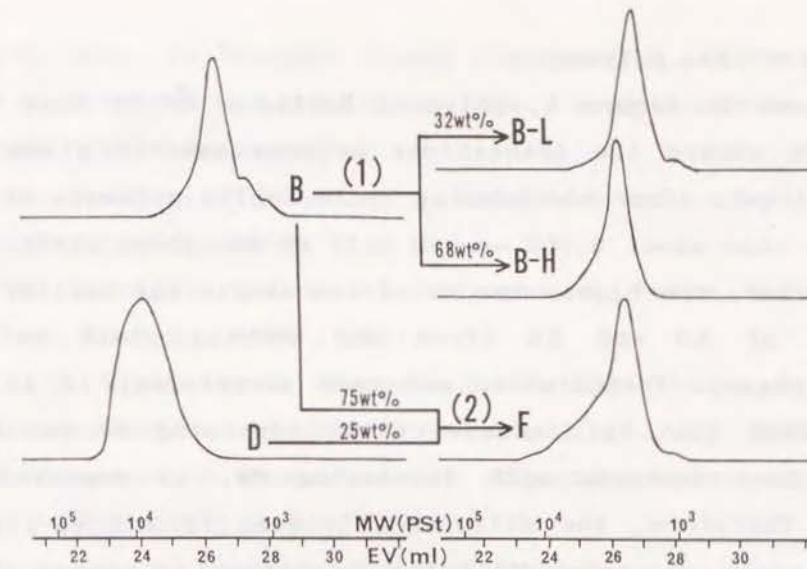
Figure 7. Molecular weight distribution of CBPVE polymers before and after (1) fractionation and (2) blending.
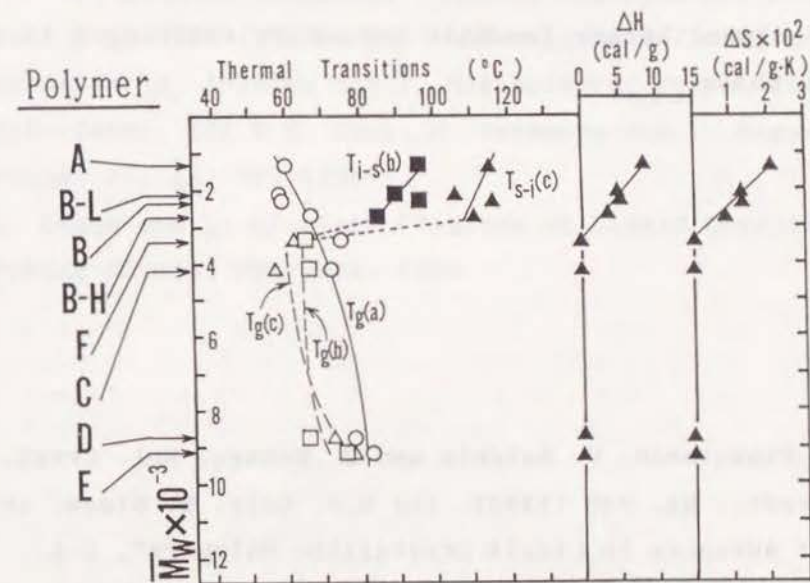
Figure 8. Thermal transition temperatures determined by DSC and thermodynamic parameters, ΔH and ΔS, for the smectic to isotropic transition as a function of $\bar{M}_w$. Designations are as follows: (a) first DSC heating cycle, ($\bigcirc$) Tg; (b) first cooling cycle, ($\square$) Tg, ($\blacksquare$) Ti-s; (c) second heating cycle, ($\triangle$) Tg, ($\blacktriangle$) Ts-i.

properties of this polymer.

As shown in Figure 8, polymers having a $\overline{M}w$ of less than about 3,000 showed the transitions between smectic glass and isotropic liquid after one heating cycle, while polymers having $\overline{M}w$ of more than about 3,000 showed only an amorphous phase, and for the former, the higher the MW of the sample the smaller was the value of ΔH and ΔS (from the smectic phase to the isotropic phase). Furthermore, and very surprising, it is not only the case that Tg increases with increasing MW but also Ti-s and Ts-i decrease with increasing MW, as depicted in Figure 8. Therefore, the difference between Tg and Ti-s also decreases with increasing MW until Tg either increases above Ti-s or overlaps with Ti-s in some MW range, apparently around a $\overline{M}n$ value of 3,000. As a result, during the cooling cycle, the higher MW polymer became immobile before it rearranged to form the smectic phase.

REFERENCES

1) (a) H. Finkelmann, U. Keichle and G. Rehage, Mol. Cryst. Liq. Cryst., 94, 343 (1983). (b) H.J. Cole, R. Simon, in "Recent Advances in Liquid Crystalline Polymers", L.L. Chapoy, Ed., Elsevier Applied Science, New York, 1985, Chapter 22.

2) H. Finkelmann, in "Polymer Liquid Crystals", A. Ciferri, W.R. Krinbaum and R.B. Meyer, Eds., Academic Press, New York, 1982, Chapter 2.

3) Chapter 5 of this thesis; Polym. J., 20, 923 (1988)

4) G.W. Gray, in "Polymer Liquid Crystals", A. Ciferri, W.R. Krigbaum and R.B. Meyer, Eds., Academic Press, New York, 1982, Chapter 1.

5) P.L. Barny, J.-C. Dubois, C. Friedrich and C. Noel, Polym. Bull. 15, 341 (1986).

6) J.M. Rodriguez-Parada and V. Percec, J. Polym. Sci., Polym. Chem. Ed., 24, 1363 (1986).

7) (a) M. Miyamoto, M. Sawamoto and T. Higashimura, Macromolecules, 17, 265 (1984); (b) ibid., 17, 2228 (1984).

8) M. Sawamoto, C. Okamoto and T. Higashimura, Macromolecules, 20, 2693 (1987).

9) T. Enoki, M. Sawamoto and T. Higashimura, J. Polym. Sci., Polym. Chem. Ed., 24, 2261 (1986).

10) (a) S. Aoshima, O. Hasegawa and T. Higashimura, Polym. Bull., 13, 229 (1985); (b) ibid., 14, 417 (1985). (c) T. Nakamura, S. Aoshima and T. Higashimura, Polym. Bull., 14, 515 (1985). (d) W.O. Choi, M. Sawamoto and T. Higashimura, Polym. J., 19, 889 (1987).

11) D. Demus and L. Richter, "Texture of Liquid Crystals", Verlag Chemie, New York, 1978.

CHAPTER 7

MOLECULAR WEIGHT EFFECTS ON THERMAL PROPERTIES OF SIDE-CHAIN LIQUID CRYSTALLINE POLY(VINYL ETHER)S WITH PENDANT ALKOXYBIPHENYL MESOGENIC GROUPS

ABSTRACT

Two vinyl ether monomers with alkoxybiphenyl groups, 2-(4'-ethoxy-4-biphenyloxy)ethyl vinyl ether (EtOVE) and 2-(4'-hexyloxy-4-biphenyloxy)ethyl vinyl ether (HexOVE), were polymerized by living cationic polymerization reactions using either the hydrogen iodide/iodine (HI/I_2) or the hydrogen iodide/zinc iodide (HI/ZnI_2) initiator system, or both. These initiators yielded polymers with narrow molecular weight distributions (MWDs) and for comparison broad MWD polymers were also prepared by using the boron trifluoride etherate (BF_3OEt_2) initiator. The thermal properties and phase transitions of these polymers were determined by DSC, by visual observation of samples on a hot stage on a polarizing microscope, by polarized light transmission intensity measurements and by wide angle X-ray diffraction analysis. The polymer from EtOVE, P(EtOVE), with a weight average molecular weight, $\overline{Mw}$, of less than about 8,000 formed both smectic and nematic liquid crystalline, LC, phases after one heating cycle. In contrast, the polymer from this monomer which had an $\overline{Mw}$ of more than about 8,000 exhibited only nematic LC phase. For the polymer from HexOVE, P(HexOVE), both the narrow and broad MWD samples showed only a nematic LC phase over the $\overline{Mw}$ range from 2,600 to 7,300. The phase transitions of both types of the polymers are discussed in relation to the molecular weight and MWD of the samples. The effect of the terminal group attached to the biphenyl group in the polymer is considered in relation to its possible steric effects.
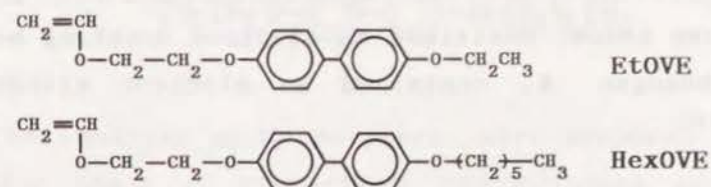
INTRODUCTION

Recently, the potential use of side chain liquid crystal-line polymer, LCP, systems for application in electro-optical devices has received much attention,[1-6] because of their combination of polymeric material properties and monomeric liquid crystalline properties. The main research activity on such side chain LCPs has been concentrated on their synthesis, on understanding their structure-property relations and on their electro-optical properties.[7, 8] Although it is known that molecular weight (MW) and molecular weight distribution (MWD) are important factors which affect the thermal properties of the LCPs, there have been few studies on their effects so far.

The author's investigations have been concerned with this relationship for side-chain LCPs, and the MW and MWD effects on the thermal properties of both narrow and broad MWD polymers were described in the preceding two chapters. The polymers studied were obtained from 2-(4'-methoxy-4-biphenyloxy)ethyl vinyl ether[9] and from 2-(4'-cyano-4-biphenyloxy)ethyl vinyl ether[10], by using the living cationic polymerization reaction recently developed by Higashimura and coworkers (for reviews see References 11-14):

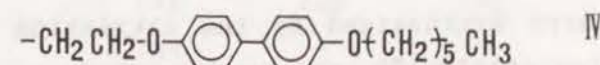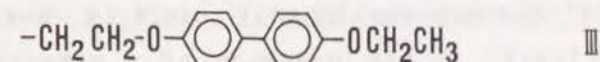$$CH_2=CH \longrightarrow -(CH_2-CH)- \\ \quad | \qquad\qquad\quad | \\ \quad O-R \qquad\qquad O-R$$

in which R represents the two different mesogenic groups. Mesogen I, shown below, contained an electron donating methoxy group, while mesogen II, contained an electron withdrawing cyano group.[9, 10]
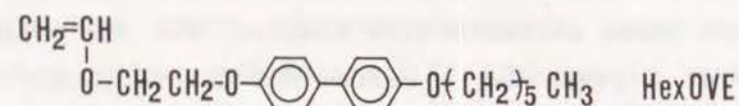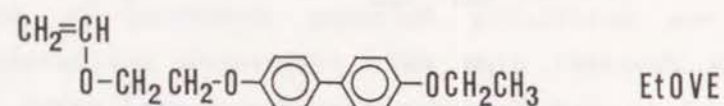

$$-CH_2CH_2-O-\langle\bigcirc\rangle-\langle\bigcirc\rangle-OCH_3 \qquad I$$

$$-CH_2CH_2-O-\langle\bigcirc\rangle-\langle\bigcirc\rangle-CN \qquad II$$
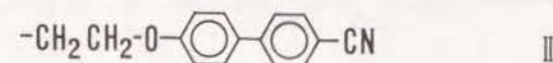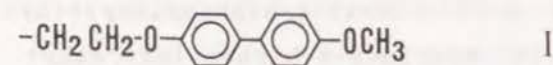
The relationships between the MW (or MWD) and the thermal properties of these polymers were complex. For the polymer with mesogen I at a given $\overline{M}n$, a narrow MWD sample showed enantiotropic liquid crystalline behavior and formed both smectic and nematic phases, but a broad MWD sample formed only a nematic phase. For the polymer with mesogen II, a low MW sample with narrow MWD formed a smectic phase, but a high MW sample or a sample with a broad MWD exhibited only an amorphous character. These phenomena were interpreted on the basis of the relationship between the transition temperature to or from the smectic phase and the glass-transition temperature, Tg. That is, the author concluded that these polymers had a monotropic smectic phase relative to the Tg.

In this chapter, polymers with mesogen III and IV having terminal alkoxy groups, either the ethoxy group or the hexyloxy group, both of which are larger in size than the previously

$$-CH_2CH_2-O-\langle\bigcirc\rangle-\langle\bigcirc\rangle-OCH_2CH_3 \qquad III$$

$$-CH_2CH_2-O-\langle\bigcirc\rangle-\langle\bigcirc\rangle-O(CH_2)_5CH_3 \qquad IV$$

described methoxy group polymers, were prepared and character-ized for their LC properties. The polymers were prepared by
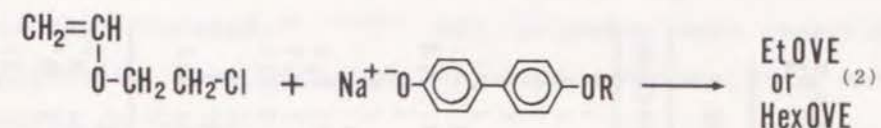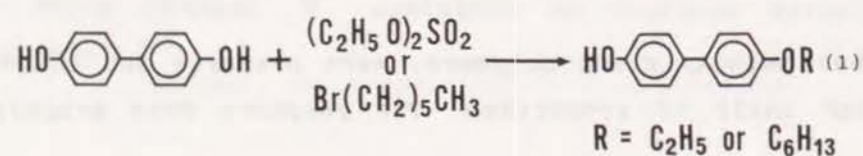
both traditional and living cationic polymerization reactions of the monomers 2-(4'-ethoxy-4-biphenyloxy)ethyl vinyl ether (EtOVE) and 2-(4'-hexyloxy-4-biphenyloxy)ethyl vinyl ether (HexOVE) shown below:

$$CH_2=CH$$
$$|$$
$$O-CH_2CH_2-O-\!\!\bigcirc\!\!-\!\!\bigcirc\!\!-OCH_2CH_3 \quad EtOVE$$

$$CH_2=CH$$
$$|$$
$$O-CH_2CH_2-O-\!\!\bigcirc\!\!-\!\!\bigcirc\!\!-O(CH_2)_5CH_3 \quad HexOVE$$

The phase transitions of the polymers were investigated in relation to their MW and MWD, and the effect of the terminal alkoxy group attached to the biphenyl group is considered in this chapter.

EXPERIMENTAL SECTION

Monomer Synthesis. 2-(4'-ethoxy-4-biphenyloxy)ethyl vinyl ether (EtOVE) and 2-(4'-hexyloxy-4-biphenyloxy)ethyl vinyl ether (HexOVE) were prepared by the phase transfer-catalyzed condensation of 2-chloroethyl vinyl ether with the sodium salt of either 4-(4'-ethoxyphenyl)phenol or 4-(4'-hexyloxyphenyl)-phenol, respectively, in the presence of a catalytic amount of tetrabutylammonium hydrogen sulphate [eq.(2)].[15] The alkoxy-phenylphenols were synthesized by the alkylation reactions of 4,4'-biphenol [eq.(1)][15,16], as shown below:

$$HO-\!\!\bigcirc\!\!-\!\!\bigcirc\!\!-OH + \begin{array}{c}(C_2H_5O)_2SO_2\\ or\\ Br(CH_2)_5CH_3\end{array} \longrightarrow HO-\!\!\bigcirc\!\!-\!\!\bigcirc\!\!-OR \quad (1)$$

$$R = C_2H_5 \text{ or } C_6H_{13}$$

$$CH_2=CH$$
$$|$$
$$O-CH_2CH_2-Cl + Na^+ {}^-O-\!\!\bigcirc\!\!-\!\!\bigcirc\!\!-OR \longrightarrow \begin{array}{c}EtOVE\\ or \quad (2)\\ HexOVE\end{array}$$

EtOVE and HexOVE were purified by recrystallization from methanol. Thermal transitions of the monomers as measured by differential scanning calorimetry (DSC) and their ^{1}H- and ^{13}C-nuclear magnetic resonance (NMR) chemical shifts are summarized in Tables 1 and 2.

Initiators and Solvents. The hydrogen iodide (HI), iodine (I_2), zinc iodide (ZnI_2) and boron trifluoride etherate (BF_3OEt_2) initiators and solvents (methylene chloride, n-hexane, and diethyl ether) used were purified as previously reported.[17-20]

Table 1.

Thermal properties [a] of the monomers

Monomer	Tm [b]	Ti [b]	Td [c]	Tc [c]
	(°C)			
EtOVE [d]	132	138	131	118
HexOVE	136	-	-	131

a) Determined by DSC.
b) Taken from the second heating cycle thermogram: Tm, melting temperature; Ti, isotropization temperature.
c) Taken from the first cooling cycle thermogram: Td, deiso-tropization temperature; Tc, recrystallization temperature.
d) Enantiotropic liquid crystalline phase (smectic) was identified with the polarizing microscope.

Table 2.

^{1}H- and ^{13}C-NMR chemical shifts[1]) of the monomers and the polymers

	EtOVE $R = C^m H_2 C^n H_3$		HexOVE $R = C^m H_2 C^n H_2 C^o H_2 C^p H_2 C^q H_2 C^r H_3$	
	^{1}H-NMR δ(ppm) proton	^{13}C-NMR δ(ppm) carbon	^{1}H-NMR δ(ppm) proton	^{13}C-NMR δ(ppm) carbon
Monomer	1.43(t) :: n	15.7 :: n	0.90(t) :: r	14.0 :: r
	4.00–	64.3 ::	1.00–	22.6 :: q
	4.40(m):a,c,d,m	67.1 &	1.90(m):n,o,p,q,r	28.4 :: o
	6.50	67.3 :: c,d	3.80–	29.2 :: n,p
	(d of d): b	87.8 :: a	4.30(m):a,c,d,m	31.6 &
	6.75–	115.5 &	6.50	66.3 & :: c,d
	7.05(m): f,k	115.7 :: f,k	(d of d): b	66.4 :: m
	7.40–	128.5 :: g,j	6.70–	68.1 :: a
	7.55(m): g,j	134.0 &	7.05(m): f,k	87.0 :: a
		134.7 :: h,i	7.25–	114.9 :: f,k
		152.4 :: b	7.60(m): g,j	127.7 :: g,j
		158.4 &		137.9 :: h,i
		158.9: e,l		151.8 :: b
				158.5 &
				159.5: e,l
Polymer	1.0–2.0: a',n	40.6 & : a'	0.90 :: r	40.7 &
	3.4–4.4:b',c,d,m	41.7: b'	1.0–2.0:a',n,o,p,q,r	41.5: a'
	6.7–7.1: f,k	74.5 ::	3.4–4.5:b',c,d,m	73.9 :: b'
	7.3–7.6: g,j	c,d,.....n2)	6.7–7.1: f,k	c,d,.....r2)
			7.2–7.6: g,j	

Monomer structure / Polymer structure

1) Chemical shifts are given in ppm relative to TMS.
2) The signals of the pendant groups(=X) are the same position as those of the monomers.

Polymerization Procedures. Cationic polymerization reactions were carried out in a dry-nitrogen atmosphere as previously reported.[9, 17-20] All polymers were purified by precipitation from methylene chloride solution into methanol and dried in vacuum.

Fractionation and Blending Procedures. P(EtOVE) sample D (see Table 3), which was obtained by initiation with BF$_3$OEt$_2$, was not completely soluble in chloroform at room temperature after precipitation into methanol even though the polymer remained soluble until the end of the polymerization reaction in methylene chloride at -5 ℃. Therefore, sample D was separated into chloroform-soluble and -insoluble fractions by extraction with chloroform at room temperature at a concentration of 100mg of polymer for 10ml of solvent. The insoluble fraction, D-H, which represented 77wt% of sample D, was recovered by filtration, and the soluble fraction, D-L, which represented the remainder was recovered by evaporation of the solvent. Both fractions were soluble in either N,N-dimethylformamide or nitrobenzene at an elevated temperature (60-80 ℃).

To prepare the blend of samples E and F (see Table 4), the two polymers were dissolved in N,N-dimethylformamide at 70 ℃. Concentration of 100mg/10ml solvent were used for the preparation of blends of D-H and A. The blended polymers (E and F) were recovered by precipitation from N,N-dimethylformamide solution into methanol and dried in vacuum before the characterization.

Characterization of Monomers and Polymers. The molecular weight distribution of the polymers was measured by gel permeation chromatography (GPC) using CHCl$_3$ as the eluent on a

Waters Associates Inc. liquid chromatograph equipped with five polystyrene gel columns (8mm × 23cm each) and refractive index (RI) detector. The number average and weight average molecular weights ($\overline{Mn}$ and $\overline{Mw}$) were calculated with the use of a standard polystyrene calibration curve. For the $CHCl_3$-insoluble polymers (samples C, D, E, F and D-H), samples were injected into the chromatograph as N,N-dimethylformamide solutions for convenience sake.

^1H- (200 or 300 MHz) and ^{13}C- (75.4 MHz) NMR spectra were obtained with Varian XL-200 or XL-300 spectrometers in $CDCl_3$ at room temperature. The chemical shifts of the ^1H- and ^{13}C-NMR spectra of the monomers (EtOVE and HexOVE) and the corresponding polymers are summarized in Table 2. As the chemical shifts of the monomers and their polymers indicate, after the polymerization the signals of the vinyloxy group in the monomers [^1H-NMR, 6.50 ppm for both EtOVE and HexOVE ($CH_2=C\underline{H}-O-$); ^{13}C-NMR, 87.8 (C^a) and 152.4 ppm (C^b) for EtOVE, 87.0 (C^a) and 151.8 ppm (C^b) for HexOVE ($\underline{C}^aH_2=\underline{C}^bH-O-$)] disappeared and new signals corresponding to the main chain methylene and methine structure [^1H-NMR, 1.0-2.0 and 3.4-4.3 ppm for both EtOVE and HexOVE ($-C\underline{H}_2-C\underline{H}-$); ^{13}C-NMR, 40.6 and 41.7 ppm for EtOVE, 40.7 and 41.5 ppm for HexOVE ($-\underline{C}H_2-CH-$), and 74.5 ppm for EtOVE, 73.9 ppm for HexOVE ($-CH_2-\underline{C}H-$)] appeared. Both ^1H- and ^{13}C-NMR spectra also showed that the signals of the pendant group (X in Table 2) are exactly the same as those of the monomers with some peak broadening.

Thermal analyses were carried out on a Perkin-Elmer DSC-2 instrument with polymer and monomer samples of 5-10 mg under a nitrogen flow at a scanning rate of 10 ℃/min. Indium and naphthalene were used for the calibration of the temperature scale. The melt behavior of the polymers was visually observed using a polarizing light microscope equipped with cross-polarizers and a hot stage.

The apparatus used for light transmission studies contained a laser, a polarizer, a Mettler hot stage and a photomultiplier. A Spectra Physics He-Ne gas laser (λ =6358 Å) was used as a light source.

X-ray diffraction experiments were carried out on a Statton flat film camera using Ni-filtered CuKα radiation (λ =1.542 Å) under reduced pressure. The powder samples were sealed in glass capillaries, and a home-made hot stage was used to control the sample temperature within 1 ℃.

RESULTS AND DISCUSSION

1. Polymerization of EtOVE and HexOVE

The cationic polymerization of EtOVE or HexOVE was carried out with the HI/I_2 and the HI/ZnI_2 initiators, both of which are reported to be living-polymerization initiator systems,[11-14, 17-19] and also with boron trifluoride etherate (BF_3OEt_2), which is a conventional cationic initiator. The polymerization conditions and the MW values of the polymers so obtained are summarized in Table 3. Figures 1 and 2 show the MWDs of the polymers.

Polymers A, B, P, Q and R were soluble in the polymerization solvent at the polymerization temperatures and in the $CHCl_3$ at room temperature for the GPC measurements. All polymers had the expected structures, as indicated by the NMR data in Table 2. As described in the preceding two chapters,[9, 10] the HI/I_2- or the HI/ZnI_2-initiated reactions gave polymers (polymers A, B, P and Q) with narrow MWDs and with $\overline{Mw}/\overline{Mn}$ ratios varying from 1.02 to 1.1. In contrast, the BF_3OEt_2-initiated

Table 3.

Cationic polymerization of EtOVE and HexOVE[1]

Monomer	Polymer designation	Initiator(mM), solvent,temp.(°C)	$[M]_0$ (M)	Reaction time(hr)	$\overline{M}_n \times 10^{-3}$ Calcd.[2]	$\overline{M}_n \times 10^{-3}$ Obsvd.[3]	$\overline{M}_w/\overline{M}_n$[3]	$\overline{DP}_n$[4]
EtOVE	A	HI/ZnI_2(11.1/0.4) Toluene, 40	0.09	24	2.3	2.0	1.1	7.0
	B	HI/I_2 (10.1/0.2) CH_2Cl_2, -5	0.10	24	2.8	2.6	1.1	9.2
	C	HI/ZnI_2 (3.1/0.2) CH_2Cl_2, -5	0.09	20	5.3	5.3	1.3	18.7
	D	BF_3OEt_2 (2.5) CH_2Cl_2, -5	0.05	24	---	4.0	2.5	14.1
	D-H	[$CHCl_3$ insoluble part (=77wt%) of D]			---	5.5	2.2	19.4
	D-L	[$CHCl_3$ soluble part (=23wt%) of D]			---	2.1	1.3	7.4
HexOVE	P	HI/ZnI_2 (5.7/0.3) CH_2Cl_2, -5	0.05	92	3.0	2.5	1.02	7.4
	Q	HI/ZnI_2 (10.1/0.4) toluene, 40	0.10	24	3.4	3.0	1.04	8.8
	R	BF_3OEt_2 (2.5) CH_2Cl_2, -5	0.05	24	---	2.8	2.6	8.2

1) All reaction conversion were close to 100%, except sample C (=64%).
2) Calcd. $\overline{M}_n$ = (MW of monomer) X ([M]consumed/[HI]$_0$)
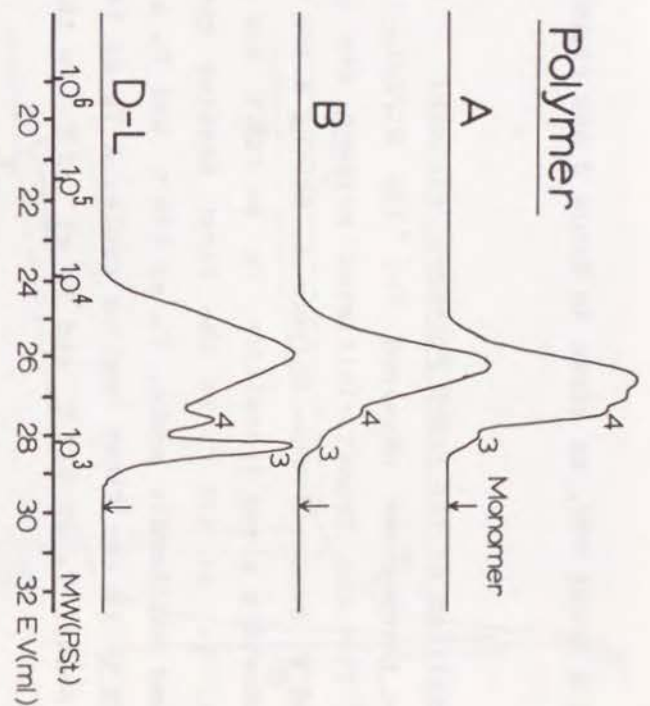3) Determined by GPC calibrated with standard polystyrene samples.
4) Number-average degree of polymerization calculated from $\overline{M}_n$(obsvd.).

Figure 1. MWD of P(EtOVE); see Table 3 for reaction conditions. Numbers near the peaks indicate the degree of polymerization of the sample.
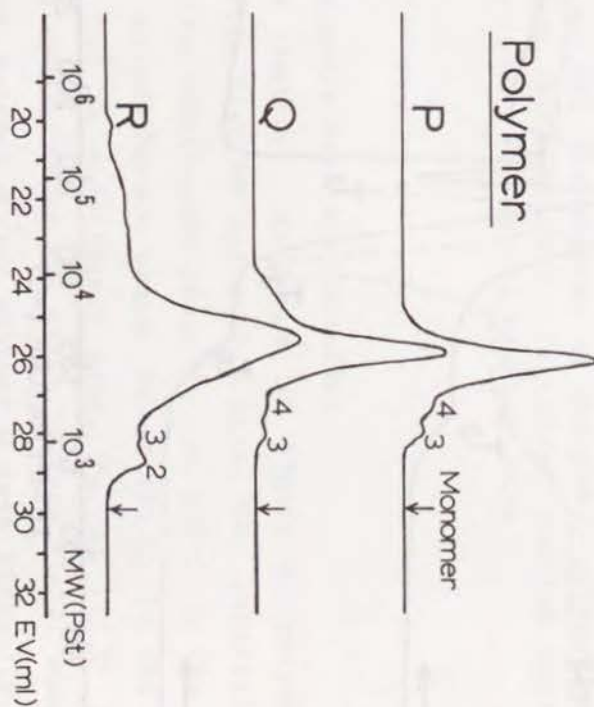

Figure 2. MWD of P(HexOVE); see Table 3 for reaction conditions. Numbers near the peaks indicate the degree of polymerization of the sample.

polymers had a broad MWD, as shown in Table 3 and Figures 1 and 2.

2. Phase Transition of the EtOVE Polymers, P(EtOVE)

Typical thermograms obtained for the HI/ZnI_2-initiated polymer and for the BF_3OEt_2-initiated polymer are shown in Figures 3 and 4, respectively. Polymer A, having a low MW and a narrow MWD showed a glass transition, Tg, at 122 ℃ and an endothermic peak, T_1, at 175 ℃ in the first heating cycle (see Figure 3), and exothermic peaks, T_2 at 176 ℃ and T_3 at 160 ℃, and Tg at 120 ℃ in the first cooling cycle. A Tg at 141 ℃ and endothermic peaks, T_4 at 177 ℃ and T_5 at 182 ℃, in the second
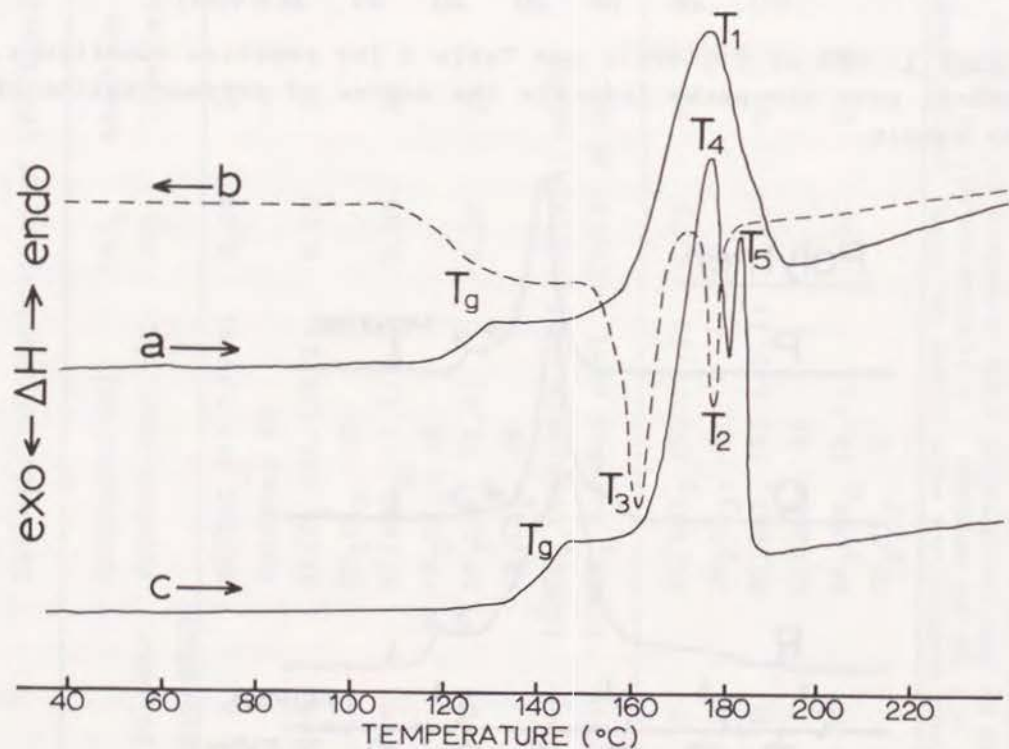

Figure 3. DSC thermograms of P(EtOVE), polymer A, obtained by initiation with HI/ZnI_2: (a) first heating cycle, (b) first cooling cycle, (c) second heating cycle.
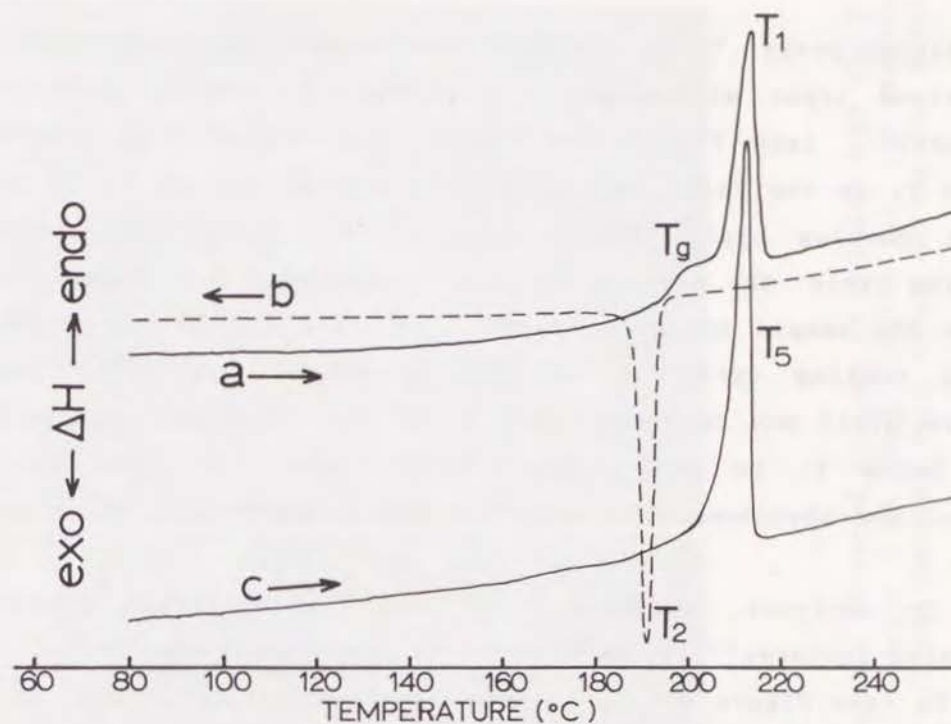

Figure 4. DSC thermograms of P(EtOVE), polymer D, obtained by initiation with BF_3OEt_2: (a) first heating cycle, (b) first cooling cycle, (c) second heating cycle.

heating cycle were also observed.

In contrast, as shown in Figure 4, polymer D, with a relatively high MW and with a broad MWD, exhibited a Tg at 195 ℃ and an endothermic peak, T_1, at 209 ℃ in the first heating cycle, an exothermic peaks, T_2 at 191 ℃, in the first cooling cycle, and an endothermic peak, T_5, at 212 ℃ in the second heating cycle. After the first heating cycle, subsequent cycles for both polymer A and polymer D gave virtually identical DSC thermograms.

To identify the phases present before and after the

transition peaks, T_1-T_5, texture observations were made with a polarized light microscope. For polymer A, nematic threaded textures[21] [see Figure 5(a)] were observed at temperatures below T_1 in the first heating cycle, between T_2 and T_3 in the first cooling cycle, and between T_4 and T_5 in the second heating cycle. The nematic threaded texture did not change even after the sample was kept below T_2 (173 ℃) for 30 min in the first cooling cycle. A smectic fan-shaped texture[21] [see Figure 5(b)] was observed below T_3 in the first cooling cycle and below T_4 in the second heating cycle. The same phase transition phenomena were observed for polymers D-L, B, E and C.

In contrast, polymers D, F and D-H exhibited nematic threaded textures[21] [Figure 5(c)] at temperatures below T_1, T_2 and T_5 (see Figure 4). The nematic texture did not change when polymer D was kept just below T_2 (188 ℃) for 30 min in the first cooling cycle.

Each transition peak and each phase before and after the peak could be identified in this manner, and the transitions are represented in Figure 6, in which Tx-y indicates the transition temperature from the x-phase to the y-phase. The assigned transitions are also listed in Table 4, and the transition temperatures of P(EtOVE) as a function of $\overline{Mw}$ are shown in Figure 7.

From the data in Table 4 and Figure 7, three conclusions can be drawn for this polymer:

(1) With increasing MW, the Tg and Tn-i increased, but Ts-n was not affected. As a result, the temperature range above Tg and below Ts-n for the smectic LC phase became increasingly narrow and, at an $\overline{Mw}$ of approximately 8,000, the smectic phase did not appear.
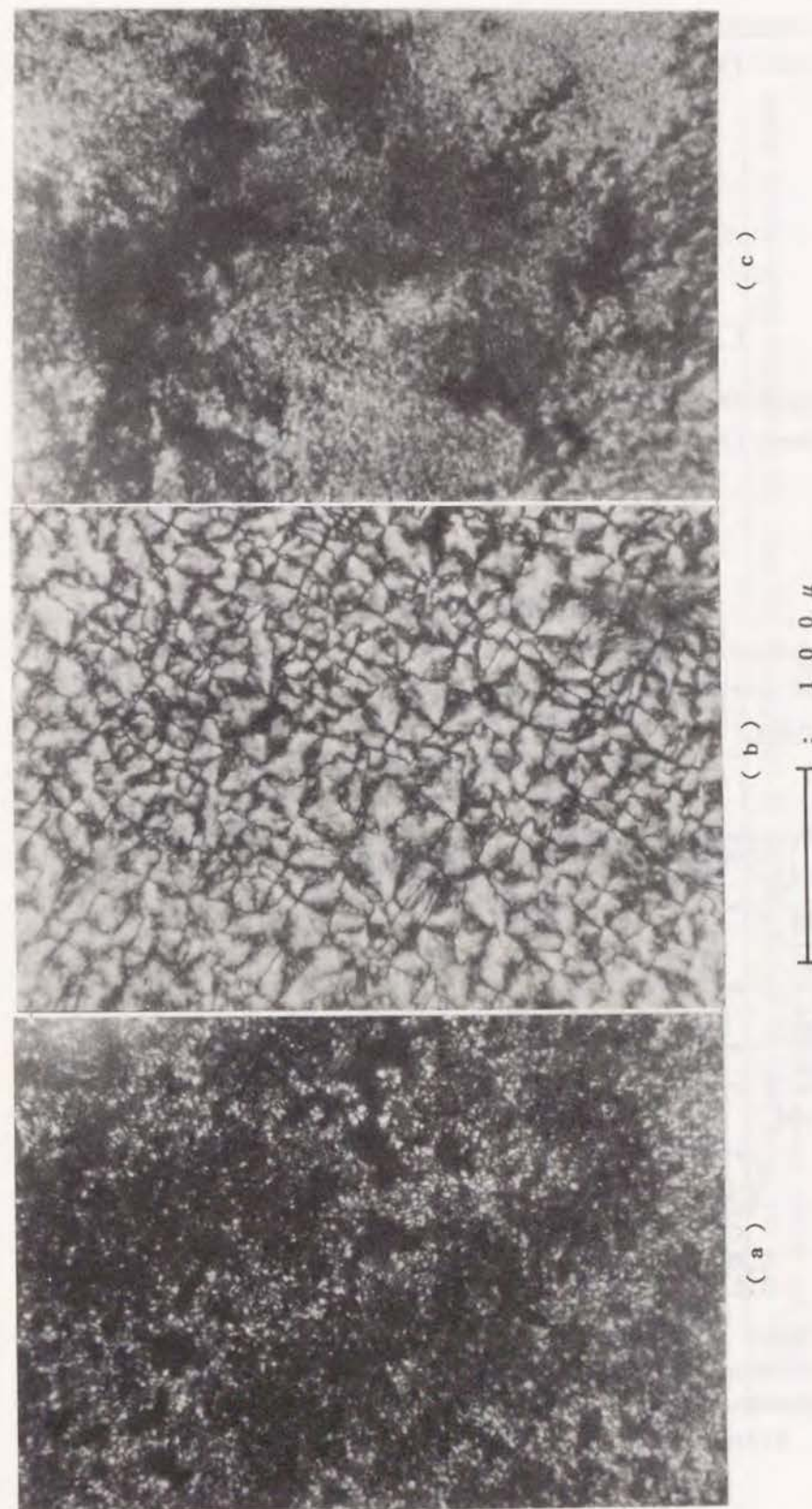
: 100 μ

Figure 5. Photomicrographs of P(EtOVE) showing: (a) nematic threaded texture of polymer A at 173 ℃ (between T_2 and T_3); (b) smectic fan-shaped texture of polymer A at 150 ℃ (below T_3); (c) nematic threaded texture of polymer D at 188 ℃ (below T_2); all photographs were taken during the first cooling cycle (original magnification: 320 ×).

Low MW poly(EtOVE) (Polymers A, D-L, B, E, and C)

Virgin Polymer: Nematic Glass

Nematic Glass — T_g → Nematic LC — $T_1(T_{n-i})$ → Isotropic Liquid — $T_2(T_{i-n})$ → Nematic LC — $T_3(T_{n-s})$ → Smectic LC — $T_4(T_{s-n})$ → Nematic LC — $T_5(T_{n-i})$ →

Smectic Glass — T_g →

High Mw poly(EtOVE) (Polymers F, D, D-H)

Virgin Polymer: Nematic Glass

Nematic Glass — T_g → Nematic LC — $T_1(T_{n-i})$ → Isotropic Liquid — $T_2(T_{i-n})\ (=T_g)$ → Nematic Glass — $T_5(T_{n-i})\ (=T_g)$ →

Figure 6. Schematic representation of the comparative thermal transitions of low and high MW samples of P(EtOVE).

$\overline{M}_W \times 10^{-3}$

POLYMER

D-H, D, F, C, E, B, D-L, A

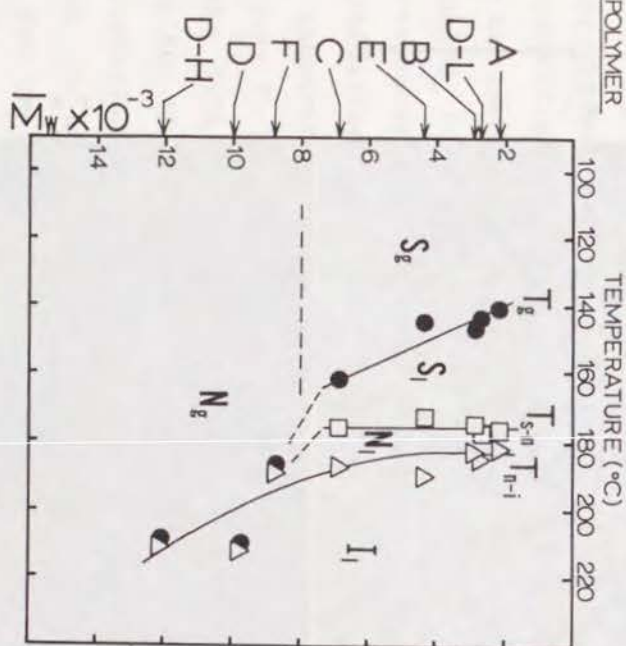S_g, S_l, N_g, N_l, I_l, T_g, T_{s-n}, T_{n-i}

TEMPERATURE (°C)

Figure 7. Phase diagram of P(EtOVE) as a function of $\overline{M}_W$, showing transition temperatures during the second heating cycle of the DSC thermograms: I, isotropic; N, nematic; S, smectic,; l, liquid; g, glass.

Table 4.

Thermal properties of Poly(EtOVE)s

Polymer designation	$\overline{M}_W \times 10^{-3}$ / $\overline{M}_n \times 10^{-3}$ / $\overline{M}_W/\overline{M}_n$	Thermal transitions(°C) by DSC — Heating cycle[1]			Cooling cycle[2]			Thermodynamic parameters[3] — ΔH (cal/g)		ΔS X 10² (cal/g·K)	
		T_g	T_{s-n}	T_{n-i}	T_{i-n}	T_{n-s}	T_g	ΔH_{s-n}	ΔH_{n-i}	ΔS_{s-n}	ΔS_{n-i}
A	2.2 / 2.0 / 1.1	122 (141)	---- (177)	175 (182)	176	160	120	9.4	2.2	2.1	0.5
D-L[4]	2.7 / 2.1 / 1.3	127 (144)	---- (178)	178 (185)	175	158	125	9.0	2.2	2.0	0.5
B	2.9 / 2.6 / 1.1	141 (147)	---- (175)	181 (183)	170	152	123	9.4	3.1	2.1	0.7
E[5]	4.4 / 2.3 / 1.9	147 (145)	---- (173)	199 (193)	167	147	125	7.1	6.0	1.6	1.3
C	6.9 / 5.3 / 1.3	173 (162)	---- (176)	194 (187)	168	153	139	5.8	6.1	1.3	1.3
F[5]	8.8 / 3.5 / 2.5	195[6] ----	---- ----	206 (189)	176	----	[6]	----	13.0	----	2.8
D	10.0 / 4.0 / 2.5	195[6] ----	---- ----	209 (212)	191	----	[6]	----	13.1	----	2.7
D-H[4]	12.1 / 5.5 / 2.2	202[6] ----	---- ----	210 (211)	191	----	[6]	----	15.2	----	3.1

1) Taken from the first heating cycle; numbers in parentheses indicate the transition temperatures taken from the second heating cycle.
2) Taken from the first cooling cycle.   3) Taken from the second heating cycle.
4) High and low MW portions of sample D by fractionation (see text).
5) Blend polymers of samples D-H and A: E, D-H/A=22/78 wt%; F, D-H/A=67/33 wt% (see text).
6) Tg may overlap with Tn-i or Ti-n.

(2) At approximately the same $\overline{M}n$, the broad distribution sample, F, had different thermal properties, including a higher Tg and Tn-i but no Ts-n, from those of the narrow distribution sample, B. Possibly, the Tg and Tn-i values were strongly affected by the higher MW fraction of the broad distribution polymer.

(3) Polymers F, D and D-H, for which the virgin polymers were recovered by precipitation into methanol, showed Tg transitions only in the first heating cycle, and they did not show clearly a Tg after one heating cycle. In some cases the Tg overlapped with the Ti-n or Tn-i transitions after one heating cycle in the same manner as described for the polymers from 2-(4'-methoxy-4-biphenyloxy)ethyl vinyl ether[9] and 2-(4'-cyano-4-biphenyloxy)ethyl vinyl ether[10].

The MW effects on the phase transitions of this polymer can be summarized as follows: during the cooling cycle, the higher MW polymers, most likely those with $\overline{M}w > 8,000$, form a glass phase and become immobile before they can reorganize from the nematic to a smectic phase, so the transition only from the isotropic to the nematic phase occurs. In contrast, when MW is low, the Tg is low too, and the sample can form a smectic phase from the nematic phase before the Tg is reached during the cooling cycle. That is, the former polymer apparently also has a monotropic smectic phase relative to Tg in the same manner as the polymers described in the preceding chapters.[9, 10]

3. Transmitted Light Intensity and X-ray Diffraction Analyses of P(EtOVE)

To confirm the phase transition behavior of P(EtOVE) observed by DSC and by use of a polarizing light microscope, two additional measurements were made: first, transmitted light intensity and, second, wide angle X-ray diffraction (WAXD).

Figures 8 and 9 show the transmitted light intensity of polymers A and D, respectively, as a function of sample temperatures in the first cooling cycle and in the second heating cycle. For polymer A in Figure 8, two changes in intensity can be seen during both the first cooling cycle and the second heating cycle. These changes correspond closely to Ti-n and Tn-s in the first cooling cycle and to Ts-n and Tn-i in the second heating cycle as measured by DSC (see Figure 3). For polymer D in Figure 9, only one change of the transmitted light intensity is seen in each scan, and this change also corresponds to either Ti-n or Tn-i as determined by DSC (see Figure 4).
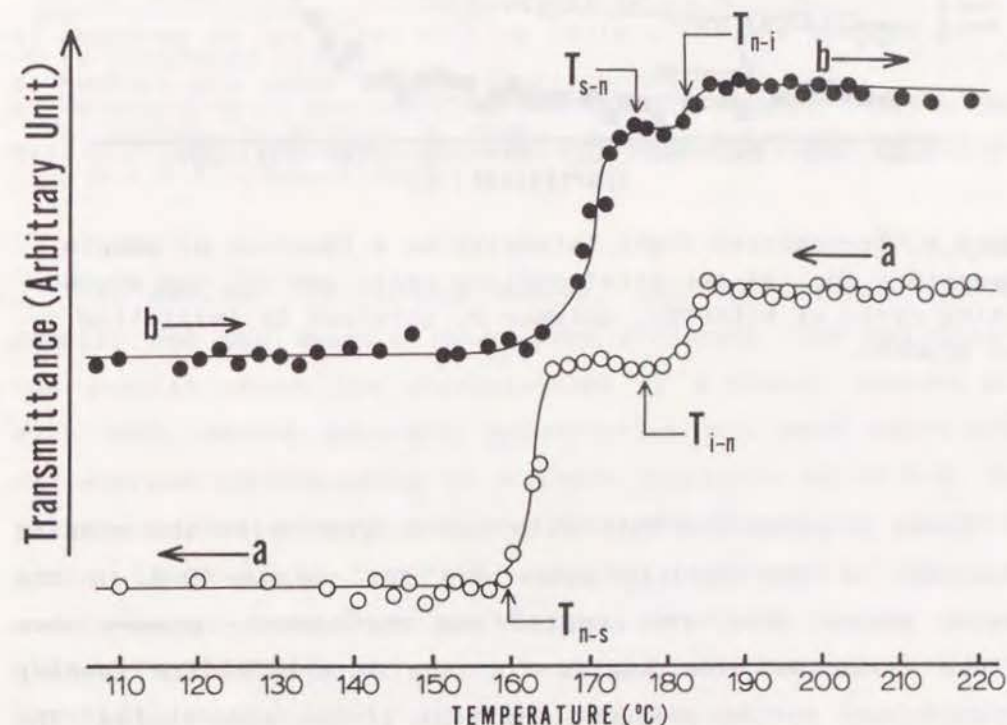

Figure 8. Transmitted light intensity as a function of sample temperature for (a) the first cooling cycle and (b) the second heating cycle of P(EtOVE), polymer A, obtained by initiation with HI/ZnI₂.
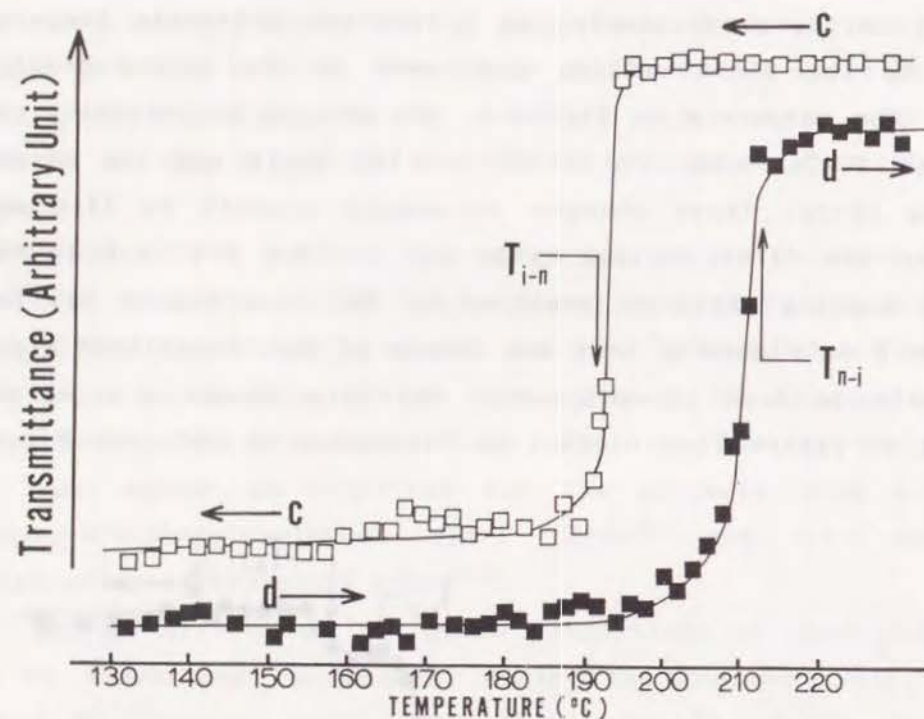
Figure 9. Transmitted light intensity as a function of sample temperature for (a) the first cooling cycle and (b) the second heating cycle of P(EtOVE), polymer D, obtained by initiation with BF$_3$OEt$_2$.

Table 5 shows the WAXD data for polymer A in the nematic phase and in the smectic phase and for polymer D-H in the nematic phase. Both the nematic and the smectic phases show diffuse rings at wide angles for the intermolecular spacing perpendicular to the mesogen long axes of the side-chains. The average intermolecular spacings observed of 4.19-4.34 Å are consistent with those reported for this type of side-chain LCP. [22, 23]

			Polymer A		Polymer D-H
			at 170 ℃ (nematic)	at 135 ℃ (smectic)	at 185 ℃ (nematic)
Small angles					
d_1 ± 1	(Å)		---	29.0(S)	---
d_2 ± 0.2	(Å)		12.8(W)	14.5(M)	13.3(W)
d_3 ± 0.2	(Å)		---	9.74(W)	---
Wide angles					
d_4 ± 0.04	(Å)		4.29(M) [d]	4.34(M) [e]	4.19(M) [f]

a) Measured in the first cooling cycle after the samples melted
   to isotropic liquid.
b) Numbers are taken from diffraction maxima.
c) Intensities of the diffractions are given in parentheses as:
   S, strong; M, medium; W, weak.
d-f) Diffuse diffraction rings with d values 3.9-5.1, 3.9-4.9,
   3.9-4.9 Å, respectively.

At smaller diffraction angles, the WAXD patterns of the nematic and the smectic phase were different. The patterns of the smectic phase are characterized by a sharp, intense ring with both medium strength second-order and weak third-order reflections corresponding to a layer thickness of 29.0 Å. This value is considerably greater than the length of the side-chain, 19-20 Å, in its fully extended conformation. Thus, the existence of some form of bilayer structure in the smectic phase, in which the molecules partially overlap, appears to be verified, as previously reported for the polymer from a cyano-biphenyl-containing acrylate monomer. [23]

For the nematic phase, diffuse rings which correspond to a distance of 12.8-13.3 Å were observed. This value is approximately the length of 4,4'-diethoxybiphenyl, so it may

arise from the intramolecular spacings parallel to the long axes of the side-chain in the same manner as some nematic main chain LCP show a diffuse ring corresponding to distances close to, or equal to, the repeating unit length.[24] This result is an indication that there is no order in the direction of the molecular long axes.

In conclusion, the transmitted light intensity and X-ray diffraction data confirm that the low MW samples of P(EtOVE) had different phase transition behavior from that of high MW samples, as summarized in Figure 6.

4. Phase Transitions of the HexOVE Polymers, P(HexOVE)

The DSC thermograms of the polymer obtained by HI/ZnI₂ initiation, P in Table 3, and by BF₃OEt₂ initiation, R in Table 3, in the polymerization of HexOVE are shown in Figure 10.
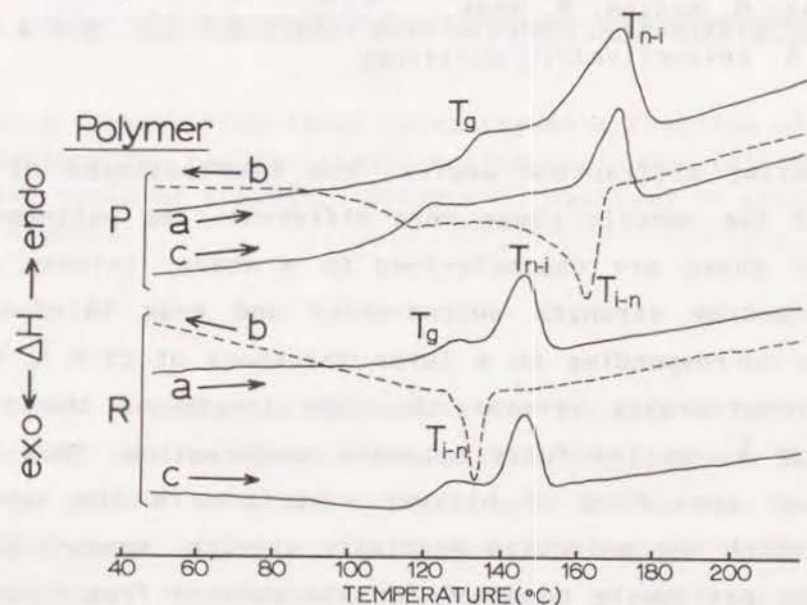
Figure 10. DSC thermograms of P(HexOVE) obtained by initiation with HI/ZnI₂, polymer P, and with BF₃OEt₂, polymer R: (a) first heating cycle, (b) first cooling cycle, (c) second heating cycle.

Photomicrographs of polymers P and R, both of which exhibit nematic threaded textures[21], are shown in Figure 11. The nematic textures did not change after the samples were kept below Ti-n for 30 min in the first cooling cycle. From these data, it may be concluded that polymers P, Q and R all form only a nematic LC phase between Tg and the isotropization temperature, Tn-i, in the molecular weight $2,600 \leq \overline{M}w \leq 7,300$. The thermal properties of these polymers are summarized in Table 6.

With increasing MW, the Tg of P(HexOVE) increased as expected, but unexpectedly Tn-i and Ti-n decreased, as shown in Table 6. As a result, the temperature range of the nematic LC phase between Tg and Tn-i or Ti-n became narrow with increasing MW. For example, polymer R, which had approximately the same $\overline{M}n$ as that of polymer P but had a broader MWD, showed a much narrower temperature range for its nematic LC phase. It appears likely, therefore, that the thermal transitions of this polymer were more strongly affected by the higher molecular weight fraction in the broad distribution sample, in the same manner as described for other LC poly(vinyl ether)s.[9,10]

5. Effect of Terminal Substituent in the Biphenyl Group

To obtain a semi-quantitative indication of the steric effect of the terminal substituents, the bulkiness factor of the substituent, R, attached to the 4'-position of the biphenyl group is calculated by the following equation:

$$\text{bulkiness factor } (\text{Å}) = [\Sigma (\text{bond length})] + [\text{van der Waals radius of the end atom}]$$

The bulkiness factor is the distance from the center of the carbon atom at the 4'-position of the biphenyl group to the end
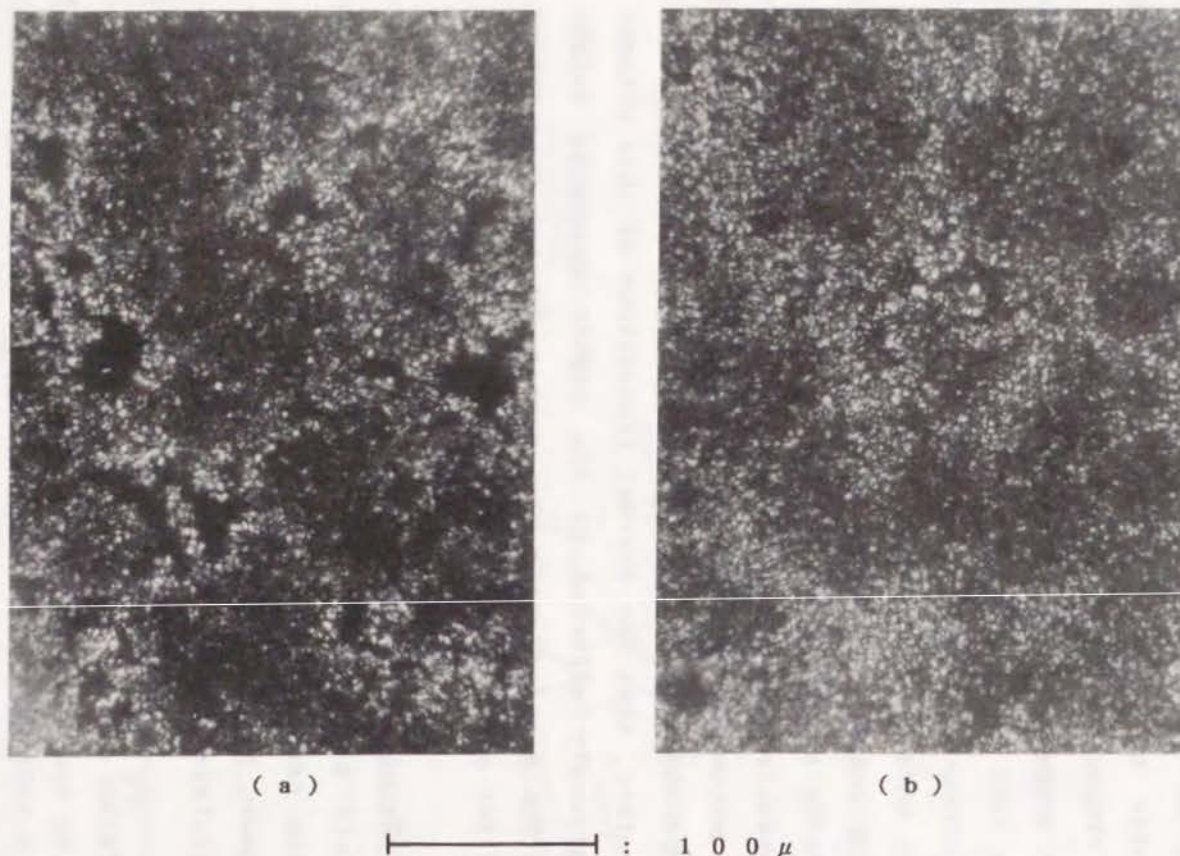
(a)   (b)

├───────────┤ : 1 0 0 µ

Figure 11. Photomicrographs of the nematic threaded textures of samples of P(HexOVE): (a) polymer P at 155 ℃ (just below Ti-n) in the first cooling cycle; (b) polymer R at 125 ℃ (just below Ti-n) in the first cooling cycle (original magnification: 320 ×).

Table 6.

Thermal properties of Poly(HexOVE)s

Polymer designation	$\overline{M}_w$ X 10^{-3} / $\overline{M}_n$ X 10^{-3} / $\overline{M}_w/\overline{M}_n$			Thermal transitions(℃) by DSC				Thermodynamic parameters[3]	
				Heating cycle[1]		Cooling cycle[2]		ΔH_{n-i} (cal/g)	ΔS_{n-i} (cal/g·K)
				T_g	T_{n-i}	T_{i-n}	T_g		
P	2.6 /	2.5 /	1.02	126 (106)	168 (169)	161	105	8.3	1.9
Q	3.1 /	3.0 /	1.04	131 (111)	171 (156)	144	108	9.9	2.3
R	7.3 /	2.8 /	2.6	127 (120)	148 (148)	135	——[4]	4.8	1.1

1) Taken from the first heating cycle; numbers in parentheses indicate the transition temperatures taken from the second heating cycle.
2) Taken from the first cooling cycle.   3) Taken from the second heating cycle.
4) Tg may overlap with Ti-n.

of the substituent and is calculated by assuming that the substituent is fully extended. The bulkiness factors so calculated and the abbreviation for each monomer unit described in Chapters 5-7 are as follows:

$$R = H: \qquad 2.3 \text{ Å}; \text{ HVE}[9]$$
$$R = CN: \qquad 4.2 \text{ Å}; \text{ CNVE}[10]$$
$$R = OMe: \qquad 5.1 \text{ Å}; \text{ MeOVE}[9]$$
$$R = OEt: \qquad 6.6 \text{ Å}; \text{ EtOVE}$$
$$R = OHex: \quad 12.8 \text{ Å}; \text{ HexOVE}$$

Figure 12 shows the general phase diagram for the polymers in this series having different terminal substituents as a function of the bulkiness factor of the substituents. The data in
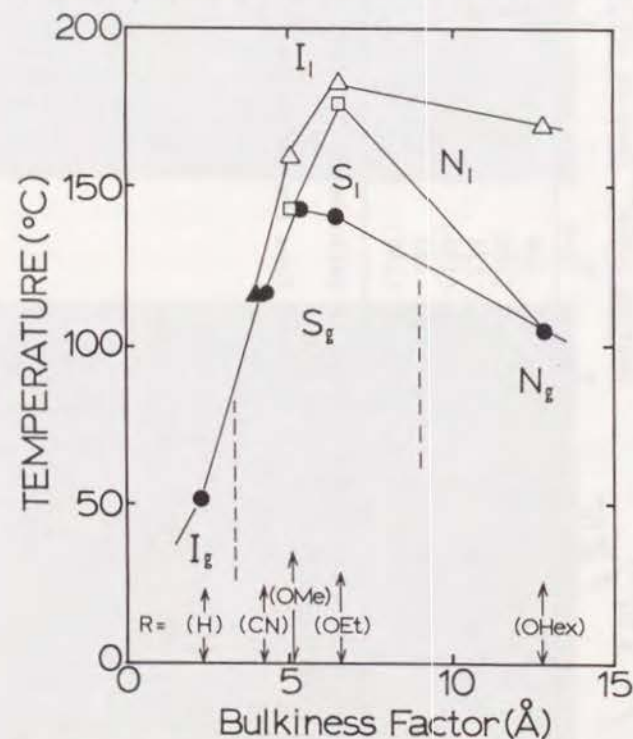
Figure 12. Phase diagram of the poly(vinyl ether)s of this series with various terminal substituents as a function of the bulkiness factor of R. Transition temperatures are those in the second heating cycle: ●, Tg; ▲, Ts-i; □, Ts-n; △, Tn-i. I, isotropic; N, nematic; S, smectic; l, liquid; g, glass.

Figure 12 are only for the polymers with narrow MWDs ($\overline{Mw}/\overline{Mn} \leq$ 1.3) and with $\overline{Mn}$ from 2,000 to 2,500. P(HVE) did not show a mesophase, but all of the other polymers in the series above exhibited at least one mesophase. With increasing bulkiness factor, the isotropization temperature of the polymers, from either the nematic or the smectic phase, increased from R=CN to R=OEt but did not increase from R=OEt to R=OHex, while the Tg increased from R=H to R=OMe but decreased from R=OMe to R=OHex. As a result, the temperature range of the LC phase became wider with increasing bulkiness factor.

Inspection of Figure 12 also reveals that each of the LC polymers exhibited different types of mesophase transitions which may be related to the different lengths of the terminal substituents. The transitions observed for each were as follows:

P(HVE), amorphous glass to isotropic liquid;
P(CNVE), smectic glass to isotropic liquid;
P(MeOVE), smectic glass to nematic liquid to isotropic liquid;
P(EtOVE), smectic glass to nematic liquid to isotropic liquid;
P(HexOVE), nematic glass to nematic liquid to isotropic liquid.

To explain these observations the author can classify the substituents according to their size (small, medium, and large) and polarity as shown in Figure 13. For example, for P(CNVE) the CN substituent is not only small but it is also highly polar, and the enhanced interaction between mesogens may aid in formation of the smectic phase instead of a nematic phase. On the other hand, for the polymers with less polar alkoxy terminal group, there may be an optimum size of R to form a smectic phase.
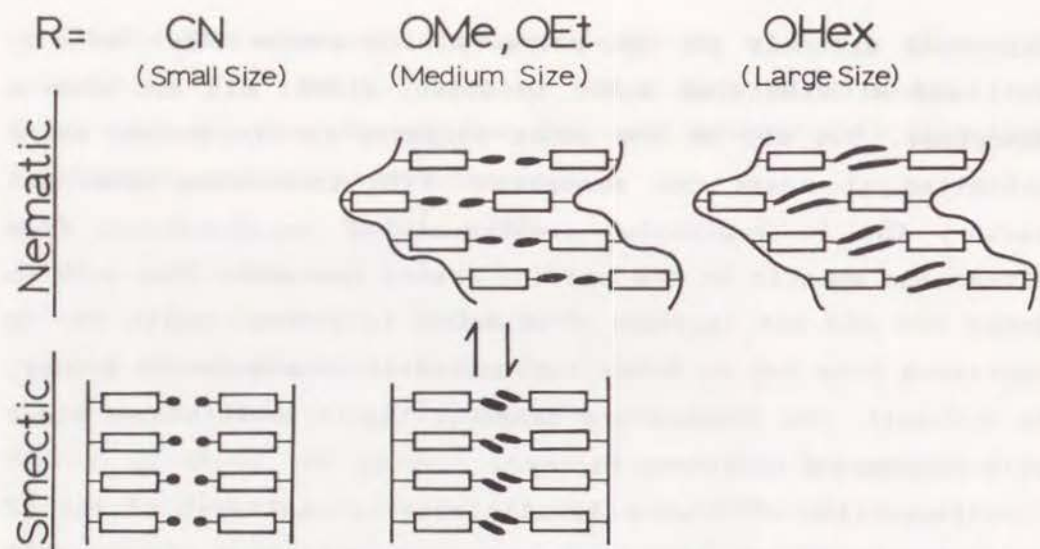
R= CN OMe,OEt OHex
(Small Size) (Medium Size) (Large Size)

Nematic

Smectic

Figure 13. Schematic representation of the relationship between size of the terminal substituent and type of mesophase.

REFERENCES

1) W.R. Krigbaum and H.J. Lader, Mol. Cryst. Liq. Cryst., 62, 87 (1980).

2) H. Finkelmann and H. Ringsdorf, Makromol. Chem., 179, 273 (1978).

3) H. Ringsdorf and A. Schneller, Br. Polym. J., 13, 43 (1981).

4) H. Ringsdorf and R. Zentel, Makromol. Chem., 180, 803 (1978).

5) H. Finkelmann, U. Keichle and G. Rehage, Mol. Cryst. Liq. Cryst., 94, 343 (1983).

6) H.J. Coles and R. Simon, "Recent Advances in Liquid Crystal-line Polymers", Ed., L.L. Chapoy, Elsevier Applied Science, New York, 1985, Chap. 22.

7) H. Finkelmann and G. Rehage, Adv. Polym. Sci., 60/61, 99 (1984).

8) V.P. Shibaev and N.A. Plate, Adv. Polym. Sci., 60/61, 173

9) Chapter 5 of this thesis; Polym. J., 20, 923 (1988).

10) Chapter 6 of this thesis; Macromolecules, 22, 3763 (1989).

11) H. Higashimura and M. Sawamoto, Adv. Polym. Sci., 62, 49 (1984).

12) T. Higashimura and M. Sawamoto, Makromol. Chem., Suppl., 12, 153 (1985).

13) M. Sawamoto and T. Higashimura, Makromol. Chem., Makromol. Symp., 3, 83 (1986).

14) T. Higashimura, S. Aoshima and M. Sawamoto, Makromol. Chem., Makromol. Symp., 3, 99 (1986).

15) J.M. Rodriguez-Parada and V. Percec, J. Polym. Sci., Polym. Chem. Ed., 24, 1363 (1986).

16) G.W. Gray, K.J. Harrison, J.A. Nash, J. Constant, D.S. Hulme, J. Kirton and E.P. Raynes, "Liquid Crystals and Ordered Fluids", Vol. 2, Eds. J.F. Johnson and R.S. Porter, Plenum Press, New York, 1974, p. 617.

17) M. Miyamoto, M. Sawamoto and T. Higashimura, Macromolecules, 17, 265 (1984).

18) M. Miyamoto, M. Sawamoto and T. Higashimura, Macromolecules, 17, 2228 (1984).

19) T. Enoki, M. Sawamoto and T. Higashimura, J. Polym. Sci., Polym. Chem. Ed., 24, 2261 (1986).

20) M. Sawamoto, C. Okamoto and T. Higashimura, Macromolecules, 20, 2693 (1987).

21) D. Demus and L. Richter, "Textures of Liquid Crystals", Verlag Chemie, New York, 1978.

22) V.V. Tsukruk, V.V. Shilov, I.I. Konstantinov, Yu.S. Lipatov and Yu.B. Amerik, Eur. Polym. J. 18, 1015 (1982).

23) P.L. Barny, J.-C. Dubois, C. Friedrich and C. Noel, Polym. Bull., 15, 341 (1986).

24) C. Noel, Chap. 9 of Ref. 6).

CHAPTER 8

SYNTHESIS OF A NOVEL COMB-LIKE POLY(VINYL ETHER) WITH PENDANT ISOPROPYLNAPHTHOXY GROUPS

ABSTRACT

A novel comb-like polymer having isopropylnaphthoxy pendant with the controlled molecular structure was synthesized by the cationic polymerization of 2-(6-isopropyl-2-naphthoxy)-ethyl vinyl ether (I) with AlEtCl$_2$ catalyst. Although the polymer's molecular weight ($\overline{M}n$: 4,000-17,000) could be controlled by the reaction conditions (solvent polarity, temperature and initial monomer concentration), the steric structure was not affected by them at all, giving almost the same amount of the meso and racemic diads irrespective of the conditions. The polymer showed only an amorphous character (Tg: 22-45 ℃) but not any liquid-crystalline phase.
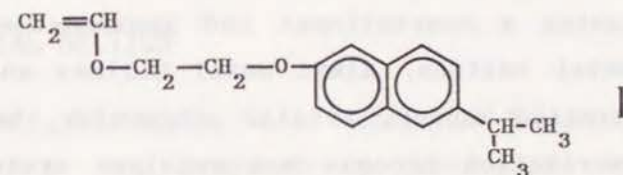
INTRODUCTION

One of the most important properties of the so-called comb-like polymers is their capacity to form a liquid crystal- line (LC) phase by incorporating a rigid-rod mesogenic side chain into a polymer structure.[1] And many types of side-chain liquid crystalline polymers (LCP), with different structures both of main chains and mesogenic side chains, have been synthesized and their properties have been investigated.[2]

Since the first examples of LC poly(vinyl ether)s with narrow molecular weight distributions (MWD) by the use of living cationic polymerization were reported by the author and Lenz,[3, 4] several research groups in the world have been actively engaged in the living polymerization of mesogenic vinyl ethers,[5, 6] because the effect of the polymer's molecular weight on the phase transitions can be determined without the undue influence of the low and high molecular weight compo- nents. From the industrial point of view, however, the cationic polymerization using a conventional and inexpensive catalyst (for example, metal halides, alkyl metal halides and so on), though less controlled manner, is also attractive, because the simplified polymerization process and catalyst system can be applied.

In this chapter, the author turned his attention to synthesis of a novel poly(vinyl ether) with an isopropyl- naphthoxy pendant using ethylaluminum dichloride ($AlEtCl_2$), one of alkyl metal halides, as a catalyst. That is, polymerizations of 2-(6-isopropyl-2-naphthoxy)ethyl vinyl ether (I) were carried out with the catalyst, in order to extend the range of cationically obtained comb-like poly(vinyl ether)s with aromatic-rigid pendants. This 6-isopropyl-2-naphthoxy pendant structure was chosen, because there are some examples of the 2,6-naphthylene structure containing main-chain LCP's,[7] and because 6-isopropyl-2-naphthol, the precursor of the monomer I , is available as a by-product of 2,6-dihydroxy-naphthalene. Furthermore, the side-chain LCP with that structure as a pendant, to the author's knowledge, has not been reported so far. The first objective, therefore, was to examine whether the poly I could show a LC phase or not. And the second objective was to investigate the effect of polymerization conditions (solvent polarity, temperature and so on) on the molecular weight, thermal properties and steric structure of the polymer. Unfortunately, this novel poly(vinyl ether) did not show any LC phase but only a glass transition as described below.
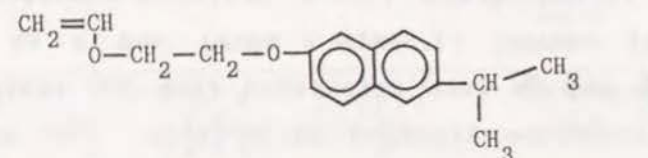
EXPERIMENTAL SECTION

Monomer Synthesis. 2-(6-isopropyl-2-naphthoxy)ethyl vinyl ether (I) was prepared by the phase-transfer-catalyzed condensation of 2-chloroethyl vinyl ether (Tokyo Kasei, purity 97%) with 6-isopropyl-2-naphthol (Mitsui Petrochemical, mp 112 ℃, purity 98%) in the presence of sodium hydroxide (equivalent to the naphthol) and a catalytic amount of tetrabutylammonium hydrogen sulfate,[8] as shown below:
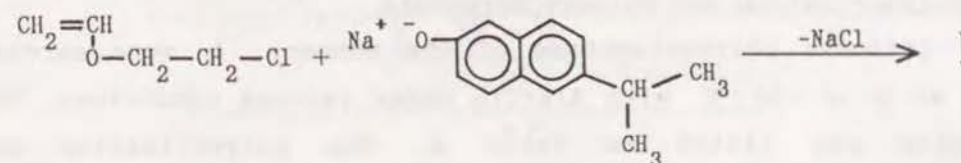
I was purified by recrystallization from ethanol three times; the isolated yield ca. 66% (based on the 6-isopropyl-2-naphthol charge), yellow needle-like crystal with mp 62 ℃ (by DSC), purity > 99 % by gas chromatography. The chemical shifts of the ¹H- and ¹³C-NMR spectra of the monomer (I) are summarized in Table 1.

Procedures. Solvents were distilled over calcium hydride before use. AlEtCl₂ (Tosoh Akzo) was used as received. Polymerizations were carried out as reported.[3, 4] Polymer yield was determined by gravimetry. The molecular weight distribution (MWD) of the polymers was measured by gel-permeation chromatography (GPC) in chloroform solutions at room temperature on a Waters liquid chromatograph (150-C ALC/GPC) equipped with a polystyrene gel column (7.5mmID × 60cm) and a UV detector (254nm). The $\overline{M}n$ and $\overline{M}w$ were calculated from GPC curves on the basis of a polystyrene standard calibration. ¹³C- and ¹H-NMR spectra were recorded on a JOEL GX-500 spectrometer (125.8 MHz and 500 MHz, respectively) in CDCl₃ at 45 ℃.

Thermal analysis was carried out by differential scanning calorimetry (DSC) on a Seiko DSC-220C instrument with polymer samples of about 10mg under a nitrogen flow at a scanning rate of 10 ℃ per min.

RESULTS AND DISCUSSION

1. Polymerization and Polymer Structure

Cationic polymerizations of the monomer I were carried out at 0 or -30 ℃ with AlEtCl₂ under various conditions. The results are listed in Table 2. The polymerization was relatively fast, reaching ca. 90 % polymer yield in 10-300 min,

Table 1.
¹H- and ¹³C-NMR chemical shifts for the monomer (I) and the polymer.[1)]

	¹H-NMR[2)]		¹³C-NMR	
	δ (ppm)	proton	δ (ppm)	carbon
Monomer[3)]	1.35 (d)	p	23.9	p
	3.05 (septet)	o	33.9	o
	4.09 (d of d)	a1	66.4	c
	4.11 (t)	c	66.5	d
	4.29 (d of d)	a2	87.1	a
	4.33 (t)	d	107.0	n
	6.56 (d of d)	b	118.7	f
	7.14 (d)	n	123.9	i
	7.16 (d of d)	f	126.1	k
	7.36 (d of d)	k	126.8	l
	7.60 (d)	i	129.1	g
	7.67 (d)	l	129.4	h
	7.70 (d)	g	133.0	m
			144.1	j
			151.6	b
			156.2	e
Polymer[4)]	1.1-1.4	p	39.4, 41.1	a'
	1.6-2.1	a'	74.3	b'
	2.8-3.0	o		
	3.6-4.1	b', c, d	other carbons in R[5)]	
	6.8-7.6	f, g, i		
		k, l, n		

1) Chemical shifts are given in ppm relative to TMS.
2) ¹H-¹H coupling constants (unit: Hz) are listed below:

$J_{a1,a2}$	$J_{a1,b}$	$J_{a2,b}$	$J_{c,d}$	$J_{f,g}$	$J_{f,n}$	$J_{i,k}$	$J_{k,l}$	$J_{o,p}$
2.2	7.0	14.3	6.8	8.9	2.5	1.7	8.4	7.0
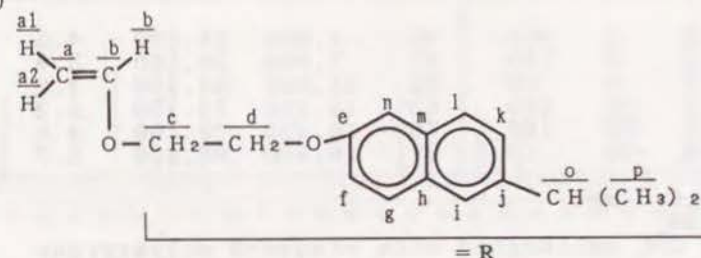
3) 4)
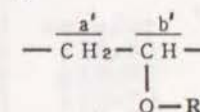
5) The signals of the pendant group (R) are at almost the same position as those of the monomer.

except for the samples obtained at the lower temperature and in CH$_2$Cl$_2$ solvent (samples D and E). All polymers were soluble in toluene and CHCl$_3$ at room temperature. The molecular weight distributions (MWD) of the polymers were shown in Figure 1. They exhibited wide MWD's, $\overline{M}w/\overline{M}n$ of 3.8-5.7, originating from AlEtCl$_2$ catalyst employed. As can be seen both in the $\overline{M}n$ and $\overline{M}w$ data in Table 2 and the MWD in Figure 1, a higher molecular weight was obtained in a more polar solvent, at a higher initial monomer concentration, [M]$_0$, and at a lower temperature, as normally observed in ionic polymerizations.

All the polymers (A - F) gave the expected comb-like structure $\rm II$, formed only by the addition reaction of the double bonds in the vinyloxy groups, as shown by the NMR results in Table 1 and Figure 2.
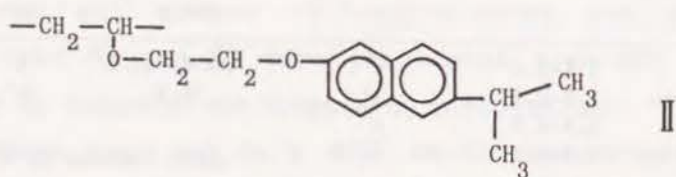
Table 2.

Cationic polymerization of
2-(6-isopropyl-2-naphthoxy)ethyl vinyl ether (I) with AlEtCl$_2$

| code | Polymn. Conditions[a] | | | | Polymer | $\overline{M}n$[c] | $\overline{M}w$[c] | $\overline{M}w/\overline{M}n$[c] | Tg[d] |
	Solvent	[M]$_0$ (M)	Temp. (℃)	Time (min)	yield (wt%)				(℃)
A[b)]	toluene	0.2	0	300	95	4,000	18,000	4.5	22
B	CH$_2$Cl$_2$	0.2	0	180	87	7,000	26,500	3.8	34
C	CH$_2$Cl$_2$	0.5	0	60	92	11,000	46,500	4.2	43
D	CH$_2$Cl$_2$	0.5	-30	180	53	14,100	73,700	5.2	43
E	CH$_2$Cl$_2$	1.0	-30	180	70	16,400	76,100	4.6	45
F	nitroethane	1.0	-30	10	97	16,900	96,800	5.7	41

a) [AlEtCl$_2$]$_0$ = 10.0 mM.
b) [H$_2$O]$_0$ = 5.0 mM.
c) Determined by GPC calibrated with standard polystyrene samples.
d) Taken from the second heating cycle (at 10 ℃ /min).
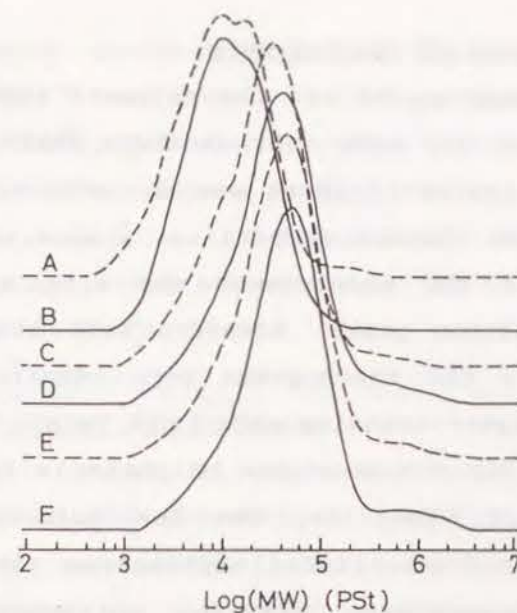
Figure 1. MWD's of the polymer obtained from $\rm I$. Sample codes as indicated: see Table 2 for reaction conditions.
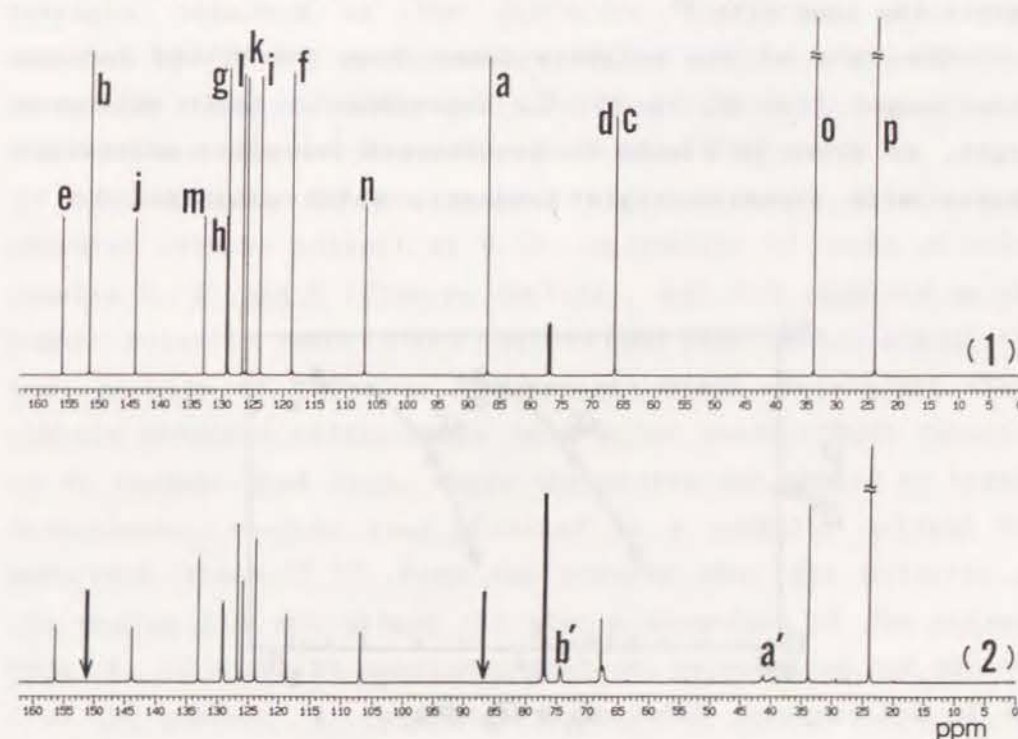

Figure 2. ^{13}C-NMR spectra of (1) $\rm I$ and (2) poly $\rm I$ obtained with AlEtCl$_2$ in CH$_2$Cl$_2$ at 0 ℃ (sample C): see Table 1 for designation of carbons.

2. Thermal Properties of the Polymers

The DSC thermograms of all the polymers showed only glass transitions but not any endo- nor exotherm peaks attributed to LC phases. To determine if there was any effect caused by the cooling rate on the thermal properties, a slow cooling rate of 2.0 ℃/min in the DSC measurement was also applied to all samples. No transition peaks, however, were observed for the samples, and their DSC thermograms were identical with those obtained at the higher scanning rate (10 ℃/min). The phenomenon that the poly I did not show any LC phase is consistent with the following fact. That is, the low molecular weight LC compounds with 2,6-disubstituted naphthalene ring gives lower isotropization temperature than the corresponding biphenyl compounds, because of the molecule's broadened structure against the long axis.[9]

The Tg's of the polymers taken from the second heating cycle ranged from 22 to 45 ℃, depending on their molecular weight, as shown in Figure 3. As observed for other poly(vinyl ether)s with aromatic rigid pendants, which exhibited no LC
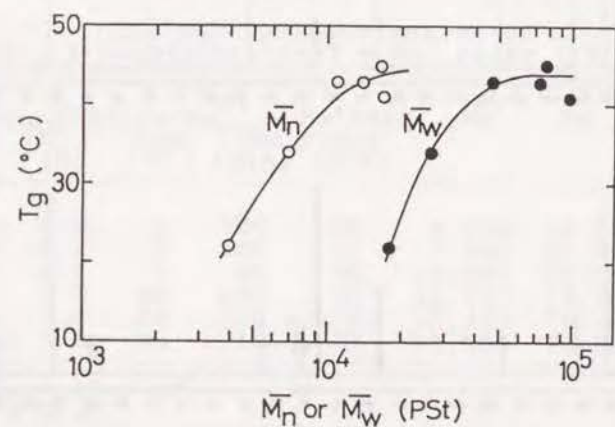
Figure 3. Tg of poly I as a function of $\overline{M}n$ and $\overline{M}w$.

phase, for example, polymers from 2-(4-biphenyloxy)ethyl vinyl ether (Tg = 56 ℃)[3] and from 2-(4-biphenylcarboxyl)ethyl vinyl ether (Tg = 32 ℃)[3], introduction of a rigid-bulky isopropyl-naphthoxy pendant group into a polymer chain also increased the Tg of poly(vinyl ether)s, in comparison with flexible alkyl groups in poly(alkyl vinyl ether)s (Tg = -33 ℃ for ethyl, -49 ℃ for propyl, and -56 ℃ for butyl).[10]

3. Steric Structure of the Polymers

The polymer's molecular weight was found to be controlled by the polarity of the polymerization medium (temperature and solvent polarity) as described above. To investigate if there was any effect of the polarity on the propagating species derived from the monomer I, the steric structures of the polymers obtained by the different conditions were then compared by ^{13}C-NMR spectroscopy. Figure 4 shows the main-chain methylene signals, which consist of two peaks corresponding to the meso and racemic diads from the higher field.[11]

The spectrum of the sample A [Figure 4(A)], obtained in nonpolar toluene solvent at 0 ℃, is similar to those of other samples C, E, and F [Figures 4(C),(E), and (F)] obtained in the higher polarity conditions, and all the samples had almost the same amounts of the meso and racemic diads. Poly(alkyl vinyl ether)s obtained cationically in a polar solvent were reported to be racemic-diad rich, where the active end should be highly dissociated, whereas that obtained in a nonpolar solvent had meso-rich diads.[12, 13] From the results that the polarity of the medium did not affect the steric structure of the polymer from I, it might be concluded that the propagating end derived from the monomer I is rather dissociated irrespective of the solvent polarity through the intramolecular self-solvation of the neighboring oxyethylene units in the 2-(6-isopropyl-2-
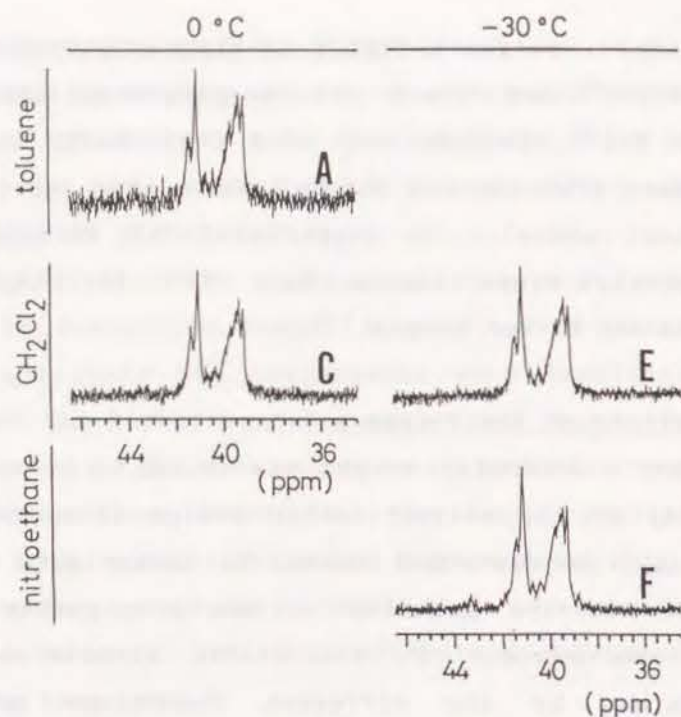
Figure 4. Partial ^{13}C-NMR spectra (main-chain methylene region)
of poly I. Polymerization temperatures, solvents and sample
codes as indicated: see Table 2 for reaction conditions.

naphthoxy)ethyloxy pendant, as proposed by Higashimura for the
poly(vinyl ether)s with polyoxyethylene pendants.[13]

In conclusion, a novel comb-like poly(vinyl ether) having
isopropyl-naphthoxy pendant with the well-defined molecular
structure could be synthesized from the monomer of
2-(6-isopropyl-2-naphthoxy)ethyl vinyl ether with AlEtCl$_2$
catalyst. Although the polymer's molecular weight could be
controlled by the polarity of the medium, it did not affect the
steric structure at all. Unfortunately, the polymer showed only
an amorphous character (Tg: 22-45 ℃) but not any LC phase.

REFERENCES

1) N.A. Plate, V.P. Shibaev, "Comb-Shaped Polymers and Liquid
   Crystals," Plenum Press, New York, N.Y., 1987.

2) (a) H. Finkelmann, "Polymer Liquid Crystals," A. Ciferri,
   W.R. Krinbaum, R.B. Meyer, Ed., Academic Press, New York,
   N.Y., 1982, Chapter 2; (b) H. Finkelmann, G. Rehage, Adv.
   Polym. Sci., 60/61, 99 (1984); (c) V.P. Shibaev, N.A. Plate,
   Adv. Polym. Sci., 60/61, 173 (1984).

3) Chapter 5 of this thesis; Polym. J., 20, 923 (1988).

4) (a) Chapter 6 of this thesis; Macromolecules, 22, 3763
   (1989); (b) Chapter 7 of this thesis; Polymer, 30, 2269
   (1989).

5) V. Percec, M. Lee, H. Jonson, J. Polym. Sci., Part A, Polym.
   Chem., 29, 327 (1991); V. Percec, M. Lee, J. Macromol. Sci.
   Chem., A 28, 651 (1991); idem, Macromolecules, 24, 1017
   (1991); ibid., 24, 2780 (1991); idem, Polym. Bull., 25, 123
   (1991); ibid., 25, 131 (1991).

6) S.G. Kostromin, N.D. Cuong, E.S. Garina, V.P. Shibaev, Mol.
   Cryst. Liq. Cryst., 193, 177 (1990);
   V. Heroguez, A. Deffieux, M. Fontanille, Makromol. Chem.,
   Makromol. Symp., 32, 199 (1990); V. Heroguez, M. Schappacher,
   E. Papon, A. Deffieux, Polym. Bull., 25, 307 (1991).

7) M.G. Dobb, J.E. McIntyre, Adv. Polym. Sci., 60/61, 61 (1984).

8) J.M. Rodriguez-Parada, V. Percec, J. Polym. Sci., Polym.
   Chem. Ed., 24, 1363 (1986).

9) G.W. Gray, Ref.2)(a), Chapter 1.

10) W.J. Schell, R. Simlea, J.J. Aklonis, J. Macromol. Sci.,
    Cem., A3, 1297 (1974); J. Lal, G.S. Trick, J. Polym. Sci.,
    Part A, 2, 4559 (1964).

11) K. Hatada, T. Kitayama, N. Matsuo, H. Yuki, Polym. J., 15,
    719 (1983).

12) Y. Ohsumi, T. Higashimura, S. Okamura, J. Polym. Sci., Part A-1, 5, 849 (1967).

13) T. Nakamura, S. Aoshima, T. Higashimura, Polym. Bull., 14, 515 (1985).

LIST OF PUBLICATIONS

CHAPTER 1	Makromol. Chem., 193, 2081 (1992)
CHAPTER 2	Makromol. Chem., 193, 2091 (1992)
CHAPTER 3	Makromol. Chem., in press
CHAPTER 4	Makromol. Chem., in press
CHAPTER 5	Polym. J., 20, 923 (1988)
CHAPTER 6	Macromolecules, 22, 3763 (1989)
CHAPTER 7	Polymer, 30, 2269 (1989)
CHAPTER 8	Polym. Bull., 28, 259 (1992)

Acknowledgments